READER INFORMATION CARD

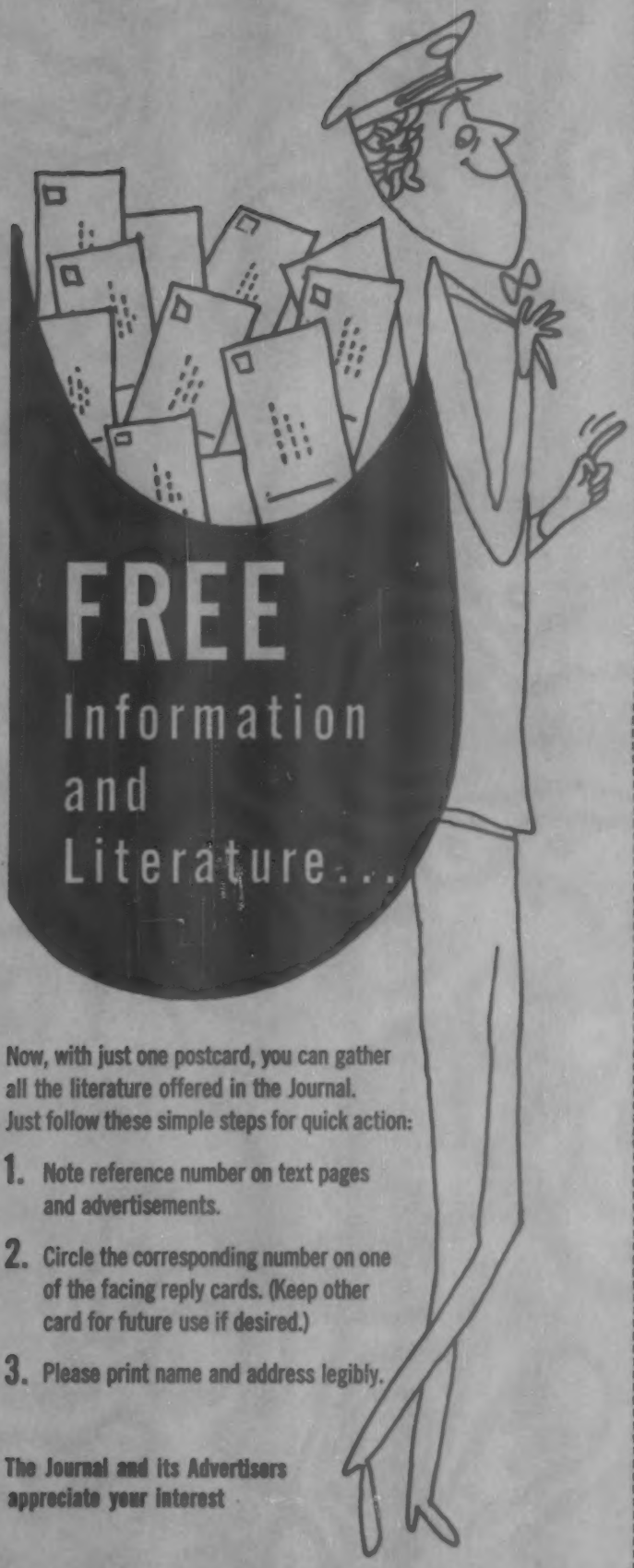

Now, with just one postcard, you can gather all the literature offered in the Journal. Just follow these simple steps for quick action:

1. Note reference number on text pages and advertisements.
2. Circle the corresponding number on one of the facing reply cards. (Keep other card for future use if desired.)
3. Please print name and address legibly.

The Journal and its Advertisers appreciate your interest

June, 1960

Card valid until August 31, 1960

Please send me, without cost or obligation, further information and literature on items circled below:

1	26	51	76	101	126
2	27	52	77	102	127
3	28	53	78	103	128
4	29	54	79	104	129
5	30	55	80	105	130
6	31	56	81	106	131
7	32	57	82	107	132
8	33	58	83	108	133
9	34	59	84	109	134
10	35	60	85	110	135
11	36	61	86	111	136
12	37	62	87	112	137
13	38	63	88	113	138
14	39	64	89	114	139
15	40	65	90	115	140
16	41	66	91	116	141
17	42	67	92	117	142
18	43	68	93	118	143
19	44	69	94	119	144
20	45	70	95	120	145
21	46	71	96	121	146
22	47	72	97	122	147
23	48	73	98	123	148
24	49	74	99	124	149
25	50	75	100	125	150

Mail me a list of AWS Publications ☐

NAME _____

TITLE _____

COMPANY _____

PRODUCT _____

ADDRESS _____

CITY & ZONE _____ STATE _____

FIRST CLASS
PERMIT NO. 9264
NEW YORK, N. Y.

Business Reply Card
No postage necessary if mailed in the United States

4¢ POSTAGE WILL BE PAID BY

Welding Journal
33 West 39th Street
New York 18, N. Y.

FIRST CLASS
PERMIT NO. 9286
NEW YORK, N. Y.

Business Reply Card
No postage necessary if mailed in the United States

4¢ POSTAGE WILL BE PAID BY

Welding Journal
33 West 39th Street
New York 18, N. Y.

June, 1960

Card valid until August 31, 1960

Please send me, without cost or obligation, further information and literature on items circled below:

1	26	51	76	101	126
2	27	52	77	102	127
3	28	53	78	103	128
4	29	54	79	104	129
5	30	55	80	105	130
6	31	56	81	106	131
7	32	57	82	107	132
8	33	58	83	108	133
9	34	59	84	109	134
10	35	60	85	110	135
11	36	61	86	111	136
12	37	62	87	112	137
13	38	63	88	113	138
14	39	64	89	114	139
15	40	65	90	115	140
16	41	66	91	116	141
17	42	67	92	117	142
18	43	68	93	118	143
19	44	69	94	119	144
20	45	70	95	120	145
21	46	71	96	121	146
22	47	72	97	122	147
23	48	73	98	123	148
24	49	74	99	124	149
25	50	75	100	125	150

Mail me a list of AWS Publications ☐

NAME _____

TITLE _____

COMPANY _____

PRODUCT _____

ADDRESS _____

CITY & ZONE _____ STATE _____

Index to ADVERTISERS

PAGE	
644	Acro Welder Mfg. Co.
Outside Back Cover	Air Reduction Sales Co.
662	All-State Welding Alloys Co., Inc.
573	Alloy Rods Company
649	Aluminum Company of America
Inside Back Cover	The American Brass Company
661	Ampco Metal, Inc.
630	The Arcair Company
666, 667	Arcos Corporation
652	Bateman Foundry & Machine
659	Cam-Lok Div., Empire Products, Inc.
628	Chicago Hardware Foundry Co.
652	Coyne Cylinder Company
669	Electric Arc, Inc.
645, 646	Eutectic Welding Alloys Corp.
629	General Vaccum Corporation
655	Glenn-Pacific Power Supply Company
670	Handy & Harman
653	Harnischfeger Corporation
567	Hobart Brothers Co.
654	Independent Engineering Company, Inc.
634	Instrument Control Co.
574	International Nickel Co., Inc.
628	Lenco, Inc.
636, 637	The Lincoln Electric Co.
571	Linde Company, Division of Union Carbide Corporation
633	Merrill Brothers
576	Miller Electric Mfg. Co., Inc.
632	National Carbide Company
651	Omark Industries, Inc.
668	Phoenix Products Company
569	Pure Carbonic Co.
648	Reynolds Metals Company
633	Royco Instruments, Inc.
648	A. O. Smith Corporation
653	S-M-S Corporation
665	Sperry Products Company
641	Stoody Company
643	Stulz-Sickles Co.
657	Sylvania Electric Products, Inc.
622	Syntron Rectifier Division
658	Tec Torch Co., Inc.
625	Tempil® Corporation
631	Thomson Electric Welder Co.
571	Union Carbide Corporation Linde Company
Inside Front Cover	Victor Equipment Co.
625	Wall Colmonoy Corporation

Welding Research

Sponsored by the Welding Research Council of the Engineering Foundation

WRC

SUPPLEMENT TO THE WELDING JOURNAL, JUNE 1960

1959 ADAMS LECTURE

The Science of Arc Welding

Evaluation of the present knowledge provides the engineer and the research man with basic concepts of volt-ampere relationship, distribution of field intensities and temperatures, metal transfer, spatter, arc forces and motion, melting rate, weld area, melting ratio and other related factors

BY CLARENCE E. JACKSON

Part III*—What the Arc Does

So far in this discussion, the physical characteristics of the tungsten-arc and consumable-electrode arc-welding processes have been considered. In order to provide a basis for a practical engineering approach to the selection of welding techniques, it will be useful to consider the performance of the arc. In projecting welding techniques for any application, a number of fundamental measurements are required. These essentially relate the effect of welding current, voltage and speed of travel on the performance of the welding process.

Volume or Area of Weld Metal Deposited

The fact that the melting rate of an electrode is expressed in many different units, sometimes is confusing. Such units as pounds per minute or hour, grams per second, and inches per minute, appear to be favored by individual workers. It is suggested that a more practical designation for melting rate is based on the volume deposited per unit time (Fig. 25).† This engineering designation is even more convenient when measurements of electrode melting rates are taken in inches per minute. The volume of metal deposited per linear inch is easily obtained by dividing the melting rate in cubic inches by the speed of travel. It has been pointed out by Wilson, *et al.*,[25] that in consumable-electrode arc welding, the total melting rate of the electrode is the melting rate caused by the arc to which is added the increase in melting rate due to the I^2R heating of the length of electrode that extends beyond the contact tip. The melting rate has also been found to be dependent upon the electrode diameter in both the inert-gas and submerged-arc processes. In order to fill a groove or to produce a fillet with a given dimension, a definite volume of weld metal per inch of length of weld is required. In order to deposit this volume or cross-sectional area of weld metal, the ratio of the current to the speed of travel is useful (Fig. 51). For a given melting rate in pounds per minute, the cross-sectional area of the

CLARENCE E. JACKSON is Associate Manager, Electric Welding Department, at the Development Laboratory, Linde Co., Division of Union Carbide Corp., Newark, N. J.

* Part I—Definition of Arc" and Part II—"Consumable-electrode Welding Arc" appeared on pages 129-s–140-s and 177-s–190-s, respectively, of the April and May 1960 issues of the WELDING JOURNAL Research Supplement.

† See page 178-s of May 1960 issue of WELDING JOURNAL Research Supplement.

deposited weld metal can be predicted.

Penetration

The penetration of a weld deposited in a groove or on the surface of a plate is generally recognized as the distance below the original surface to which the molten metal progresses. A study of the factors which influence penetration for any given welding process indicates that current, voltage and travel are important in the results which are obtained. Of these three items, the welding current is the most significant, while the travel and voltage are less important. In determining the penetration for any particular weld, from a fundamental study, it is assumed that penetration is the distance below the level of molten metal in the crater which the base metal is melted. Figure 52 shows the combined effect of current, welding voltage, speed of travel on penetration for a series of experiments with covered electrodes. A similar relationship is noted with submerged-arc welding and also with inert-gas consumable-electrode for mild steel; these results shown in Figs. 53 and 54 indicate the general application of the welding-technique performance factor. In a series of tests using the submerged-arc process, the results reported by Hayashi[53] covering a wide range of welding conditions gave the relation shown in Fig. 55.

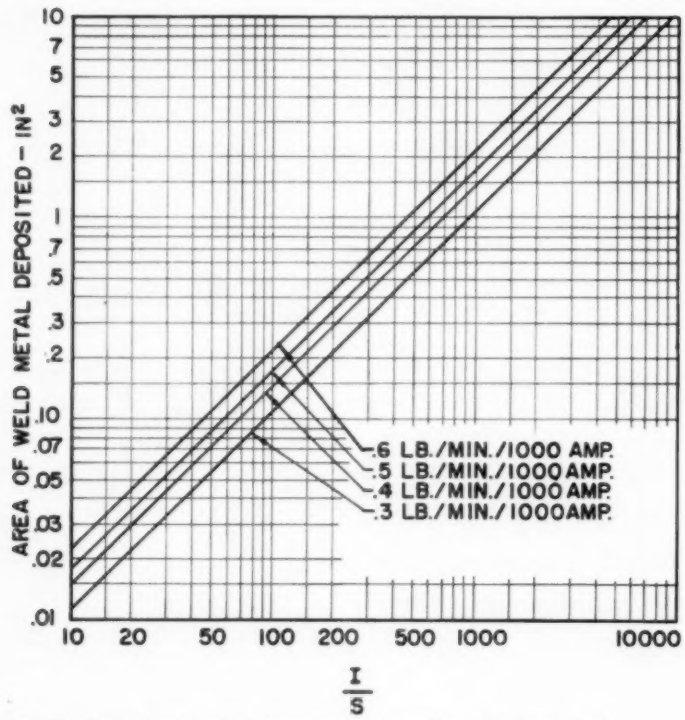

Fig. 51—Area of weld metal deposited is determined by the ratio of current (I) to the speed of travel (S) for any electrode melting rate

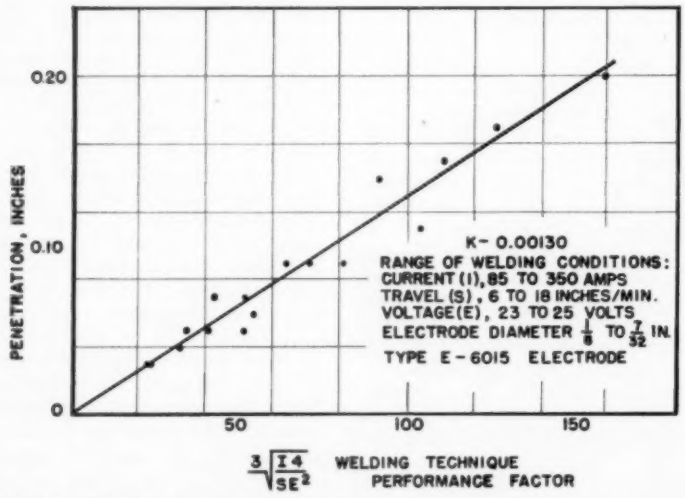

Fig. 52—Effect of current, welding voltage and speed of travel on penetration in the covered-electrode process

In applying empirical relationships, the level of the crater is important. In many cases, the penetration is roughly the penetration below the surface of the plate since the crater is essentially level with the surface. The true arc length cannot be measured directly except when there is negligible penetration because, although a projected image of the arc may be readily recorded, a fraction of the arc may be below the plate level. It has been suggested by Needham and Smith, that the extension of the arc below the plate may be nearly equal to the penetration in etched macrospecimens. Certainly the arc cannot extend beyond the fused zone. Fusing of the plate material by heat flow is limited by the steep thermal gradient at the crater periphery.

Very few data have been reported which show the effect of welding technique on crater formation. From a theoretical standpoint, the force acting toward the crater will be given by the following relation:

$$F = KI^2 \log \frac{r_1}{r_2}$$

Where:

r_1 = radius of arc at crater
r_2 = radius of arc at electrode
I = current, amperes
K = constant
F = force toward crater

From this it is seen that the force at the crater will increase with an increase in current with a given electrode or with a decrease in the diameter of the electrode for a given current. This suggests that penetration should increase with current density; McElrath[22] reports a series of tests which substantiates this conclusion (Fig. 56). Such increase in penetration is more likely accompanied by an increase in

Table 8—Comparison of Effect of Welding Technique on Melting Rate, Nugget Area, Melting Ratio and Penetration; Both Measured and Calculated Values Are Shown

Welding technique			Melting rate electrode lb/min		Nugget area, in.		Melting ratio, %		Penetration, in.	
Amp	V	Ipm	Measured	Calculated	Measured	Calculated	Measured	Calculated	Measured	Calculated
290	26	10	0.12	0.12	0.08	0.09	51.0	55.4	0.12	0.18
800	26	27.4	0.42	0.37	0.18	0.18	60.7	73.2	0.39	0.42
900	34	10	0.49	0.43	0.49	0.53	65.5	71.0	...	...
500	30	20.1	0.22	0.22	0.14	0.14	72.0	73.0	0.28	0.23
580	26	20.1	0.25	0.25	0.14	0.14	68.7	69.1	0.26	0.29
435	26	15.1	0.19	0.19	0.11	0.15	60.4	56.3	0.17	0.22
420	36	20.1	0.16	0.18	0.10	0.09	70.6	68.0	0.22	0.18
290	26	10	0.11	0.11	0.09	0.09	52.0	55.4	0.13	0.18
500	30	27.4	0.22	0.22	0.10	0.09	74.3	78.6	0.23	0.22
135	26	4.7	0.04	0.05	0.04	0.06	46.0	31.2	0.07	0.07

crater depth. Further investigation is needed in order to study all the factors which control crater formation and the resulting penetration.

Weld-metal Nugget Area

In any study of electric-arc welding, some indication of the total quality of metal which is fused is important. The quantity of base metal fused, together with the electrode consumed, provides the molten metal which, properly positioned by the welding process, must necessarily form the weld joint. In the fused-metal area, both the molten metal transferred from the electrode and the quantity of base metal fused increases with the welding current. In a like manner, as the speed of travel is increased for a given current, this area will decrease. The area from many tests seems to be relatively unaffected by normal changes in the welding voltage. The weld-metal area is controlled by the current and speed of travel used, and, for the data which are available, is related directly to the 1.716 power of the current and inversely to the first power of the speed of travel as shown in Fig. 57 for the submerged-arc process. A similar relationship also is applicable to the inert-gas consumable-electrode process as shown in Fig. 58. An equation for the data in Fig. 57 is as follows:

$$\text{Log } A = 0.903 \log \frac{I^{1.716}}{S} - 3.95$$

Where:

A = area of weld nugget, sq. in.
I = welding current, amp
S = travel, ipm

Melting Ratio

Wilson, *et al.*,[23] have suggested an equation for the melting rate for a steel electrode for the submerged-arc process as follows:

$$MR = \frac{I}{1000}\left[0.35 + d^2 + 2.08 \times 10^{-7}\left(\frac{IL}{d^2}\right)^{1.22}\right]$$

Where:

MR = melting rate, lb/min

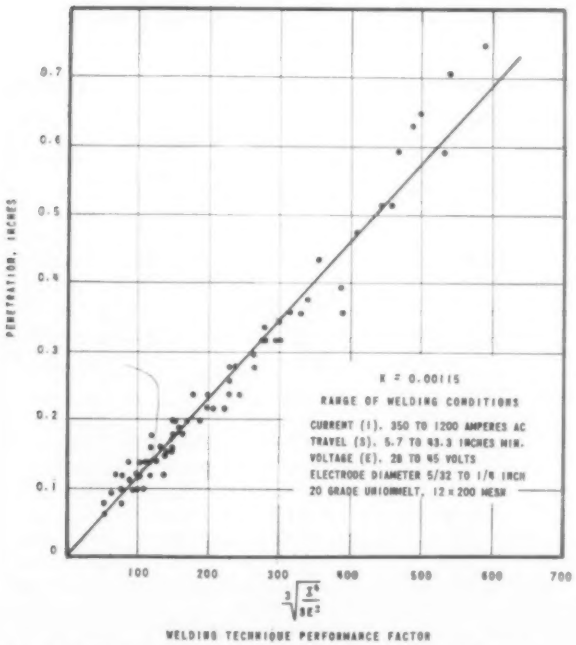
PENETRATION, INCHES
K = 0.00115
RANGE OF WELDING CONDITIONS
CURRENT (I). 350 TO 1200 AMPERES AC
TRAVEL (S). 5.7 TO 93.3 INCHES MIN.
VOLTAGE (E). 28 TO 45 VOLTS
ELECTRODE DIAMETER 5/32 TO 1/8 INCH
20 GRADE UNIONMELT, 12 x 200 MESH
WELDING TECHNIQUE PERFORMANCE FACTOR

Fig. 53—Effect of welding technique on penetration in the submerged-arc process

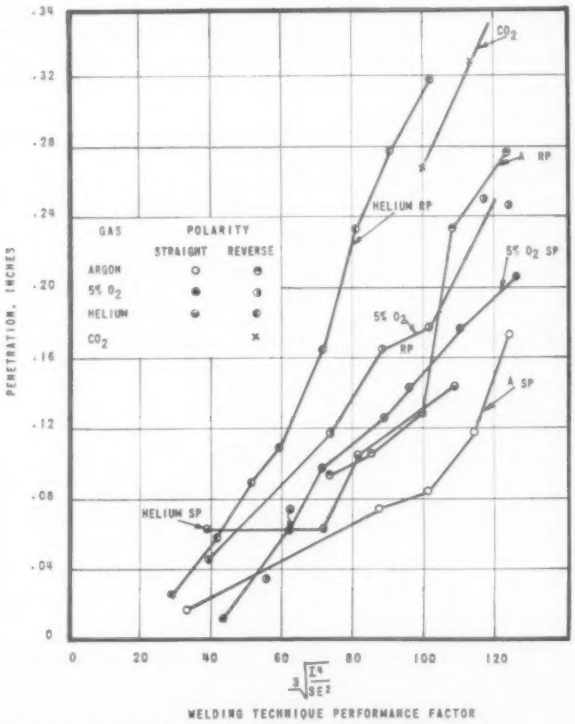

Fig. 54—Effect of technique on penetration in the inert-gas consumable-electrode process

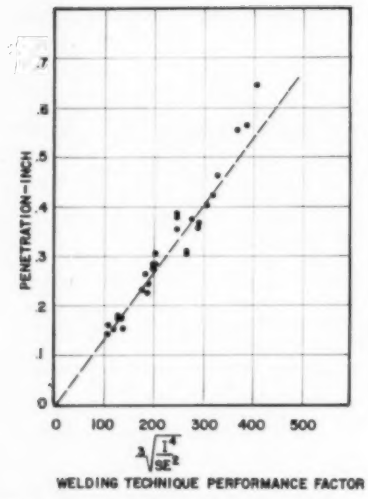

Fig. 55—Penetration for submerged-arc welding[53]

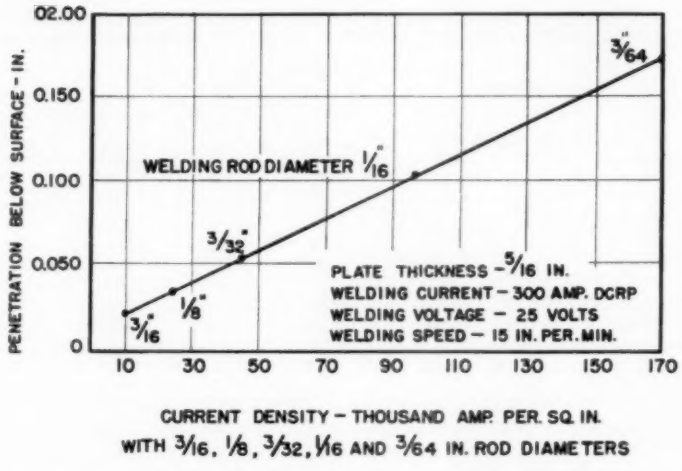
PENETRATION BELOW SURFACE - IN.
WELDING ROD DIAMETER 1/16"
3/32"
1/8"
3/16"
3/64"
PLATE THICKNESS - 5/16 IN.
WELDING CURRENT - 300 AMP. DCRP
WELDING VOLTAGE - 25 VOLTS
WELDING SPEED - 15 IN. PER. MIN.
CURRENT DENSITY - THOUSAND AMP. PER. SQ. IN.
WITH 3/16, 1/8, 3/32, 1/16 AND 3/64 IN. ROD DIAMETERS

Fig. 56—Penetration vs. current density[22]

d = electrode diameter, in.
I = current, amp
L = electrode extension, in.

It is now possible to estimate the ratio of the volume of the base metal melted to total weld metal melted for a range of welding techniques. The results of such a calculation are compared with actual measurements for a series of submerged-arc welding tests in Table 8; the agreement is reasonable.

Heat Effect of Weld Nugget

The electric-arc welding process fuses a volume of weld metal. In order to produce this volume of weld metal, energy is consumed. From studies of the energy distribution in electric-arc welding, it has been pointed out that improved efficiency of energy utilization is expected with higher currents and higher speeds. The weld-nugget area increases at a rate faster than the first power of current. In welding literature, the total energy input is often expressed as joules per linear inch. In these days of increased use of automatic welding processes, with higher speeds and higher-strength steels, it is important to recognize that comparisons based on total energy may not be applicable[54] and that the factors affecting the energy distribution must be considered.

In order to determine the effect of current and travel on the weld-metal nugget area, fifteen welds were deposited using the submerged-arc process on the surface of a steel plate (A212). These surface beads were deposited with currents from 135 to 800 amp with the travel adjusted to give an energy input of 45,000 joules per linear inch. The area of cross section taken from these welds ranged from 0.044 to 0.186 sq in., Table 9. Two cross sections are shown in Fig. 59. The maximum cooling

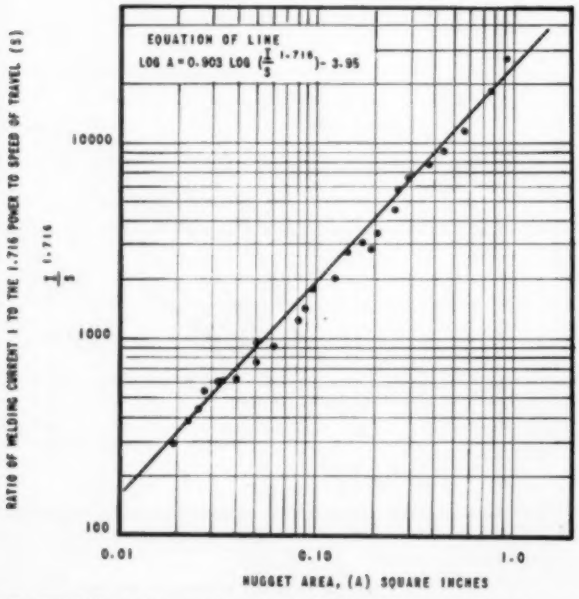
EQUATION OF LINE
LOG A = 0.903 LOG (I^1.716/S) - 3.95
RATIO OF WELDING CURRENT I TO THE 1.716 POWER TO SPEED OF TRAVEL (S)
NUGGET AREA, (A) SQUARE INCHES

Fig. 57—Effect of current and speed of travel on nugget area in the submerged-arc process

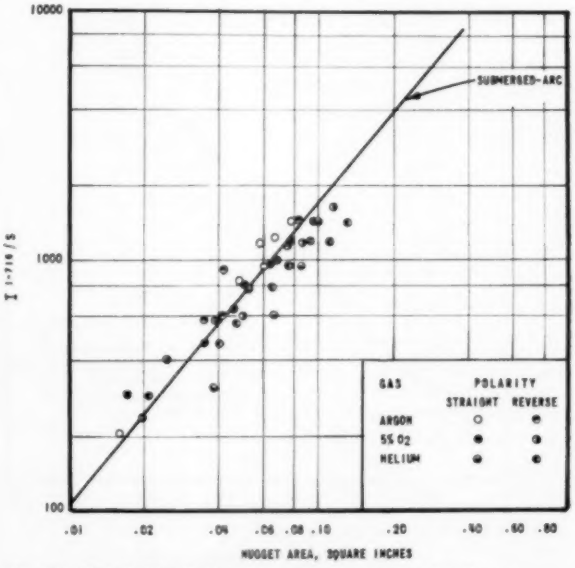

Fig. 58—Effect of technique on nugget area with inert-gas consumable-electrode arc welding

Table 9—Effect of Welding Technique on Nugget Area

Welding technique			Energy input, joules per linear inch	Nugget area, sq in.	
Amp	V	Ipm		Actual	Calculated
290	26	10	45,250	0.084	0.092
435	26	15.1	45,000	0.115	0.149
580	26	20.1	45,000	0.160	0.143
580	26	20.1	45,000	0.165	0.143
500	30	20.1	44,800	0.138	0.143
420	36	20.1	45,100	0.102	0.087
503	30	20.1	45,000	0.117	0.143
580	26	20.1	45,000	0.143	0.143
580	26	20.1	45,000	0.143	0.143
800	26	27.4	45,500	0.186	0.178
800	26	27.4	45,500	0.185	0.178
800	26	27.4	45,500	0.173	0.178
290	26	10	45,400	0.087	0.092
135	26	4.7	44,800	0.044	0.059

rate in the heat-affected zone is determined by the volume of molten metal in the weld bead; the hardness in the heat-affected zone for any steel is controlled by this cooling rate. As shown in Fig. 60, the maximum hardness in the heat-affected zone decreases as the nugget area increases even though the power input in joules per linear inch is constant.

Data are gradually being accumulated covering the performance of the various factors which may be controlled in the application of any arc-welding process. The welding engineer is now able to go to the drawing board and establish approximate welding techniques for initial tests and further predict the effects of specified changes in welding conditions.

Discussion

Useful concepts for the engineering application of the welding arc have been proposed. The melting rate of an electrode depends upon the electrode diameter, extension and current level. Penetration below the level of the crater increases with current and decreases with speed of travel and welding voltage. The effect of welding technique on melting ratio and nugget area has been pointed out.

Because of the fact that the consumable-electrode arc-welding processes include such a wide range of conditions, many questions remain to be answered, in spite of the extensive investigations reported. There is need for a more comprehensive study of crater mechanics. The factors which control the solidification pattern of the molten weld metal will aid in understanding such phenomena as undercutting and molten-metal viscosity. Although a fair understanding exists of the factors which control the melting rate of the electrode, there is need for further data in order to provide engineering scope over the entire field. The techniques which are available for studying the spatial relation in the submerged-arc process will be useful in systematically investigating the effects of current density, electrode diameters, flux compositions and other factors. The new processes using carbon dioxide have not been studied from a fundamental standpoint.

The welding fraternity is approaching a clear-cut scientific understanding of the many factors which control arc welding. Many investigators have contributed; many investigators will continue to contribute.

Closure

Engineering knowledge starts with the accumulation of empirical data, which to begin with, can only be qualitative. As new approaches are used, and especially when new methods of measurements or new techniques for studying the phenomena become available, these qualitative data gradually develop into quantitative data which serve as a basis for the theoretical analysis of the phenomena which we are studying. Only when the engineering data become quantitive, can we deal with the why and wherefore of the field. A special plea is made for a broadening of the range of arc-welding data which are studied; often a small amount of data taken in order to extrapolate restricted data will establish trends, and will be useful in developing a pattern.

The physical description of the arc-welding zone is rapidly becoming more exact, particular for the inert-gas-shielded tungsten-arc process. Considerable data have been presented for the consumable-electrode processes, although these are more complicated and will require ingenious approaches in future investigations. The relationships which exist for the inert-gas and

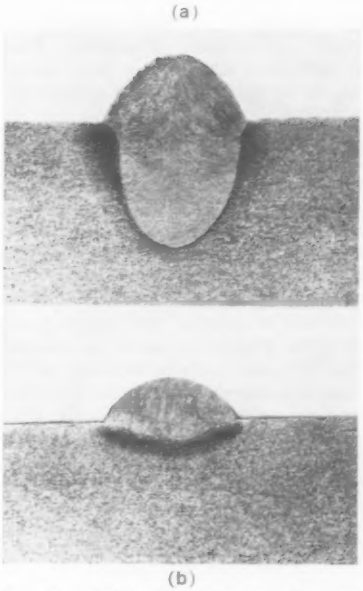

Fig. 59—(a) Weld deposited using 800 amp, 26 v and 27.4-ipm travel at 45,500 joules per linear inch, (b) weld deposited using 135 amp, 26 v and 4.7-ipm travel at 44,800 joules per linear inch

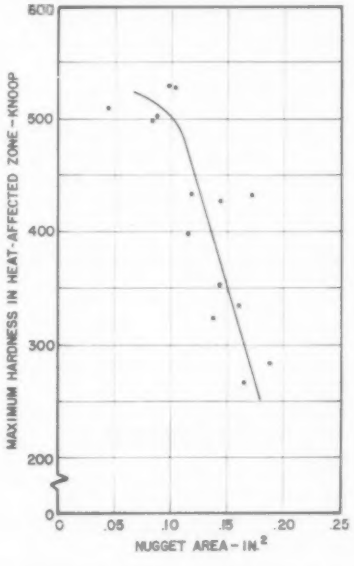

Fig. 60—The maximum hardness in the heat-affected zone decreases as the nugget area increases even though all deposited with approximately 45,000 joules per linear inch

submerged-arc consumable-electrode arc-welding processes will be useful in developing new techniques for applications using modern materials.

It is hoped that this presentation will stimulate investigation in some of the fields where the data are meager. Although a good practical understanding exists, there are large areas which will require further attention. As new welding processes are introduced, new basic problems will be raised. Although many welding engineers have a sound intuitive approach to welding problems, as more basic data become available, welding engineering will continue to grow into an exact science—that engineering "science of welding" envisioned by Dr. Adams.

References

53. Hayashi, K., Private communication, 1953.

54. Jackson, C. E., and Goodwin, W. J., "Effect of Variations in Welding Technique on the Transition Behavior of Welded Specimens," Part II, THE WELDING JOURNAL, **27** (5), Research Suppl., 234-s to 266-s (1948).

55. Alexander, P., "The Abridgement of the Stability of the Welding Arc," *J. Am. Inst. Elec. Engrs.*, **47**, 109–112, February 1928.

56. Benner, R. H., and Jones, T. B., "Atmospheric Water Vapor Effects on D-C Arc Electrode Burn-Off Rates," THE WELDING JOURNAL, **36** (0), Research Suppl., 263-s to 264-s (1957).

57. Boulton, N. S., and Martin, H. E. L., "Temperature Distribution During Welding," *Proc. Inst. Mech. Engrs.*, **133,** 295–339, 1936.

58. Breymeier, R. T., "Metal Transfer in Sigma Welding," THE WELDING JOURNAL, **31** (5), 393–399 (1952).

59. Busz-Peuckert, G., and Finkelnburg, W., "On Anode Mechanisms of Thermal Argon Arcs," *Z. Physik*, **144,** 244–251, 1956.

60. d'Herbemont, G., "Deep Penetration Welding with Covered Electrodes," *Soudage et Techniques Connexes*, Vol. 12, pp. 15–20, January-February 1958.

61. Fett, G. H., "Cathode Drop of an Arc," *Welding Journal*, Vol. 21, pp. 27s–29s, January 1942.

62. Gaubert, A., "Deep Penetration Welding with Covered Electrodes," *Soudage et Techniques Connexes*, **12,** 5–14, January-February 1958.

63. Gunnert, R., "Penetration and Travel Speed in Metal-Arc Welding," AMERICAN WELDING SOCIETY JOURNAL, **27** (1), 542 (1935).

64. Hazlett, T. H., "Coating Ingredients" Influence on Surface Tension, Arc Stability and Bead Shape," THE WELDING JOURNAL, **36** (1), Research Suppl., 18-s to 22-s (1957).

65. Helmbrecht, W. H., and Oyler, G. W., "Shielding Gases for Inert-Gas Welding," THE WELDING JOURNAL, **36** (10), 969–979 (1957).

66. Hull, W. G., and Needham, J. C., "Self-Adjusting Arc and Controlled-Arc Welding Processes," *Welding Research*, **7,** 80–95, August 1953.

67. Jackson, C. E., and Shrubsall, A. E., "Control of Penetration and Melting Ratio with Welding Technique," THE WELDING JOURNAL, **32** (4), Research Suppl., 172-s to 178-s (1953).

68. Jones, T. B., Kouwenhoven, W. B., and Skolnik, M., "Heat Effects in Anode Spots of High-Current Arcs," *Ibid.*, **28** (10), Research Suppl., 461-s to 465-s (1949).

69. Keller, R. J., and Koss, J., "The Carbon-Dioxide-Shielded Metal-Arc Welding Process," *Ibid.*, **35** (2), 145–151 (1956).

70. Larson, L. J., "Metal Transfer in the Metallic Arc," *Ibid.*, **21** (2), Research Suppl., 107-s to 112-s (1942).

71. Needham, J. C., *The Transfer of Material, Temperature and Stability in the Electric Welding Arc*, British Welding Association Report R27, London, 1946.

72. Needham, J. C., and Smith, A. A., "Arc and Bead Characteristics of the Aluminum Self-Adjusting Arc," *British Welding Journal*, **5,** 66–76, 1958.

73. Orton, L. H., and Needham, J. C., *Microsecond Phenomena in the Steel Welding Arc*, Electrical Research Association Report Z/T79, London, 1949.

74. Paschkis, V., "Establishment of Cooling Curves of Welds by Means of Electrical Analogy," THE WELDING JOURNAL, **22** (10), Research Suppl., 462-s to 483-s (1943).

75. Richter, K. E., and Essig, J. F. M., "Consumable-Electrode Inert-Gas Welding with Small-Diameter Wires," *Ibid.*, **36** (9), 893–899 (1957).

76. Rosenthal, D., and Schmerber, R., "Thermal Study of Arc Welding Experimental Verification of Theoretical Formulas," *Ibid.*, **17** (4), Research Suppl., 2-s to 8-s (1938).

77. Rothschild, G. R., "Carbon-Dioxide-Shielded Consumable-Electrode Arc Welding," *Ibid.*, **35** (1), 19–29 (1956).

78. Spraragen, W., and Claussen, G. E., "Temperature Distribution During Welding, a Review of the Literature to January 1, 1937," *Ibid.*, **16** (9), Research Suppl., 4-s to 10-s (1937).

79. Von Conrady, H., "The Transfer of Material in the Welding Arc," *Elektroschweissung*, **11,** 109–114, 1940.

80. Wienecke, R., "Concerning Physical Processes in Electric Arcs," *Schweissen und Schneiden*, **9,** 428–434, September 1957.

A Request for Corrosion Complaints Involving 316L Weld Metal

Service exposure of Type 316L stainless steel, in the as-welded condition, seems to lead to weld corrosion under a variety of conditions. Too little information has been published to permit prediction of this attack.

The WRC High Alloys Subcommittee investigating this subject are soliciting information about any such experience which the readers of this journal can report. A post card to 1500 S. 50th St., Philadelphia 43, Pa., will initiate the correspondence necessary to explore the conditions under which the weld corrosion occurred.

Effect of Elevated-Temperature Exposure on Heavy-Section Pressure-Vessel Steels

PVRC-sponsored investigation describes the effect of aging at room temperature, 500 and 700° F on the embrittlement of carbon and alloy pressure-vessel steels

BY A. W. PENSE, J. H. GROSS AND R. D. STOUT

ABSTRACT. Previous PVRC investigations have indicated the suitability of high-strength steels for pressure-vessel applications in conventional thicknesses and also in heavy sections, particularly if the heavy sections are spray-quenched and stress-relieved. However, concern has been expressed regarding the effect of extended exposure at elevated temperatures on the mechanical properties of heavy-section pressure-vessel steels in applications such as power boilers and nuclear and chemical reactors.

The present investigation describes the effect of exposure at room temperature, 500, and 700° F for times up to 16,000 hr on the tensile properties and the notch ductility of simulated spray-quenched and normalized heavy-section pressure-vessel steels.

The results of the study indicate that no significant embrittlement (greater than 25° F increase in transition temperature) occurred in any of the steels after aging at room temperature or 500° F for times up to 16,000 hr. After aging at 700° F, certain alloy steels (T-1, HY80, HY65 and A203) exhibited an embrittlement of 40 to 100° F increase in the transition temperature. The maximum embrittlement, which occurred at about 8000 hr at 700° F, appeared to be independent of the condition of the steel—spray-quenched or normalized and stress-relieved or stress-relieved, strained and restress-relieved. After 16,000 hr at 700° F the stress-relieved steels showed the same embrittlement as after 8000 hr, whereas the strained and restress-relieved specimens exhibited a tendency to recover from the maximum embrittlement. The 700° F embrittlement was accompanied by a corresponding increase in the tensile strength.

The results obtained did not suggest a specific mechanism by which the embrittlement occurs. However, only the steels containing nickel were observed to embrittle.

A. W. PENSE, J. H. GROSS and R. D. STOUT are associated with the Department of Metallurgical Engineering, Lehigh University, Bethlehem, Pa.

Paper presented at AWS 41st Annual Meeting held in Los Angeles, Calif., April 25–29, 1960.

Introduction

During the past ten years, the Pressure Vessel Research Committee has sponsored investigations to determine the suitability of high-strength steels for pressure-vessel construction. The interest in high-strength steels stems from the increased pressure and temperature requirements for modern pressure-vessel applications and the problems encountered in meeting these requirements with conventional carbon-steel plate materials. Initial studies[1, 2, 3] on selected $^3/_4$- and 1-in. thick high-strength steels indicated that the plastic fatigue strength, room and elevated-temperature tensile strength and notch toughness were superior to the corresponding properties of the carbon steels, and that the ductility and weldability were only slightly reduced. Similar results were also obtained in a comparison[4] of 4-in. thick carbon- and high-strength steels. A subsequent investigation[5] indicated that a further improvement in mechanical properties of the 4-in. thick high-strength steels was obtained by accelerated cooling—spray quenching—providing a stress-relieving treatment followed the spray quenching. The most recent study[6] showed that the spray-quenched steels exhibited about the same susceptibility to embrittlement from cold-forming, cold-forming and aging and extended stress-relieving as the conventionally treated steels. Thus, the superiority of the spray-quenched steels should be retained after normal fabrication operations.

The preceding studies demonstrated the general suitability of high-strength steels, spray-quenched and conventionally treated, for ambient-temperature pressure-vessel applications. However, boilers, chemical pressure vessels and nuclear-reaction pressure vessels commonly operate at elevated temperatures for extended periods of time. At present, little or no information is available on the effect of extended elevated-temperature exposure on the mechanical properties of heavy-section steels, particularly on heavy-section high-strength steels in the spray-quenched condition. Of particular interest are changes in the tensile properties that might affect continued operation at elevated temperatures and changes in notch toughness that may influence safety during shut-down operations. The present investigation extends the available information on extended exposure at room temperature, 500 and 700° F on the tensile properties and notch ductility of these steels in the spray-quenched and in the normalized condition.

Experimental Procedure

The experimental procedure consisted of exposing two carbon steels (A285 and A212) and seven alloy high-strength steels (48s5, A302, A203, HY65, A387, HY80, and T-1) to elevated temperatures of 500 and 700° F for periods of 2000, 8000, and 16,000 hr. The steels were exposed as $^1/_2$-in. thick plates which were either oil quenched (to simulate the microstructure near the surface of a spray-quenched 4-in. thick plate) and stress relieved at the recommended stress-relieving temperatures, or were cooled in a foil-lined box (to simulate the microstructure of a normalized 4-in. thick plate) and stress relieved. Addi-

Table 1—Chemical Analysis (%) and Heat-treating Temperatures

Steel	Grade[a]	C	Mn	P	S	Si	Ni	Cr	Mo	V	Ti	Cu	B	Austenitizing temperature, ° F	Stress relief or tempering temperature, ° F
ASTM A285	C	0.20	0.53	0.020	0.016	...	...	...	...	...	...	...	...	1650	1150
48s5	HT	0.15	1.09	0.033	0.028	0.18	...	...	...	0.09	0.009	...	...	1650	1150
ASTM A212	B	0.28	0.70	0.010	0.021	0.24	...	...	...	...	...	...	...	1650	1150
ASTM A203	D	0.15	0.64	0.010	0.026	0.22	3.64	...	...	...	...	...	...	1650	1150
HY 65		0.12	0.48	0.013	0.032	0.21	2.16	...	0.39	...	...	0.70	...	1750	1200
ASTM A302	B	0.20	1.32	0.022	0.030	0.25	...	...	0.42	...	...	...	...	1650	1150
ASTM A387	D	0.09	0.44	0.013	0.011	0.25	...	2.18	0.96	...	...	...	...	1700	1350
T-1		0.15	0.93	0.015	0.022	0.27	0.89	0.48	0.44	0.06	...	...	0.0031	1700	1200
HY 80	High	0.15	0.28	0.016	0.015	0.19	2.86	1.72	0.50	...	...	...	...	1650	1150

[a] All steels were firebox quality where applicable.

tional specimens of all steels in the same two base conditions were strained 5% after heat treatment, restress relieved and then exposed at 500 and 700° F. Specimens of each steel were also prepared in the base conditions, strained 5% and exposed at room temperature for 1, 13, 26, 52 and 104 weeks (168, 2184, 4368, 8736 and 17,472 hr).

Following exposure, the tensile properties and notch ductility of the steels were evaluated. Standard 0.252 - inch - diameter tension - test specimens cut parallel to the rolling direction of the plate and Charpy V-notch impact specimens cut parallel to the rolling direction and notched transversely to the surface of the plate were prepared from each test plate. The chemical composition and the temperatures of heat treatment for each steel are given in Table 1.

Experimental Results and Discussion

The tensile properties—yield and tensile strength, elongation and reduction of area—and the impact properties—transition temperature based on 15 ft-lb, 15 mil and 50% fibrous fracture—for the nine steels in their various conditions of prolonged exposure at room temperature, 500 and 700° F are presented in complete tabular form in WRC Reports of Progress, June issue. To allow a convenient comparison of the effect of the aging treatments on the nine steels, the impact properties and selected tensile properties are presented graphically in Figs. 1 through 8.

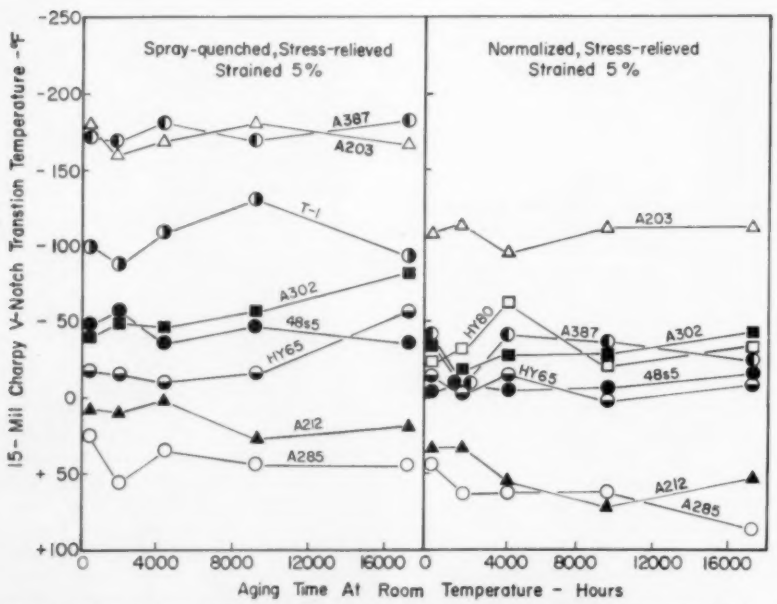

Fig. 1—Effect of room-temperature aging on the notch toughness of spray-quenched and normalized pressure-vessel steels after 5% plastic strain

Figure 1 shows the transition temperatures of the spray-quenched and stress-relieved and the normalized and stress-relieved steels after 5% plastic strain and aging at room temperature for periods of one week to two years. The results indicate that there is little or no tendency for these steels to strain age at room temperature for times up to two years. Since the spray-quenched as well as the normalized steels were insensitive to the room-temperature aging treatment, any initial superiority in notch ductility for the spray-quenched steels was retained after the aging treatment.

The effect of aging at 500° F for times up to 16,000 hr on the notch ductility of the normalized and stress-relieved steels is presented in Fig. 2. Also shown is the effect of the 500° F aging on the steels in the stress-relieved, strained 5% and restress-relieved condition. For the most part, the changes in transition temperature after the various aging times are within 25° F of the value prior to aging. The observed changes in notch toughness are not considered significant since they are typical of the scatter commonly encountered in transition-temperature determinations. Figure 3 illustrates the effect of the 500° F aging treatment on the notch ductility of the spray-quenched steels. The results are similar to those presented in Fig. 2 and confirm the observation that these steels in the stress-relieved condition or in the stress-relieved, strained and restress-relieved condition are not significantly embrittled by exposure at 500° F for times up to 16,000 hr (approximately two years).

After aging at 700° F, the carbon steels and certain of the alloy steels (48s5, A302 and A387) again exhibited no significant susceptibility to embrittlement as illustrated in

Figs. 4 and 5 for the same conditions as the 500° aging. However, the other alloy steels (HY65, T-1, HY80 and A203) showed a substantial embrittlement in all conditions—spray-quenched or normalized and stress-relieved or stress-relieved, strained and restress-relieved. In general, the steels in all conditions exhibited significant embrittlement after 2000 hr at 700° F and reached a maximum by 8000 hr at 700° F. Although the maximum embrittlement varied for the four steels (40 to 100° F increase in the 15-mil Charpy V-notch transition temperature) the condition of the steel had no appreciable effect on the general pattern of embrittlement or the maximum embrittlement. One exception to this observation is the tendency for the stress-relieved, strained and restress-relieved material to recover some notch ductility between 8000 and 16,000 hr, whereas the stress-relieved material exhibited about the same embrittlement after 8000 and 16,000 hr at 700° F.

Figure 6 reveals that the increase in transition temperature for the four embrittled steels was accompanied by a proportionate increase in the tensile strength. Examination of the data obtained also shows that the yield strength increased and the elongation and reduction of area decreased as the embrittlement at 700° F increased. The increase in tensile strength with embrittlement is great enough so that the embrittlement could probably be detected by hardness measurements. This behavior is interesting because many embrittling phenomena cannot be detected readily by changes in tensile properties.

In spite of the embrittlement observed in four of the alloy steels, all of the alloy steels, except HY65, exhibited better notch toughness than the carbon steels in all conditions including exposure at 700° F. This behavior is illustrated in Fig. 7 for the stress-relieved condition and in Fig. 8 for the stress-relieved, strained and restress-relieved condition. These graphs again show that the maximum embrittlement (cross-hatched part) after aging at 700° F varies with the steels but is essentially independent of the treatment imposed upon the steels.

The results obtained to date have not indicated any specific mechanism by which the embrittlement occurs. Limited additional studies at higher aging temperatures suggest that the 700° F embrittlement may be an extension of temper embrittlement to lower temperatures. Although embrittlement has been reported in fully hardened alloy steels of the type studied in this program but usually at higher carbon contents, Jaffe's interpretive report[7] indicates that essentially no information is available on time-temperature embrittlement of pressure-vessel steels, particularly in the unhardened condition. Examination of the chemical composition of the four alloy steels that exhibited embrittlement after aging at 700° F reveals that nickel is the only element common to these four steels and not present in the other five steels. The role that nickel may play, if any, in the observed embrittlement is not clear. For example,

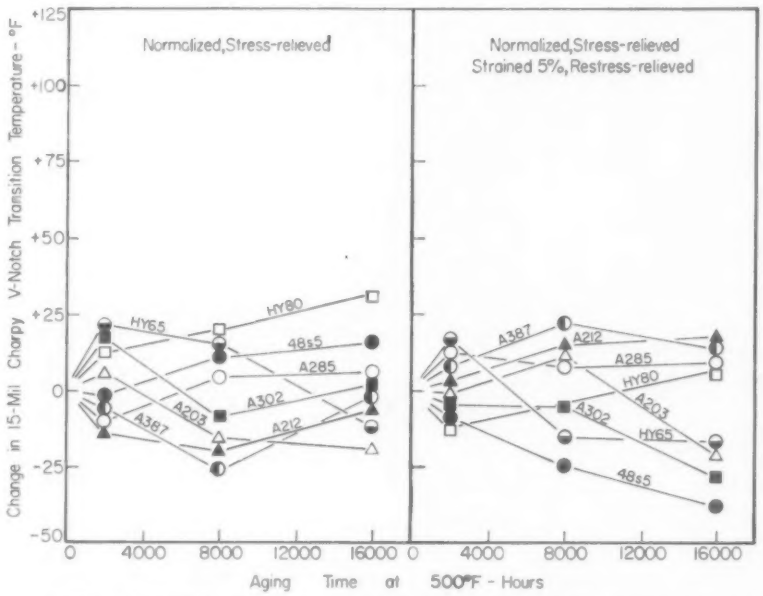

Fig. 2—Effect of aging at 500° F on the notch toughness of normalized pressure-vessel steels in the stress-relieved conditions and in the stress-relieved, strained and restress-relieved condition

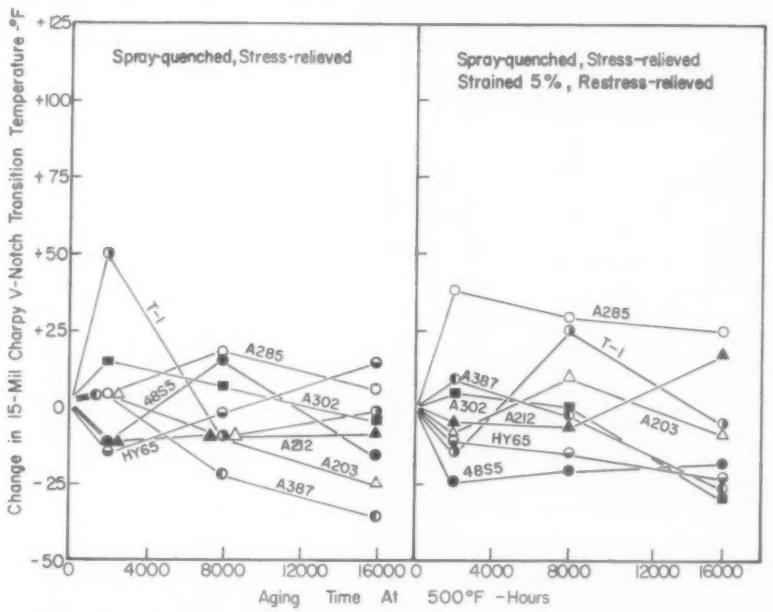

Fig. 3—Effect of aging at 500° F on the notch toughness of spray-quenched pressure-vessel steels in the stress-relieved condition and in the stress-relieved, strained and restress-relieved condition

the nonnickel-bearing steels may exhibit embrittlement at a slightly higher aging temperature. Thus, the effect of nickel could be related to a lowering of the embrittling temperature in the same way nickel lowers the critical temperature. This and similar approaches to the cause and elimination of the observed embrittlement are currently under study.

Summary

The results of the present investigation on the effect of aging at room temperature, 500 and 700° F on the embrittlement of carbon and alloy pressure-vessel steels may be summarized as follows:

1. Effect of temperature and time.
   (*a*) Prolonged aging at room temperature after straining resulted in no additional embrittlement.
   (*b*) Exposure at 500° F for times up to 16,000 hr produced no significant embrittlement for any of the steels in any condition.
   (*c*) Exposure at 700° F resulted in embrittlement as great as 100° F increase in transition temperature for certain alloy steels.
   (*d*) At 700° F the maximum embrittlement occurred at about 8000-hr exposure. Beyond 8000-hr exposure no additional embrittlement was observed and the strained and restress-relieved condition tended to recover.
2. Effect of heat treatment and cold work.
   (*a*) After stress relieving, the spray-quenched steels exhibited about the same sensitivity to embrittlement as the normalized steels. Therefore, any initial superiority in notch toughness for the spray-quenched steels over the normalized steels was retained after exposure.
   (*b*) The maximum embrittlement at 700° F exhibited by steels in the strained and restress-relieved condition was essentially the same as in the stress-relieved condition. However, steels in the strained and restress-relieved condition showed a greater tendency to recover from the embrittlement.
3. Effect of steel composition.
   (*a*) The carbon steels and certain alloy steels were not significantly embrittled by any of the exposure treatments.
   (*b*) Only the alloy steels containing nickel exhibited embrittlement greater than 30° F increase in the transition temperature.

The embrittlement of the alloy steels at 700° F was accompanied by a proportional increase in the tensile strength.

The specific mechanism of embrittlement that resulted from aging at 700° F was not established. However, limited additional studies indicate a similarity to temper embrittlement.

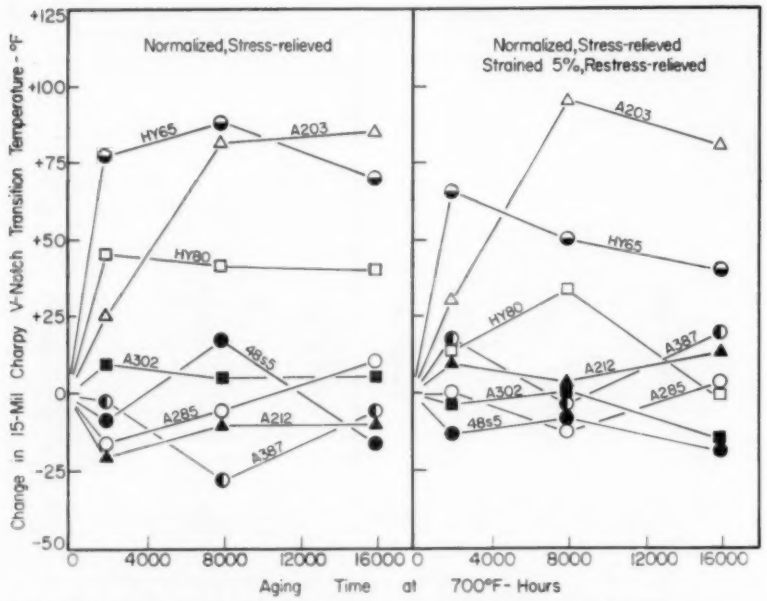

Fig. 4—Effect of aging at 700° F on the notch toughness of normalized pressure-vessel steels in the stress-relieved condition and in the stress-relieved, strained and restress-relieved condition

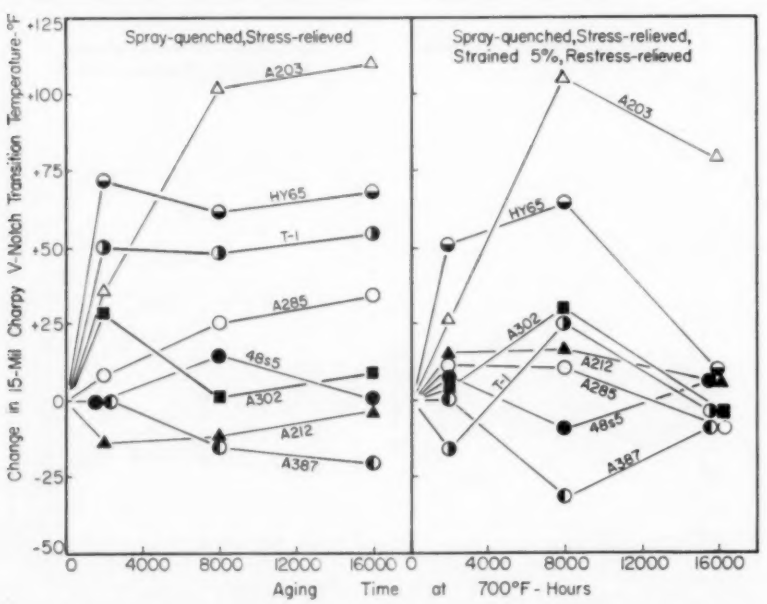

Fig. 5—Effect of aging at 700° F on the notch toughness of spray-quenched pressure-vessel steels in the stress-relieved condition and in stress-relieved, strained and restress-relieved condition

Acknowledgment

The investigation reported herein was sponsored by the Materials

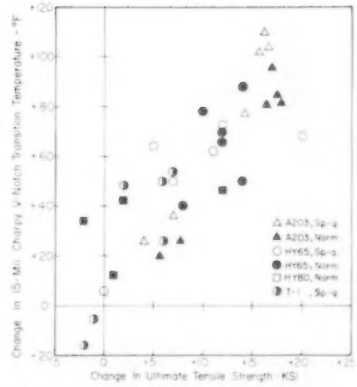

Fig. 6—Increase in tensile strength accompanying 700° F embrittlement of certain pressure-vessel steels

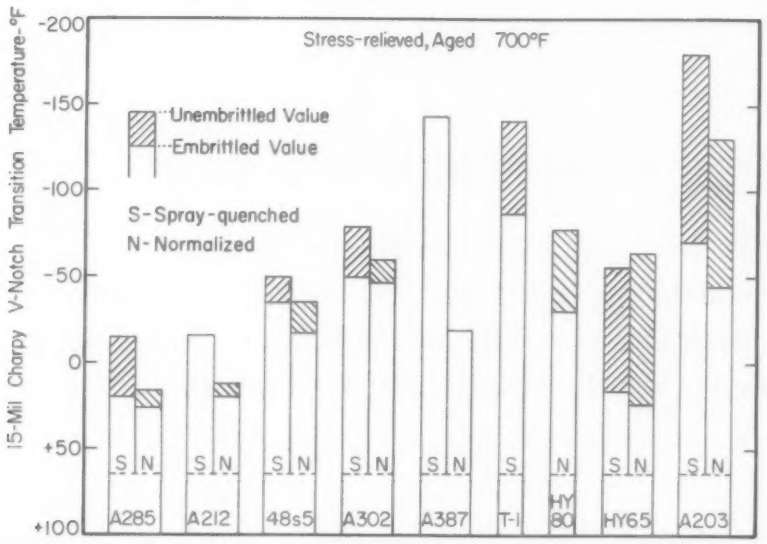

Fig. 7—Maximum embrittlement exhibited by spray-quenched and normalized pressure-vessel steels in the stress-relieved condition after aging at 700° F

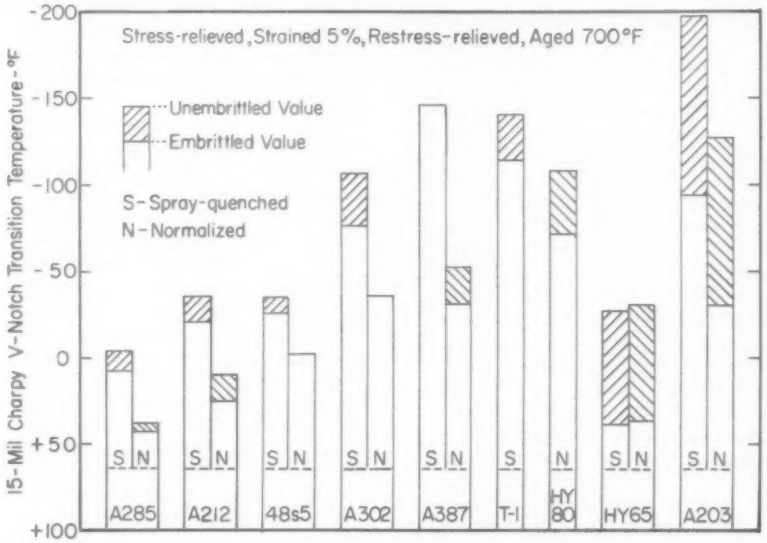

Fig. 8—Maximum embrittlement exhibited by spray-quenched and normalized pressure-vessel steels in the stress-relieved, strained and restress-relieved condition after aging at 700° F

Division of the Pressure Vessel Research Committee and guided by the Subcommittee on Research on High-Strength Steels, F. Eberle, Chairman. The authors are indebted to PVRC for support of the investigation and to the subcommittee for direction and encouragement.

References

1. Gross, J. H., and Stout, R. D., "The Performance of High-Strength Pressure-Vessel Steels," THE WELDING JOURNAL **35** (3), Research Suppl., 115-s to 119-s (1956).

2. Bunk, A. P., "Welding Procedure Qualification Tests for Six High-Yield-Strength Steels," *Ibid.*, **34** (4), Research Suppl., 197-s to 206-s (1955).

3. Kooistra, L. F., "Effect of Plastic Fatigue on Pressure-Vessel Materials and Design," *Ibid.*, **36** (3), Research Suppl., 121-s to 130-s (1957).

4. Gross, J. H., and Stout, R. D., "Properties and Weldability of High-Strength Pressure-Vessel Steels in Heavy Sections," *Ibid.*, **36** (3), Research Suppl., 157-s to 167-s (1957).

5. Gross, J. H., Kottcamp, E. H., and Stout, R. D., "Effect of Heat Treatment on the Microstructure and Low-Temperature Properties of Pressure-Vessel Steels," *Ibid.*, **37** (4), Research Suppl., 160-s to 168-s (1958).

6. Rubin, A. I., Gross, J. H., and Stout, R. D., "Effect of Heat Treatment and Fabrication on Heavy-Section Pressure-Vessel Steels," *Ibid.*, **38** (4), Research Suppl., 182-s to 187-s (1959).

7. Jaffe, L. D., "Temper Brittleness of Pressure-Vessel Steels," *Ibid.*, **34** (3), Research Suppl., 141-s to 150-s (1955).

INSTRUCTIONS FOR PROSPECTIVE AUTHORS

Authors who plan to submit papers for publication in the WELDING JOURNAL are invited to send for a free copy of the booklet "Instructions and Suggestions for Authors." All requests should be addressed to Editor, WELDING JOURNAL, American Welding Society, 33 W. 39th St., New York 18, N. Y.

Weld Metals in Nickel-Base Alloys

Laboratory investigation indicates that sound welds in these alloys tend to have good strength, ductility and toughness at normal and low temperatures. Best results are secured from argon-shielded Ni-Cr-Fe-Cb type welds

BY J. HEUSCHKEL

Introduction

Nickel-base alloy structures are being fabricated by welding, although such alloys were not originally designed for that specific mode of joining. The resulting products are widely used in industry for corrosion-resistant and elevated-temperature applications. Some porosity or cracking may occur during the welding operations.[1-3] The welds contain from 64 to 97% nickel; that is, pure-nickel weld metals are not used commercially. All but the Ni-Ti type alloy compositions are nonmagnetic. No suitable published data exist on the elevated-temperature properties of these weld metals to serve as a guide in defining the regions wherein they are weak and/or brittle.

Within the nuclear-power industry there has been a recent tendency to shift, or to consider shifting, from the use of AISI 300 austenitic stainless steels to such nickel-base alloys as the Ni-Cr-Fe type, largely because of expected improved resistance to stress-corrosion cracking. Following the marginal difficulties already experienced in the welding of some of the AISI 300 series of commercially available austenitic stainless steels,[4-6] it is appropriate that the temperature effects on the properties of sound, nickel-base alloy weld metals be firmly established. Such information provides a basis for judging the susceptibility to hot cracking during welding, subsequent heat treatments and service. It also provides further perspective on the general problem of hot brittleness in metals. Accordingly, tests were conducted on all-weld-metal tensile specimens in the as-deposited condition, made with existing nickel-titanium, nickel-chromium-iron-columbium, nickel-chromium-iron-titanium and nickel-copper type electrodes.

The deposits contain nickel, chromium, iron, copper, titanium, columbium (= niobium), tantalum, manganese, silicon, molybdenum, carbon and/or aluminum.[1-3] Sound welds, in these alloys, tend to have good strength, ductility and toughness at normal and low temperatures. They also tend to have low ductility, as little as 4% total elongation, across a several-hundred-degree temperature range, which varies with alloy type, from 1200 to 2200° F. In these alloy systems, the conditions are once more encountered where marginal success in welding operations may be experienced because of the inherent characteristics of the metals. Knowing these characteristics, however, permits a more rational approach to the selection of composition limits, joint designs, welding procedures and heat treatments for particular service conditions. Best results were secured from argon-shielded Ni-Cr-Fe-Cb type welds, where a minimum total elongation of 34% was secured.

Experimental Objectives

The tests described were conducted to provide basic technical and engineering information on the compositions, short-time tensile properties, microstructures and hardnesses of as-deposited weld metals, and to observe how those properties are altered by temperature. It is recognized that designers need other information but as a guide for recommendations in welded applications, it was first necessary to determine if brittle ranges exist and, if so, to define those ranges.

Except for welds in the Ni-Cr-Fe-Ti type alloy, conventional 25-degree included-angle, U-grooved, unrestrained, flat butt joints were made, double thickness bars being used as an expedient because the 5/8-in. thick stock desired was not readily available. Ni-Cr-Fe-Ti type alloy flats were not available in any thickness and longitudinally U-grooved pipe was used for making these welds. Test welds in this case were, therefore, subject to more restraint during initial cool-down than those in the other alloy systems. Ten welds were made (see Figs. 1 to 10). Two others, not being reported in detail, involved dissimilar-metal combinations, a Ni-Cr-Fe alloy welded to plain-carbon steel, but, in general, the base metal was of the same composition type as the electrode. Both argon and covered-electrode shielded arcs were used. Tensile specimens 0.357 in. in diam were prepared with their longitudinal axes coincident with the longitudinal axes of the welds. Chemical analyses were secured from the ruptured shanks of these specimens. In no case was the weld-metal sulfur content more than 0.009%, or the phosphorus content over 0.007%. The cobalt contents were less than 0.05%.

Chemistry of Arc Transfer of Metal

Argon-shielded Arcs

Five bare-wire electrode welds were made with the argon-shielded arc (see Figs. 1, 3, 6 and 10). Data were secured to provide a back-

J. HEUSCHKEL is Consulting Welding Engineer, Westinghouse Research Laboratories, Pittsburgh 35, Pa.

Paper presented at the AWS National Fall Meeting held in Detroit, Mich., Sept. 28–Oct. 1, 1959.

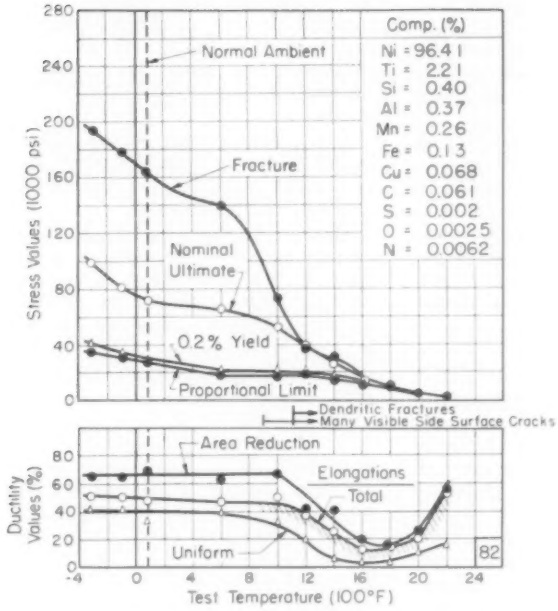

Fig. 1—Temperature-stress-ductility relations for Ni-Ti type welds (argon shielded)

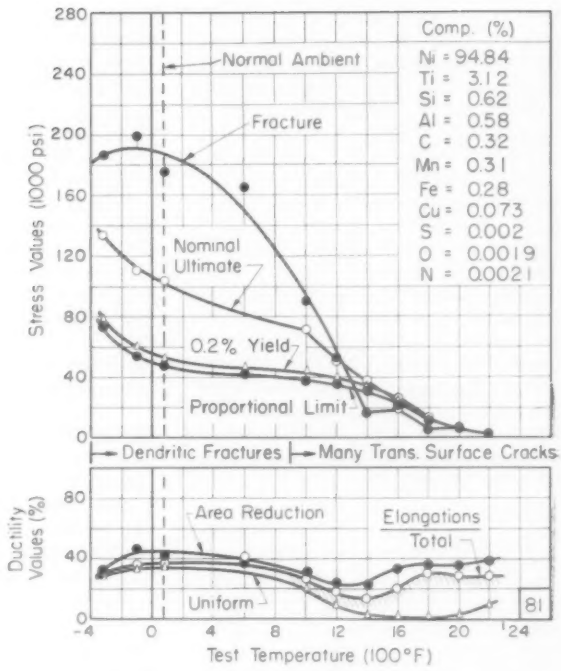

Fig. 2—Temperature-stress-ductility relations for Ni-Ti type welds (covered-electrode shielded)

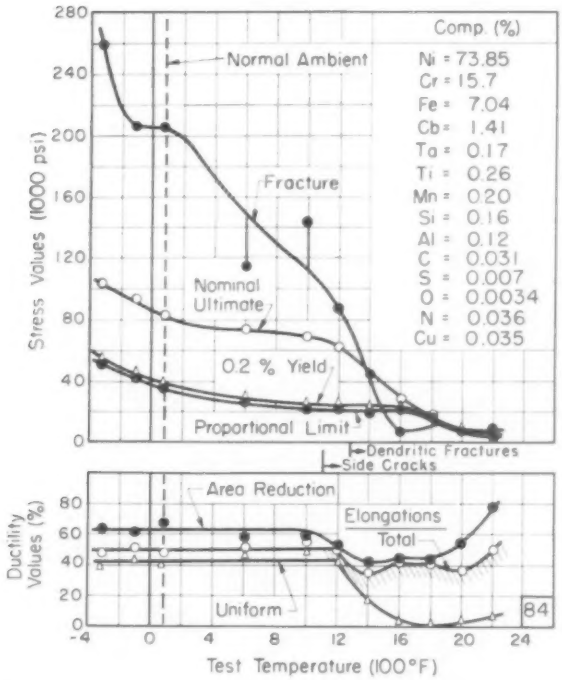

Fig. 3—Temperature-stress-ductility relations for Ni-Cr-Fe-Cb type welds (argon shielded)

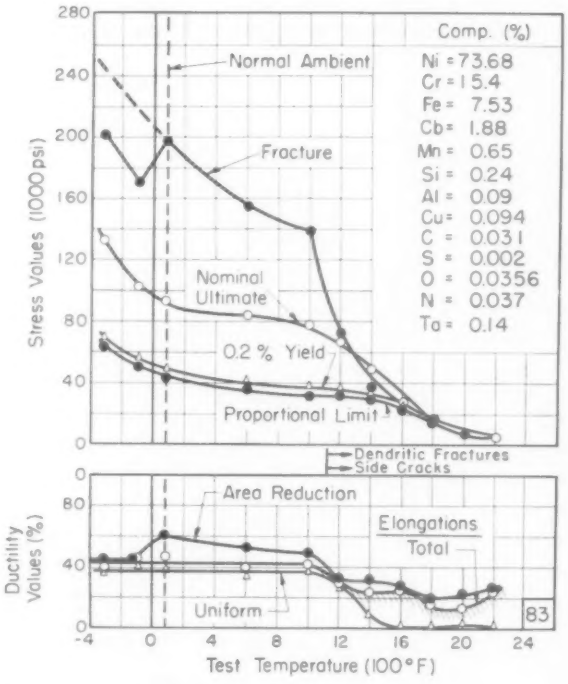

Fig. 4—Temperature-stress-ductility relations for Ni-Cr-Fe-Cb type welds (covered-electrode shielded)

ground for evaluating the amount of each element lost in the gross transfer of metal across the arc where the argon envelope is surrounded by air. This is the normal production condition.

The nickel mass is the same, relatively, in the weld deposit as in the wire; i.e., the weight loss suffered from oxidization, evaporation and spatter of molten globules does not alter the total percentage of nickel.

If the ratio of the alloying element present in the weld, in weight percent, to the corresponding amount originally present in the wire is called the arc transfer ratio, the lowest value of that ratio, for the several more prominent elements in the argon-shielded nickel-base alloy arc welds, is:

Iron	0.98
Chromium	0.96
Manganese	0.95
Carbon	0.95
Titanium	0.82
Silicon	0.81
Aluminum	0.79
Columbium	0.78
Tantalum	0.65

The lower the order in which an element appears on this list, the more effective it is as a deoxidizer, or the more susceptible it is to evaporation.

Because of the losses of other elements, there is a slight relative gain in copper content in the Ni-Cu type weld metals over the percentage present in the bare wire.

There is no general increase in nitrogen and oxygen contents, indicating that efficient arc shielding is obtained.

When joining base metals of similar composition with the argon-shielded process, if that composition is to be maintained, all of the alloying elements desired in the deposited weld metal must be present in the wire in an amount inversely proportional to the ratios listed in the above tabulation.

Covered Electrodes

The electrode coverings contain Ca, Na, or Na_3Al fluorides. Adequate ventilation should be provided when using these materials. In this respect, they are no different from the stainless steels.

Oxides of Ti, Al, Si, Mg, Mo, Cr and/or Ca, ferroalloys, organic materials and binders are also present in the coverings. Only two of the electrode coverings contain more than 10% of organic materials. Transfer of alloying elements across the covered-electrode arc is a complex phenomenon. All, part, or none of the alloying element found in the weld may come from the wire; the other source is the covering.

Chromium and copper, where used, are added through the core wire, the average transfer ratio being 0.95 for chromium. Some copper in the Ni-Cu type alloys is brought over from the electrode covering as impurities in the ferroalloys.

Iron, where used as an alloy, comes basically from the core wire, but some is added via the ferroalloys in the covering.

Carbon, manganese and silicon are usually higher in the weld deposit than in the core wire, indicating that all three elements are present in the electrode coverings in significant amounts.

Aluminum is transferred from the core wire, but the transfer ratio is only about 0.51.

Titanium is transferred from the core wire in full amount, partly because enough is placed in the covering to compensate for transfer losses. This contrasts with the circulated opinion of the manufacturers of covered stainless-steel electrodes, who claim that titanium cannot be effectively transferred across the covered-electrode arc.

There is little difference between the oxygen, nitrogen, phosphorus and sulfur contents of the welds; all are low. The low oxygen contents of the nickel-base alloy weld metals are partially related to the

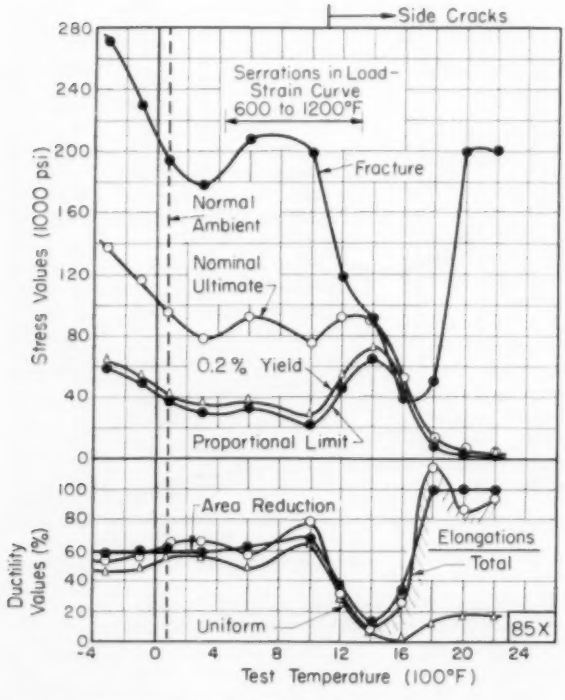

Fig. 5—Temperature-stress-ductility relations for annealed Ni-Cr-Fe-Ti type base metal

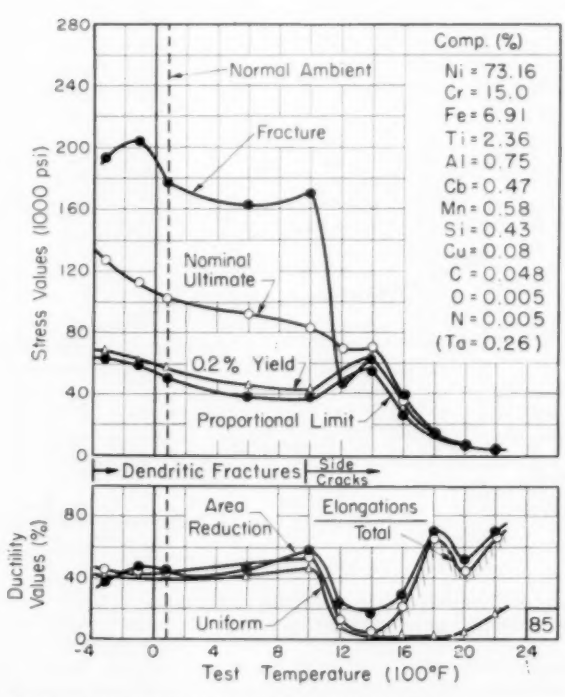

Fig. 6—Temperature-stress-ductility relations for Ni-Cr-Fe-Ti type weld metal (argon shielded)

high amounts of deoxidizers present in the electrode wires as alloys, and in the coverings as ferroalloys or metallic powders.

Temperature Dependence of Tensile Properties

Tensile tests on 0.357-in. diam unnotched tensile specimens, cut from the center of the welds, were made at a 750% per hour constant strain rate across a temperature range from −320 to +2200° F for all but three of the welds. One series was tested down to −452° F. The other two exceptions were not tested below room temperature. Load-strain curves to rupture were recorded automatically in every case.

The temperature dependence of the short-time tensile strength and ductility of the as-deposited weld-metal specimens are shown graphically in Figs. 1 to 10 inclusive.

Basically, these welds show about the same temperature response as was found previously for welds in the AISI 300 series stainless steels.[5-7] With few exceptions, as temperature decreases below normal ambients down to liquid-nitrogen levels, −320° F, there is little or no change in ductility. There is a slight (39%) rise in the proportional limit and yield stresses, a modest (33%) increase in tensile strength and from zero to a substantial (74%) increase in fracture stress. These are, in general, good metals for low-temperature service. Of the several compositions, the Ni-Cu type is best for very low temperatures. But significant decreases in ductility were found in most of the elevated-temperature tests. Also, welds in the Ni-Cr-Fe-Ti compositions showed a sharp increase in yield strength at, or near, 1400° F, with corresponding losses in ductility (see Figs. 5 and 6).

The detailed response secured from the twelve welds tested was:

Ni-Ti Type Weld, Argon Shielded

The argon-shielded Ni-Ti type alloy weld metal, with Si-Al-Mn present in more than trivial amounts, has subambient-temperature tensile properties characteristic of f.c.c. metals, Fig. 1. It is dendritic and large-grained, with normal orientation, but is characterized by the presence of many small particles both within the grain matrix and at the grain boundaries. The larger particles are about 0.0001 in. in actual diameter. For a commercially available product, the phosphorus, sulfur, oxygen and nitrogen contents are low.

As temperatures decrease from the ambient down to −320° F, the yield strength rises 37%, the nominal ultimate strength rises 39%, and the fracture strength rises 18%. There is no decrease in ductility down to −320° F.

As temperature rises from the ambient to 600° F, the strength drops slightly. Also, up to that temperature, the ductility, as measured by elongation to reach maximum load (uniform elongation), total elongation to rupture, and area reduction at fracture, are all about constant; the average values being 38.6, 47.6 and 64.2% respectively. Between +600 and −320° F, all of the ruptured specimens exhibit a mottled side surface appearance (see Fig. 11), and at × 30 magnification with the binocular microscope under strong light there were no visible evidences of side surface cracks.

At 1000° F, the fracture strength has dropped to slightly less than 50% of the room-temperature value and, for all temperatures above 1000° F, the fractures are no longer of the 45 deg "satin" to "unglazed porcelain" type, but are instead of the separated dendritic reed type (see Fig. 12). Full ductility is maintained up to 1000° F (see Fig. 1).

Above 1200° F, up to the maximum of 2200° F tested, all strength values progressively approach zero,

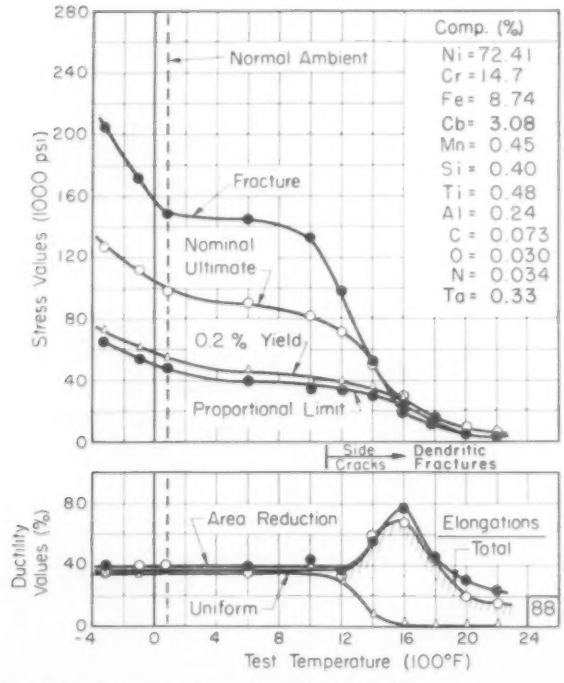

Fig. 7—Temperature-stress-ductility relations for Ni-Cr-Fe-Cb type weld metal (covered-electrode shielded)

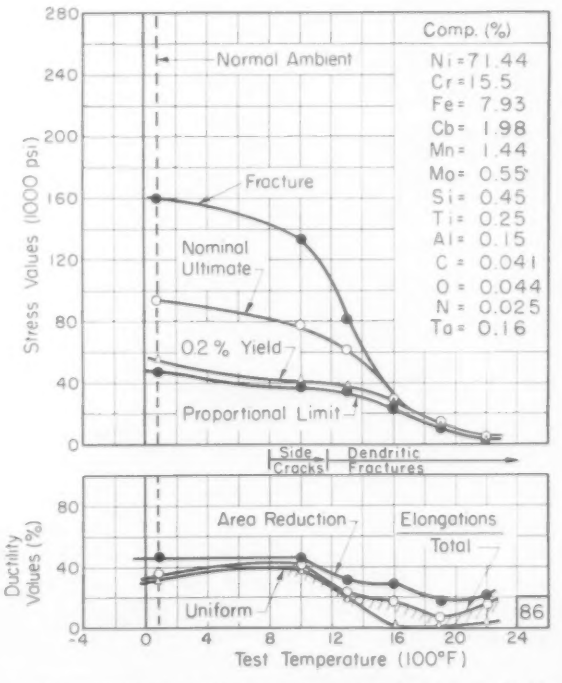

Fig. 8—Temperature-stress-ductility relations for Ni-Cr-Fe-Cb-Mn type weld metal (covered-electrode shielded)

which would be expected for pure nickel to be at about 2650° F. For the 2.2% Ti nickel alloy, this zero-strength level is expected at a slightly lower temperature.

Minimum ductility is reached between 1500 and 1900° F. All specimens tested at and above 1000° F exhibit numerous side cracks (see Fig. 11), and the final fracture is simply the one region where the most and largest of such cracks converged into a common schism. The total elongation values obtained above 1000° F may be misleadingly high because they include the sum of all crack widths. For this reason the "total-elongation" curves are hatched for those temperature ranges across which such side cracks were observed on the finally ruptured specimens.

Above 1800° F, all of the ductility indices rise to reveal the characteristic presence of the temperature-ductility dip previously described for similar deposits in austenitic Cr-Ni steel weld metals.[5] There are reasons to believe that this is associated with internal microstructural changes in these metals. The as-deposited hot-brittleness problem in austenitic steels is therefore not circumvented by the lone expedient of changing from Fe-Cr-Ni steels to a f.c.c. Ni-Ti alloy, even when used with argon shielding under ideal laboratory conditions.

Ni-Ti Type Weld, Covered-electrode Shielded

The companion weld, deposited with covered electrodes (see Fig. 2), reflects more than a change in arc shielding. The argon-shielded weld was made in three layers; the covered-electrode weld in nine beads. The microstructure is correspondingly finer but the basic dendritic grains are still "large." The covered-electrode weld also contains more Ti (+0.91%), C (+0.26), Si (+0.22), Al (+0.21) and Mn (+0.05) than the argon-shielded deposit. The P, S, O, and N contents of this weld were low.

The stress-temperature relations are roughly the same as for the argon-shielded weld, but the welds are generally stronger at any selected temperature, probably because of the higher alloy contents. A less-pronounced ductility dip exists, and its location is shifted down to between 1200 and 1600° F, probably because of the higher titanium content. The ductility is less across most of the temperature range, but it is more ductile within the 1600 to 2100° F range. At −320° F, the ductility, by all criteria, was decreasing.

The specimen appearances were about the same, except that the fracture surfaces revealed the dendritic structure at *all* test temperatures. Side surface cracks, on the ruptured specimens, were visible only for tests made at and above 1000° F.

Except within the 1600–2100° F range, the ductility of the argon-shielded weld is superior to the covered-electrode one, but, in general, the covered-electrode weld is stronger. If it is assumed that, on the first cool-down of the weld metal, the same strength-ductility relations exist at each temperature as is shown by the test specimens, the prevailing fracture strength-elongation relations during that cool-down would be as shown in Fig. 13. As the temperature falls below 2200° F, the fracture strength rises (reading Figs. 1 and 2 from right to left) and, when the ductility also rises, the potential for cracking is lower. But, when ductility falls disproportionately with increasing strength as the temperature is lowered, one can expect cracking in the presence of adequate local strain. Note that strain hardening does not occur at these high temperatures and maximum resistance to loading occurs at strains of about 1% in an unnotched specimen. With the argon-shielded welds, one could anticipate that cracking would be most likely to occur at 1600° F under restrained notched conditions, and between 1300 and 1600° F with the covered-electrode weld under similar conditions. As both

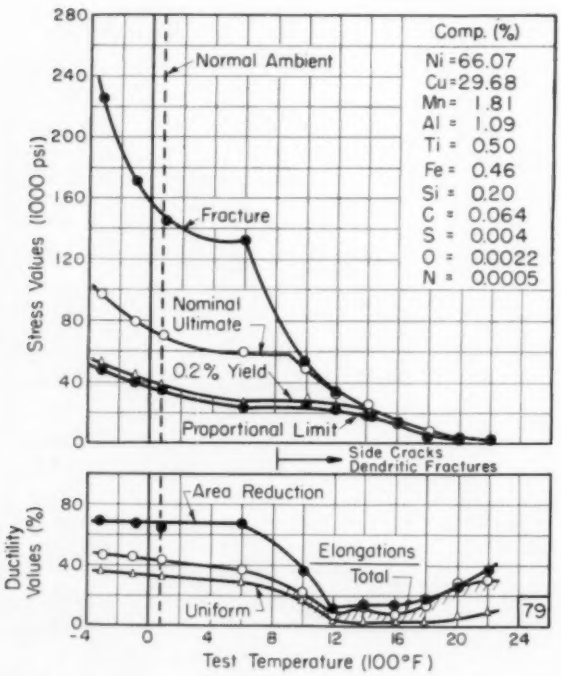

Fig. 9—Temperature-strength-ductility relations for Ni-Cu type weld metal (covered-electrode shielded)

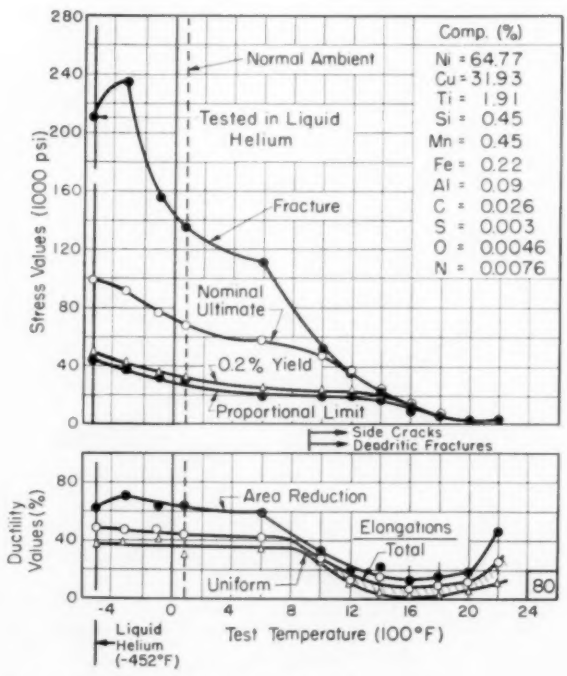

Fig. 10—Temperature-stress-ductility relations for Ni-Cu type weld metal (argon shielded)

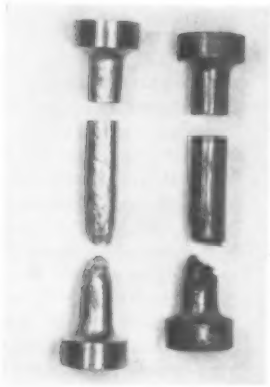
←Cut for hardness readings
←Tensile fracture
Typical of
800° F to −320° F
(Mottled flowed surface with no detectable cracks at X 30)
Typical of
>1000° F
(Smooth surface with from few to many surface fissures)

Fig. 11—Typical appearance of ruptured specimens

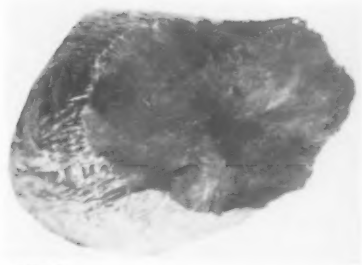

<800° F

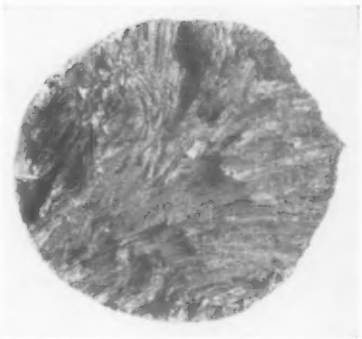

>1000° F

Fig. 12—Typical fractures

strength and ductility rise, with further decreasing temperatures, the capacity of the metal to absorb energy increases and cracking is not expected to occur in these metals.

Ni-Cr-Fe-Cb Type Weld, Argon Shielded

The yield strength vs. temperature relations for the argon-shielded Ni-Cr-Fe-Cb type weld metal (see Fig. 3), are again typical of f.c.c. metals. These include the low rise in yield strength at the suppressed temperatures, down to −320° F, and the gradually drooping shelf that extends as temperature increases above the ambient, in this case, up to 1600° F. Above 1600° F, the yield strengths decrease rapidly with increased temperatures.

The ultimate strength vs. temperature curve is almost parallel to the yield-stress curve except that the fall-off on rising temperature begins at 1100° F. The fracture stress starts deteriorating at some temperature near 1000° F.

The ductility of this metal is excellent from −320° F up to, and including, 1200° F. There is a slight dip in ductility between 1200 and 2000° F, but it is not severe; at its lowest, the elongation is 34.3% and the area reduction is 41.5%, both at 1400° F. Strain hardening occurs up to, and including, 1200° F, but decreases rapidly above that temperature to a low amount at and above 1800° F.

Random transverse cracking occurred on straining above the ultimate load (uniform elongation) value for all temperatures above 1000° F and fractures show the irregular dendritic reed type for all temperatures over 1200° F.

A feathery dendritic × 10 macrostructure reveals sharply delineated grain boundaries at × 100 and × 1000 magnifications with secondary constituents distributed throughout the grains.*

Ni-Cr-Fe-Cb Type Weld, Covered Electrode

The covered-electrode Ni-Cr-Fe-Cb type weld metal has the same general characteristics as the argon-shielded one, with which it is almost identical chemically, but the ductility is inferior across the entire temperature range (see Fig. 4). The low-ductility point, 13.1% total

* These structures are not reproduced in this paper to keep length within reasonable limit.

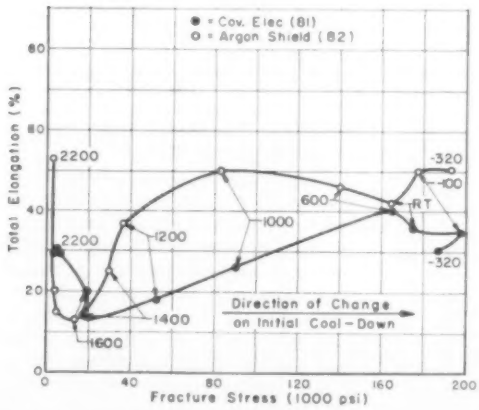

Fig. 13—Relation between fracture stress and elongation for Ni-Ti type weld metals

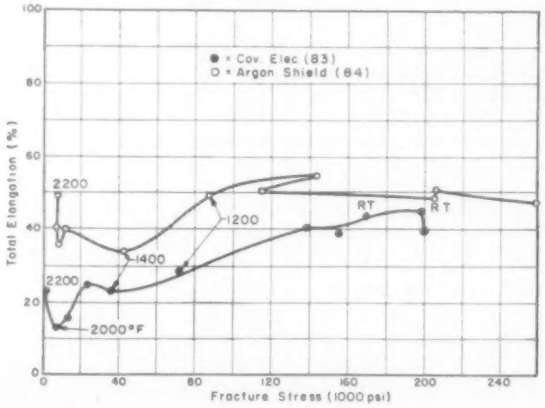

Fig. 14—Relations between fracture stress and elongation for Ni-Cr-Fe-Cb type weld metals

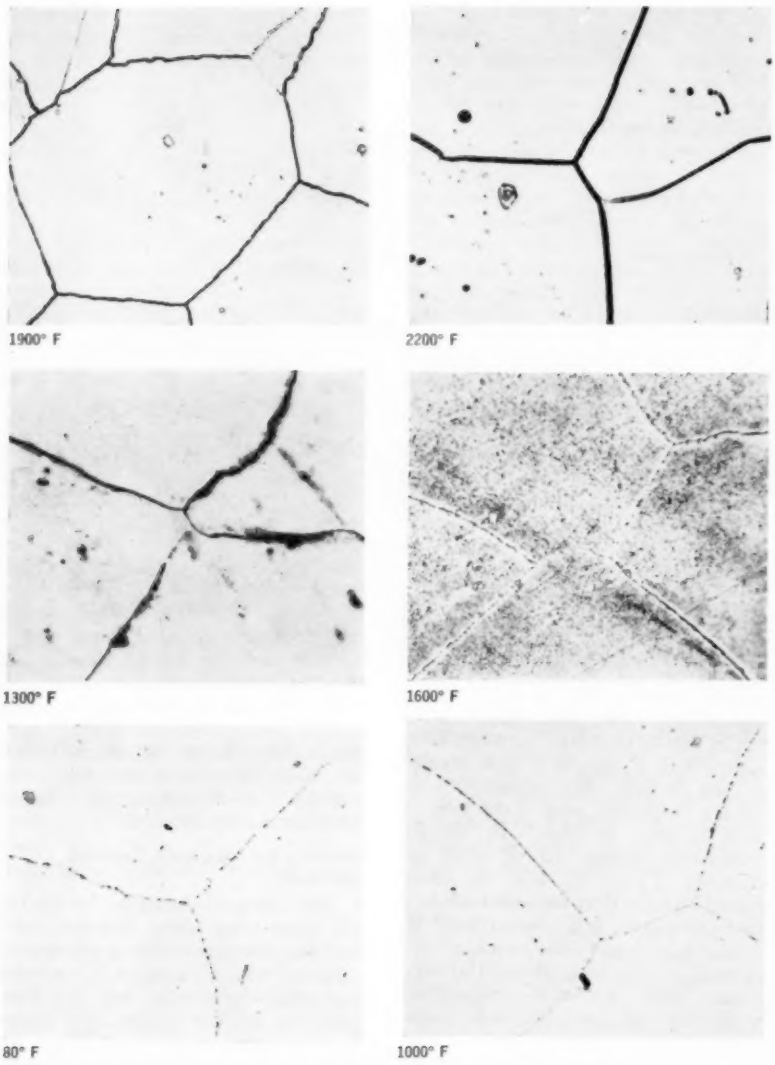

Fig. 15—Structures of Ni-Cr-Fe-Ti type base metal at X 1000. (From unstrained ends of tensile specimens tested at temperatures listed.) (Reduced by approx. 1/2 upon reproduction)

elongation, is between 1700 and 2100° F.

Treating the temperature-strength-ductility relations for the Ni-Cr-Fe-Cb type welds, as was done for the Ni-Ti ones, it would be expected that a minimum tendency for cracking would exist with the argon-shielded welds (see Fig. 14). Covered-electrode welds would be expected to crack only near the 2000° F level.

Ni-Cr-Fe-Ti-Type Alloys

The Ni-Cr-Fe-Ti type base, and weld, metals and one variation of the weld metal, have special characteristics. For the base metal, a slight increase occurs in yield strength as the temperature increases from 300 to 600° F, then decreases as the temperature rises to 1000° F, and then it rises sharply to a maximum at 1400° F (see Fig. 5). As the strengths increase, the ductility decreases disproportionately. The minimum ductility at 1400° F is 7.4% total elongation and 13.4% area reduction. At 1600° F, the fractures in the base metal had the appearance of grain separations in a compact of wet sand. At 1800° F, and above, the metal is very ductile; >99.2% area reduction at 1800, 2000, and 2200° F. At 1800° F, the total elongation is 107.9%.

The certified analysis (%) of the tube stock involved is:

Nickel	73.10
Chromium	15.04
Iron	6.67
Titanium	2.49
Cb + Ta	0.87
Aluminum	0.81
Manganese	0.56
Silicon	0.34
Copper	0.05
Carbon	0.04

A precipitation-hardening mechanism, effective in the annealed base metal, is temperature dependent and is effective at two levels. Between >300 and <600° F and again between >1000 and <1600° F, the mechanism causes increases in yield strengths with minor increases in tensile strength (see Fig. 5). Serrations occur in the load-strain curves only within the 600–1200° F range, i.e., when there is a maximum gap between fracture and yield strengths. Such serrations are associated with precipitation-hardening phenomena occurring during strain hardening. This occurs in low-carbon steel welds at about 300° F[5] and in some precipitation-hardening stainless steels at 1200° F.

The titanium compounds that precipitate within the <600 to >1400° F range cause the increased yield, ultimate and fracture strengths (see Fig. 15). The overall increase in the grain strengthening components, caused by the presence of the precipitate, without a proportionate increase in cohesive strength between the grains produces the low-ductility rupture at 1400° F. At 1600° F, the difference between the fracture stress and the yield and ultimate stresses is a minimum. It is here that the sand-compact type failure occurs (see Fig 15). As the temperature increases further, the return of the precipitate into solution in the matrix results in excellent ductility at lowered strengths, normal for the temperature levels. This effect, except for the time scale, is analogous to the formation and re-entry into solution of the brittle sigma phase in the austenitic matrix Fe-Cr-Ni steels as temperatures progressively increase.

Ni-Cr-Fe-Ti Type Welds, Argon- or Covered-electrode Shielded

The argon-shielded Ni-Cr-Fe-Ti type weld metal (Fig. 6) had tensile characteristics roughly similar to those of the base metal as related to temperature, except that a rise in yield strength does not occur at 600° F. A pronounced rise in yield strength does occur at >1000 and <1600° F, with a corresponding disproportionate drop in ductility, 4.2% total elongation on one specimen and only 2.8% on a recheck. At 1800° F, and above, the duc-

tility is good; >51% area reduction and >44% total elongation. The fracture stress is poor for all temperatures above 1000° F.

The covered-electrode shielded welds had similar characteristics, except that the ductility across most of the temperature range was poor. This weld contained some cracks in the as-deposited condition. At 1300° F, the total elongation was <1% and the area reduction 11.3%. These data are not included in detail. (See Fig. 16 for microstructures).

A weld of similar composition made between a Ni-Cr-Fe alloy and plain-carbon structural steel with argon shielding and a commercially available electrode also exhibited a rise in yield strength at 1400° F, with the corresponding ductility dip, 7% total elongation.

Significantly, these three welds are the only ones of the basic Ni-Cr-Fe composition series studied that contain high titanium, from 2.35 to 2.66%. Of the 12 welds covered by this study, only these three exhibited the high-yield-strength characteristic at 1400° F. It is therefore the titanium that makes the difference in the Ni-Cr-Fe combination, but the presence of titanium in nickel (see Figs. 1 and 2) and in the Ni-Cu alloys (see Fig 10) has no such effect in the short-time tensile test. There is, however, some evidence of this phenomenon in the hardness data (see Fig. 18) for the unstrained metal.

Additional welds of the covered-electrode Ni-Cr-Fe-Cb type (see Figs. 7 and 8) with low titanium (Ti 0.25/0.48), did not exhibit the yield stress rise or the ductility dip at 1400° F. A weld made with a covered electrode that is no longer commercially available (see Fig. 7) exhibits no anomalies in strength-temperature relations and shows good ductility up to and including 2200° F, with a ductility rise at >1200 and <2000° F. Another covered-electrode weld (see Fig. 8) containing 0.25% titanium, also exhibited no anomalies in the strength-temperature relations, but it had a minimum ductility at 1900° F. At that temperature, the total elongation was only 7.1%. Both of these welds contained defects of the porosity-cracking type from their original solidification. The first root bead of this deposit cracked badly. Unfortunately, from a property determination point of view, the variable restraint conditions in the tube has had its influence on these results, but that condition has, at the same time, provided information to show that, in

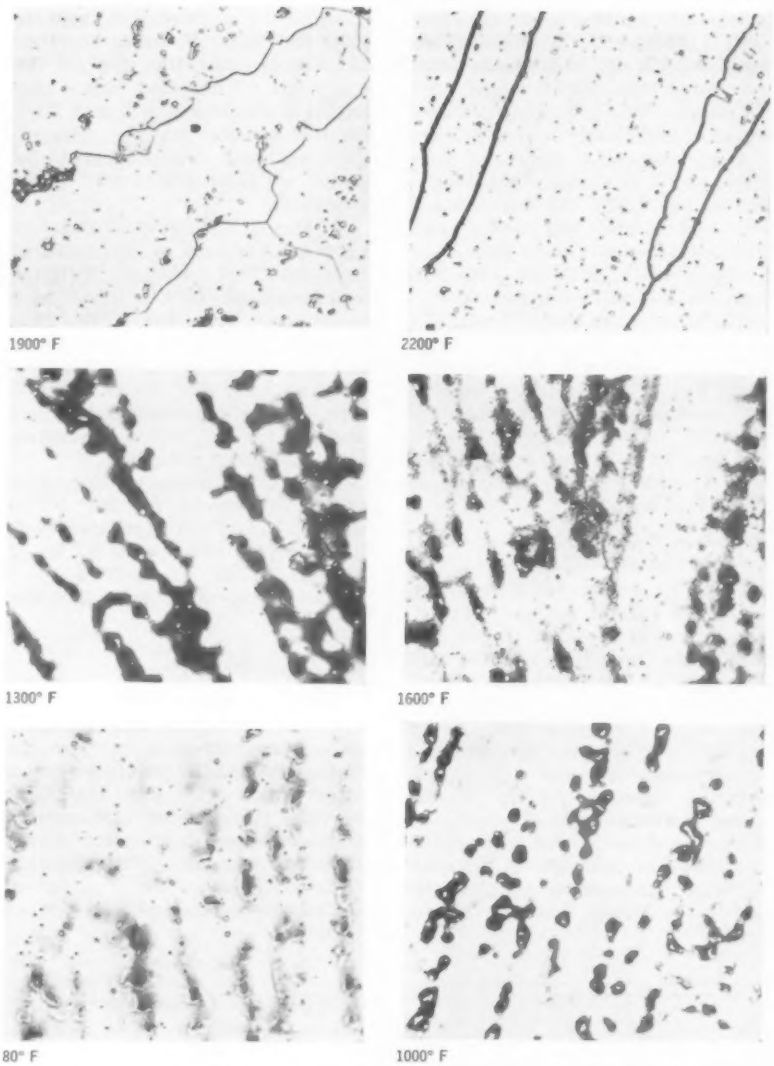

Fig. 16—Structures of covered-electrode Ni-Cr-Fe-Cb-Ti-Ta type welds at X 1000. (From unstrained ends of tensile specimens tested at temperatures listed). (Reduced by approx. 1/2 upon reproduction)

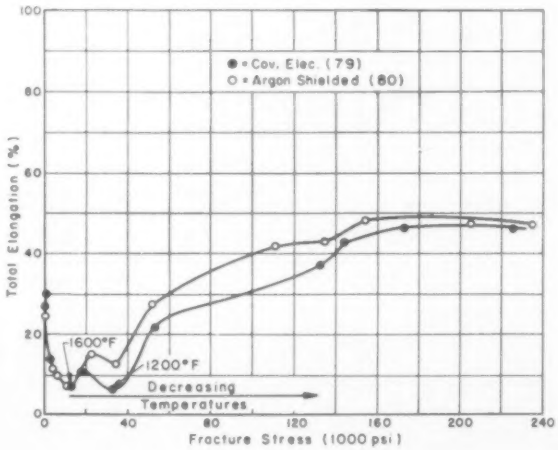

Fig. 17—Fracture stress vs. elongation relationships for Ni-Cu type weld metals

production, caution must be exercised in the selection and use of these compositions. A weld made with the same electrode between two flat pieces of Ni-Cr-Fe alloy and carbon steel had closely similar properties, but somewhat improved ductility, 13.2% minimum total elongation at 1800° F. The iron content was higher and the nickel and chromium contents lower because of enrichment and dilution resulting from the carbon-steel member.

The choice between Cb and Ti as additions to the Ni-Cr-Fe alloy series is therefore a delicate one. More than 2% Ti, with or without Cb, produces precipitation hardening and 1400° F embrittlement; less than 0.5% Ti with too high Cb, >1.9%, produces low ductility at 1800° F or higher.

Ni-Cu Type Welds, Covered Electrode and Argon Shielded

Ni-Cu type weld metals (see Figs. 9 and 10) exhibit normal temperature-strength relations up to the 2200° F maximum investigated. The fracture strengths are poor above 600° F, but are excellent at the very low temperatures. There is little difference between the covered-electrode and the argon-shielded deposits. At 600° F and lower, the ductility is excellent, but a marked deterioration in ductility is already in evidence as the temperature increases up to 1000° F, and these values continue to degenerate to a minimum between 1200 and 2000° F, being less than 15% total elongation for all but one point within that range, and having a minima of 6.2 and 7.1% total elongation for the covered-electrode and argon-shielded deposits at 1200 and 1600° F respectively.

Of special academic interest are the results secured at liquid helium temperatures (−452° F) with the argon-shielded Ni-Cu alloy weld metal (see Fig. 10). The yield strength maintained its relatively low rate of rise down to that temperature, only 4.5° above absolute zero, while maintaining excellent ductility, 47.3% total elongation and 61.8% area reduction.

The fracture stress vs. elongation values are shown for the Ni-Cu welds in Fig. 17. The critical cracking temperatures appear to be at 1600 and 1200° F; 1600° F being the most critical for both shielding methods.

Hardness Variations

Hardness traverses were made on the unstrained butt ends and in the strained shanks 0.75 in. from the ends of most of the tensile specimens after rupture (see Fig. 11). This provided independent information on the effects of the thermal and of the thermal-stress cycles (see Figs. 18 to 21).

The covered-electrode Ni-Ti type welds were softened when heated to and above 1700° F (Fig. 18), but the argon-shielded welds were essentially unaffected by brief (20 min) exposure to any of the 2200° F maximum test temperatures. For both cases, there was evidence o hardening at 1400° F. Strain hardening occurred up to 1280 and 1440° F, respectively, lower curve, but it was most appreciable below 1100° F.

Ni-Cr-Fe-Cb type welds (Fig. 19) had essentially the same response, regardless of shielding mechanism. The as-deposited welds were softened slightly upon exposure to temperatures above 1600° F. The strain hardening was about constant up to 1000° F. It decreased rapidly above that temperature, to very small amounts at and above 1700° F.

The Ni-Cr-Fe-Ti type base metal hardness-temperature responses revealed softening of the strained metal above 1400° F and hardening of the unstrained metal after exposure to temperatures of 1200° F and above. The hardness increase in the unstrained metal is the result of a precipitation phenomenon previously discussed. These weld metals, containing >2.0% titanium, respond, in general, in the same manner as the base metal (see Fig. 20), but in a more pronounced manner. The unstrained metal increases in hardness after exposure

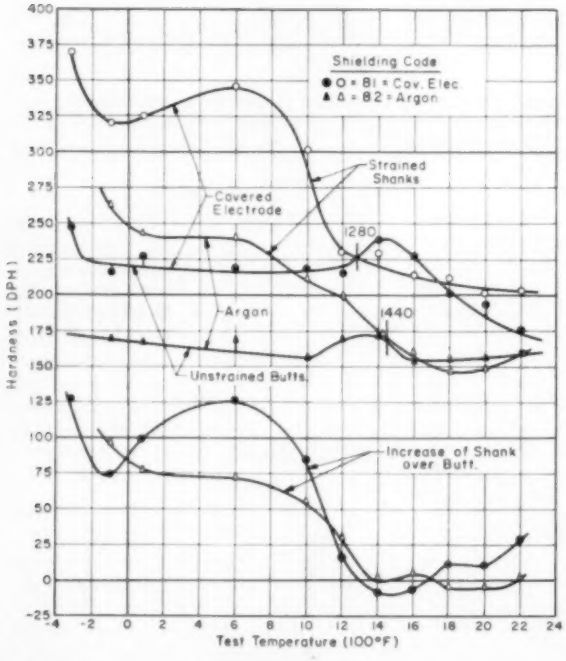

Fig. 18—Hardness data for Ni-Ti type welds

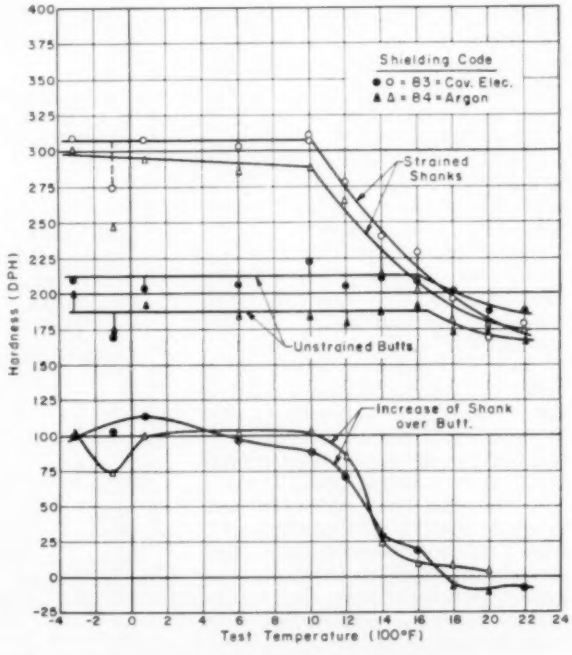

Fig. 19—Hardness data for Ni-Cr-Fe-Cb type welds

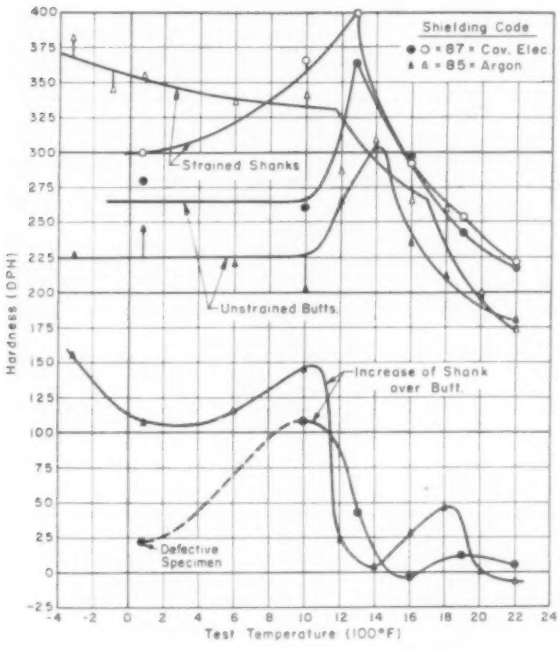

Fig. 20—Hardness data for Ni-Cr-Fe-Ti type welds

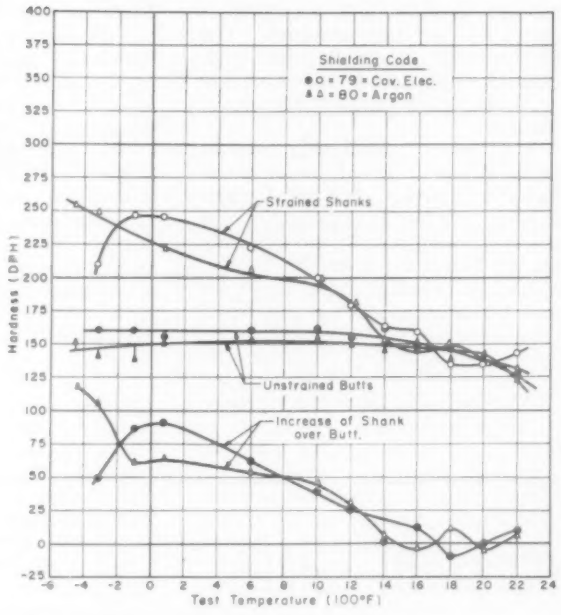

Fig. 21—Hardness data for Ni-Cu type welds

to temperatures above 1000° F. This increases to a maximum at 1400° F, and for higher temperatures the hardness progressively decreases as the precipitate returns into solution. The net result is that there is little difference between the hardness of the strained and unstrained metal for exposures to temperatures of 1400° F and above. Modified electrodes, producing welds containing columbium, do not exhibit the precipitation-hardening phenomenon. These metals are softened somewhat by exposure to temperatures above 1400° F and the maximum straining hardness decreases as the temperatures exceed 1000° F. No net increase in hardness occurs from straining at temperatures of 1800° F and above.

A titanium-bearing deposit, made between a Ni-Cr-Fe alloy and plain-carbon steel, again shows the 1400° F increase in hardness in the unstrained weld metal. This weld is the only one of the entire series that shows at least some strain hardening at all test temperatures.

Ni-Cu type welds showed the least sensitivity to strain hardness (see Fig. 21). They were softened by exposure to temperatures above 1800° F and revealed no precipitation-hardening effects.

In general, all of the nickel-base alloy welds, except the Ni-Cu group, increased about 100 DPH in the uniformly strained metal over that in the unstrained butts, up to about 1000° F. This differential dropped to from less than 25 DPH to a negative value above 1200° F for the Ni-Ti and the Ni-Cu type welds (see Figs. 18 and 21); above 1400° F for the Ni-Cr-Fe-Cb and Ni-Cr-Fe-Ti welds (see Figs. 19 and 20); and above 1600° F for the Ni-Cr-Fe-Cb-Ti welds.

There is a general near-linear relation between the amount of strain at uniform load and the strain hardening increase, although this is more pronounced in some compositions than in others. For a 40% uniform strain, the hardness increase ranges from 60 in the Ni-Cu type welds to as high as 150 for the Ni-Ti and the Ni-Cr-Fe-Ti welds. In the high-temperature tests there was little uniform, and total, strain; also, there is little increase in hardness at those temperatures. In general, for a given strain, the hardness increase is less in the argon-shielded welds than in the covered-electrode ones.

Magnetic Characteristics

Magne-gage readings showed all the welds to be nonmagnetic, except the Ni-Ti alloy series. These two welds had the magnetic equivalent of more than 35% ferrite in the total mass.

Conclusions

1. The transfer efficiencies of the primary alloying elements across the welding arc in the nickel-base alloys are:

	Shielding	
Element	Argon	Covered electrode
Fe	0.98	>1.0[a]
Cr	0.96	>0.95[b]
Mn	0.95	0.85[b]
C	0.95	...
Ti	0.82	0.92[a]
Si	0.81	>1.0[a]
Al	0.79	0.51[c]
Cb	0.78	>1.0[a]
Ta	0.65	>1.0[a]

[a] Net for fortified covering.
[b] Net for unfortified covering.
[c] Independent of covering fortification.

2. Any desired composition in nickel-base alloy weld metals can be secured by either shielding technique by properly balancing wire and covering compositions.

3. Ni-Cu type alloy welds are low in ductility at all temperatures above 1200° F, but are very ductile below 800° F and down to liquid-helium temperatures.

4. Ni-Ti type alloy welds have a low-ductility dip centered at 1800° F.

5. Ni-Cr-Fe-Cb type alloy welds have maximum hot ductility, particularly when argon shielded.

6. Welds in the Ni-Cr-Fe series become precipitation hardened and very brittle at 1400° F when more than 2% Ti is added to the deposit, regardless of the arc shielding media.

7. Ni-Cr-Fe-Ti type alloy welds are not only hot brittle but are crack sensitive under nominal levels of restraint.

8. Ni-Cu, Ni-Ti and Ni-Cr-

Fe-Cb type alloy welds have excellent ductility and strength at extremely low temperatures. The yield stress tends to rise with lowered temperatures about in line with accepted values for f.c.c. metals.

9. Strain hardening below 1000° F is basically a function of the amount of strain, and for a given amount of strain it is a minimum in the Ni-Cu alloys and a maximum in the Ni-Ti and Ni-Cr-Fe-Ti alloys.

10. All welds in these alloys are nonmagnetic except for the Ni-Ti compositions.

Acknowledgments

Analyses of the weld deposits were provided by the Westinghouse Engineering Departments. Covering analyses were made by J. F. Reed, and spectrographic analyses by J. Senko, Technology Department, Research Laboratories. Welds were made by P. T. Ehrhardt; magnetic readings by C. J. Dorsch, and hardness readings by C. J. Dorsch and G. R. McGraw, all of the Research Metals Joining Section. Tensile tests were made by W. H. Pryle and R. R. Hovan, and metallographic examinations by R. L. Anderson, all of the Research Metallurgy Department.

References

1. Pease, G. R. "The Practical Welding Metallurgy of Nickel and High Nickel Alloys," THE WELDING JOURNAL, **38** (7), Research Suppl., 330 to 334-s (1957).

2. Pease, G. R., Brien, R. E., and Legrand P. E. "The Control of Porosity in High Nickel Alloy Welds," *Ibid.*, **37** (8), Research Suppl., 354-s to 360-s (1958).

3. T. E. Kihlgren and C. E. Lacy. "The Control of Weld Hot Cracking in Nickel-Chromium-Iron Alloys," *Ibid.*, **25** (11), Research Suppl., 769-s to 775-s (1946).

4. Poole, L. K. "The Incidence of Cracking in Welding Type 347 Steels," *Ibid.*, **32** (8), Research Suppl., 403-s to 412-s (1953).

5. Heuschkel, J. "Initial Characteristics of Chromium-Nickel Steel Weld Metals," *Ibid.*, **34** (10), Research Suppl., 484-s to 504-s (1955).

6. Heuschkel, J. "Time-Temperature Dependence of Austenitic Stainless Steel Welded Joint Components," *Ibid.*, **35** Research Suppl. (12), 569-s to 581-s (1956).

7. Heuschkel, J. "Dependence of Steel Weld Properties on Lattice Structure," *Ibid.*, **35** (2), 82-s to 90-s (1956).

8. Heuschkel, J. "Effects of Temperature on Weld Metal Properties," *Ibid.*, **33** (8), 388-s to 397-s (1954).

BULLETIN SERIES

Requests for single copies should be sent to the
AMERICAN WELDING SOCIETY, 29 W. 39th St., New York 18, N. Y.

Requests for bulk lots of ten or more, should be sent to the
WELDING RESEARCH COUNCIL, 29 W. 39th St., New York 18, N. Y.

No. 53 **Plastic Design of Pinned-Base "Lean-to" Type Frames,** by Robert L. Ketter and Bung-Tseng Yen, September 1959. $1.00.

No. 54 **Bending of 2:1 and 3:1 Open-Crown Ellipsoidal Shells,** by G. D. Galletly, October 1959. $1.00.

No. 55 **Fourth Technical Progress Report of the Ship Structure Committee,** November 1959. $1.00.

No. 56 **Interpretive Report on Welding Titanium and Titanium Alloys,** by G. E. Faulkner and C. B. Voldrich, December 1959. $1.00.

No. 57 **Some Observations on the Brittle Fracture,** by G. M. Boyd, January 1960. $1.00.

No. 58 **Strength of Aluminum Alloy 6061-T4 Thick-Walled Cylindrical Vessels Subjected to Internal Pressures,** by J. Marin and Tu-Lung Weng, March 1960. $1.00.

No. 59 **Factors Which Affect Low-Alloy Weld Metal Notch-Toughness,** by S. S. Sagan and H. C. Campbell, April 1960. $1.00.

No. 60 **(1) Interpretive Commentary on the Application of Theory to Experimental Results for Stresses and Deflections Due to Local Loads on Cylindrical Shells,** by P. P. Bijlaard and E. T. Cranch; **(2) An Experimental Investigation of Stresses in the Neighborhood of Attachments to a Cylindrical Shell,** by E. T. Cranch, May 1960. $2.00.

No. 61 **Interpretive Report on Welding of Nickel Clad and Stainless Clad Steel Plate,** by W. H. Funk, June 1960. $1.00.

Resistance Seam Welding of Terne Plate

The changes in welding variables necessary for seam welding terne plate are described, and the welds produced are compared with welds having a zinc coating

BY HORACE F. GREER AND M. L. BEGEMAN

Introduction

Coated-steel sheets have wide application in industry for products which must be resistant to corrosion and have liquid-tight seams. This report is one of several which deals with the uses of resistance seam welding as a method for producing acceptable welded joints. The first two reports compared the results of welding uncoated and zinc-coated low-carbon steel at the welding conditions for uncoated steels, and established the fact that coated materials require different machine settings to produce welds of consistent high quality. This report describes the changes in welding variables necessary for seam welding terne plate and compares the welds produced with welds having a zinc coating.

Terne plate is sheet steel which has been coated with an alloy of lead and tin. The normal composition of the terne-alloy coating is 75% lead and 25% tin; however, wide variations in composition are not uncommon. The reason for a proportion of tin in terne metal is that lead, by itself, is insoluble in both solid and liquid iron, so there is no tendency for lead to wet the steel or to bond itself to a steel surface by alloying. The addition of 25% tin enhances the adhering property of the lead-alloy coating to such an extent that by weight, only a half or a third as much is required to achieve the same protection as would be required for lead or zinc, respectively.

Effect of Metallic Coatings on a Resistance Weld

The presence of any low-melting-point coating on the surface of a weldment involves some difficulty in seam welding in that the coating tends to alloy with the wheel electrodes, and some provision is necessary for cleaning the wheel surface. Another effect of coatings is to increase the number of layers of metal initially present between the electrodes from two to six, thereby increasing the electrical resistance as compared to uncoated steel. The melting of a coating in the course of making a seam weld introduces a third effect—that of being a cooling medium or heat sink for the area surrounding the weld, tending to restrict the maximum temperature reached.

The problem of electrode pickup may be countered by employing a knurled driving roller to break up the alloyed material on the electrode face. This technique proved reasonably satisfactory in welding terne plate although the electrode pickup was found to progress rapidly.

A resistance weld is made by an application of force and heat generated by resistance to the passage of an electric current; the presence of extra layers of metal in a weld area affecting the manner in which heat is produced in the weld region. With uncoated weldments, the three primary resistances are the contact resistances between the electrodes and weldments, plus the interface resistance between the weldments. The electrode-weldment contact resistances are small, and heat generated at the outside surfaces is dissipated by flood cooling. It is the heat generated at the interface which produces the weld.

For coated weldments, the major resistances are still the contact resistances; however, the distribution of resistance across the weldments changes once the welding is begun. With the first generation of heat, the low-melting-point coating liquefies and is squeezed away from the weld area by the force applied by the electrodes. Ideally, the displacement of the liquid coating results in a steel-to-steel contact at the sheet interface, and welding then proceeds as in uncoated materials. There is, however, the possibility that some of the coating will be trapped in the weld area and remain as an inclusion defect. The requirement that the liquefied coating be forced from the weld area dictates the use of higher electrode forces when welding coated materials.

The melting of the coating produces cooling in the weld area and represents a heat loss to the base metal. To compensate for the heat deficit, either the electrical resistance or the welding current must be increased. No "extra" heat is generated due to increased electrical resistance because the initial resistance decreases in accordance with melting of the coating until its value is that of the two steel weldments in close contact. The increased heating required for the welding of coated steel can be achieved only by an increase in the welding current.

In summary, it is seen that a metallic coating introduces the following considerations to the seam-welding process: (1) the problem of the coating alloying with the electrode; (2) the problem of securing a steel-to-steel contact at the interface; and (3) the problem of countering the cooling effect associated with melting of the coating.

Equipment and Materials

A circular seam-welding machine was employed to produce the seam welds involved in this study. With a power input of 440 v and 60 cycle current, the transformer for the welding machine was rated at 250 kva. Control of the current

HORACE F. GREER is Research Engineer, Convair, Vandenburg Air Force Base, Calif.; formerly a graduate student RWMA Fellowship, the University of Texas, Austin, Texas, and M. L. BEGEMAN is Professor of Mechanical Engineering, the University of Texas.

Paper presented at AWS 41st Annual Meeting held in Los Angeles, Calif., April 25–29, 1960.

Table 1—Information on Terne-coated Steel Sheet

Gage	Coating weight, oz/ft²	Coating class, oz/ft²	Steel C, %	Steel Mn, %	Steel P, %	Steel S, %	Terne Pb, %	Terne Sn, %
22	0.48	0.55	0.06	0.41	0.008	0.021	72.77	27.23
22	0.37	0.45	0.07	0.39	0.008	0.024	78.23	21.17
20	0.33	0.35	0.05	0.30	0.008	0.028	75.17	24.83
18	0.45	0.55	0.05	0.26	0.008	0.041	73.26	26.74

variables associated with the welding process was provided by a thyratron control unit. This fully electronic control permitted the selection of "on" and "off" times of 1 to 32 cycles in one cycle increments, and provided for current variation by means of a phase control which adjusted the basic sine wave to correspond to the selected percent heat.

The copper-base electrodes employed were made of a RWMA Class II alloy recommended for seam welding coated steels. The electrodes were 10 in. in diam and $^1/_2$ in. thick, with the face width reduced to $^5/_{16}$ in. by 10-deg tapers, and $^1/_{16}$-in. radii provided at the face edges. The resulting electrode face was $^9/_{32}$-in. wide and fitted snugly into the driving roller. Knurled driving rollers were employed to rotate the electrodes.

Materials. Steel sheets for production of terne-coated sheet steels are supplied in three qualities; namely, "commercial," "drawing" and "physical," according to whether ductility or mechanical tests are specified. The materials used in this investigation were hot-dip coated 22-, 20- and 18-gage commercial-quality steel sheets. This means that the steel sheets were produced from rimmed, capped or semikilled steel, at the producer's option. Table 1 summarizes information given on the shipping documents of the material used in this investigation, and shows the coating weight as determined by ASTM triple-spot test, and corresponding "coating class," plus the chemical analyses of the steel and terne alloy.

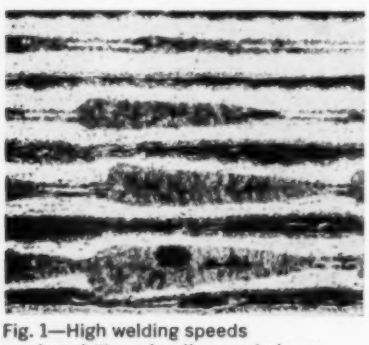

Fig. 1—High welding speeds produced "tear-drop" nugget shape

Procedure

The resistance-seam-welding process is complicated by interrelation of its four major variables, namely, electrode force, current timing, welding current and welding speed. To establish optimum conditions, a systematic variation of the welding variables must be made using some arbitrarily selected initial settings. The investigational procedure described below proved satisfactory and was applied to each of the three gages investigated.

Selection of Welding Speeds and Timing (for initial experiments). A welding speed of 60 ipm was selected because work with other coated steels indicated that this was the optimum speed. In addition, a speed of 100 ipm was investigated because of the industrial trend toward higher welding speeds. A current timing for making the first welds was selected by consulting a welding schedule for uncoated steels and increasing the recommended heating time by one cycle. This timing was used to establish the optimum electrode force. The optimum timing was not determined until later in the investigation.

Determination of Optimum Electrode Force. Using the arbitrarily selected welding speed and current timing, welds were made at several settings of electrode force, and for each electrode force the welding current was varied to produce a series of welds. The welds produced in this manner were often not of top quality, but a clearly defined region of better-quality welds was distinguishable in each investigation made. The electrode force that produced the better welds was designated as "optimum."

The procedure described above was applied uniformly to each of the three gages of material; with the exception that, for the 22-gage material, optimum force investigations were conducted at three welding speeds, namely, 60, 100 and 150 ipm, to confirm that no change in optimum electrode force accompanied a change in welding speed.

Determination of Optimum Timing and Welding Current. With the established optimum electrode force, welds were made with variation in welding current for each of several current timings. From these welds, the optimum current timing and welding current were determined.

Welding Technique. In preparation for the welding operation, weldments were wiped free of loose dirt and dust with a clean cloth. No other preparation was deemed necessary, for the surface was only slightly oiled. The welds were made by superimposing one 1-x 30-in. strip upon another and then seam welding along the center of the strips. From these welded strips, specimens were taken for metallurgical examination, X-ray evaluation, and corrosion testing.

Metallurgical Examination. Metallurgical examination of the welds consisted of measuring the nugget penetration* and inspecting the welds for defects. Both longitudinal and transverse sections were employed. The longitudinal sections were used in studying defects such as microscopic and visual transverse cracks, lack of nugget overlap and the extent of porosity; while transverse sections were needed to reveal unsymmetrical nuggets.

Corrosion Testing. To determine the corrosion resistance of terne plate after it was welded, specimens possessing the heaviest coating of terne, 0.48 oz per sq ft, were subjected to 100% humidity at room temperature for four months, November through February, and inspected periodically for corrosion.

Results

Percent nugget penetration was used as the first criteria for evaluation of weld quality, but complete evaluation was based upon inspection for weld defects and upon peel-and pillow-test performance. Measurement of nugget penetration was made using longitudinally sectioned specimens, for this exposed several nuggets in each seam weld and allowed an average assessment of penetration.

Effect of Welding-speed Varia-

* Nugget penetration is defined to be the ratio of weld-nugget thickness to the total thickness of the joint.

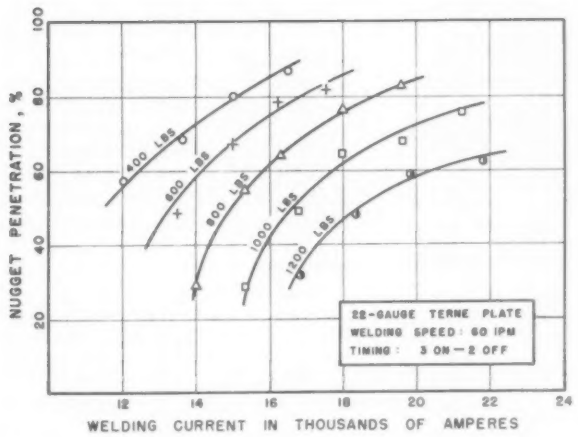

Fig. 2—Effect of electrode force on nugget penetration and welding current for 22-gage terne plate welded at 60 ipm

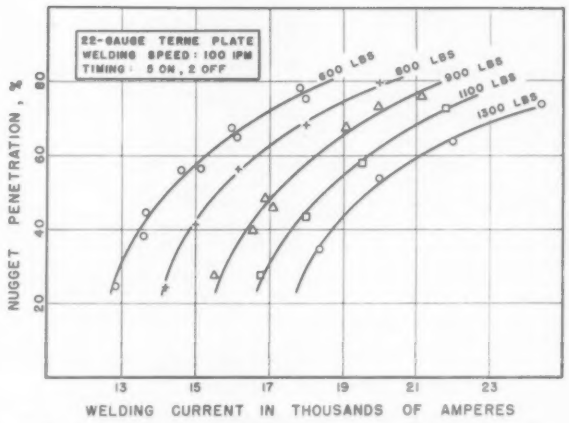

Fig. 3—Effect of electrode force on nugget penetration and welding current for 22-gage terne plate welded at 100 ipm

tion. To determine the effect of welding speed on optimum electrode force, welds were made in 22-gage material at speeds of 60, 100 and 150 ipm, with various electrode forces, and a current timing of 4 cycles on and 2 off. It was found that the optimum electrode force was unaffected by changes in welding speed. For 22-gage sheet, the optimum electrode force was 900 lb. One effect of increased welding speed was that each increase in speed required an increase in current in order to achieve a given nugget penetration. The increase in current was required because more material was passing between the electrodes per unit time, due to increased speed, and additional heat (current) was required to weld the "extra" material.

It was also found that an increase in the welding speed increased nugget spacing and altered nugget shape. Nugget spacing was barely sufficient to produce tangency of the nuggets at 100 ipm, so this speed was the upper limit for producing seam welds. The effect of increased welding speed on nugget shape was to change the contour from oval to "tear drop" as shown in Fig. 1. Large voids occurred frequently in the thickest portion of the weld nugget near the plane of the interface due to premature release of electrode force inherent with high welding speed.

The shape of the nugget shows that, after the initial impulse of current, the amount of heat generated decreased. The decrease in nugget thickness was the result of increased electrical resistance caused by heating of the steel. After the first impulse of current, the material adjacent to the weld area was preheated by conduction, and portions of the subsequent current flow were diverted around the nugget region, thus reducing the heat generated in the trailing weld area. One effect of the diverted current was the formation of twin projections at the interface periphery of almost every nugget.

The fact that the "diverted-current" phenomenon is common to all welds was shown by the presence of the projections on welds made both at 150 and 60 ipm as shown in Fig. 1 and later in Fig. 4, respectively. The overlapping nuggets at low welding speeds obscure the decreased heating effect, but the wide nugget spacing of the higher welding speeds distributes the decrease in nugget thickness and produces the "tear-drop" shape.

Effect of Electrode-force Variation. Figures 2 and 3 show the results of welds made in 22-gage terne plate with variations in electrode force at welding speeds of 60 and 100 ipm, respectively. The maximum pentrations obtainable without excessive flashing and electrode sticking were 80% in 22-gage, 70% in 20-gage and 50% in 18-gage terne plate which are approximately the maximum pene-

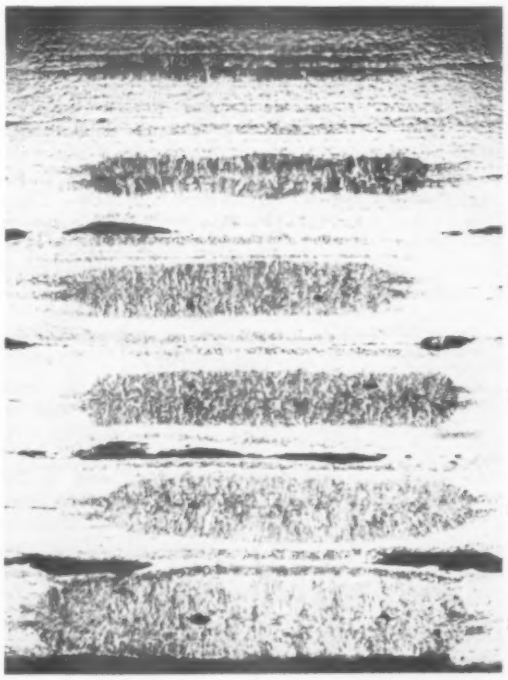

Fig. 4—Macrograph showing the normal increase in nugget size which accompanies increased welding current. Welds were made in 22-gage terne plate with 900-lb electrode force and welding speed of 60 ipm. × 12. (Reduced by 20% upon reproduction)

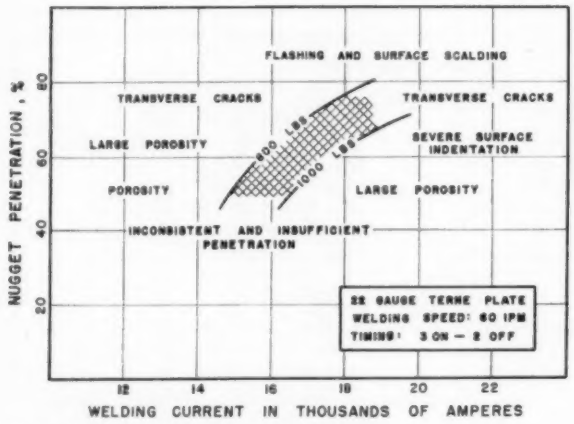

Fig. 5—Region of optimum welds (shaded area) and defects encountered outside the optimum region for 22-gage terne plate welded at 60 ipm

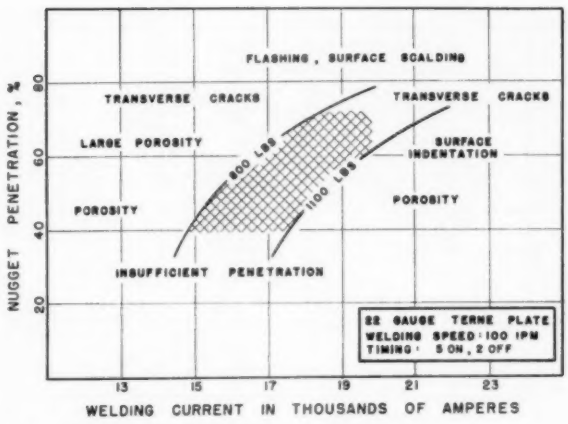

Fig. 6—Region of optimum welds (shaded area) and defects encountered outside the optimum region for 22-gage terne plate welded at 100 ipm

trations obtained in galvanized steel of the same gage. Figures 2 and 3 also illustrate that an increase in electrode force requires an increase in current to maintain a given penetration.

The macrographs in Fig. 4 show, for 22-gage material welded at 60 ipm, the effect of current variation at an electrode force of 900 lb. The weld produced at 15,000 amp did not possess complete penetration and was unsatisfactory under pillow testing. Welds made with 16,000, 17,000, 18,000, 19,000 and 20,000 amp show the normal increase in nugget size associated with an increased current.

For the electrode forces investigated, it was noted that the weld defects could be grouped into zones or regions in which a particular weld defect predominated. The shaded areas in Figs. 5 and 6 indicate regions of optimum weld quality. The figures also point out the defects encountered if conditions are outside the optimum zone. Figures 5 and 6 are 22-gage material at welding speeds of 60 and 100 ipm, respectively.

The limits of the optimum regions for each of three gages were set by excessive flashing and electrode sticking at the higher penetrations and by insufficient bonding or joining at the lower penetrations. The lateral boundaries of the optimum region were not so easily defined, for the change in weld quality was gradual. The boundaries were drawn in the light of the observation that acceptable welds could be achieved with electrode forces 100 lb. above or below the designated optimum electrode force. The optimum forces for 22-, 20- and 18-gage material were found to be 900, 1000 and 1100 lb, respectively, which are partially the same as the electrode forces recommended by Volek[1] and Allen[2] for seam welding the corresponding gages of galvanized steel. The only difference in recommended electrode forces was that for 22-gage material both Volek and Allen recommended 1200-lb electrode force; however, their welds were essentially pressure welds with no real nugget formation. Welds made with 900-lb electrode force possessed large well-defined nuggets as was shown in Fig. 4.

Where defects were present, these were similar in all gages of material except that transverse cracks were detected in the 22-gage material and not in the 20- and 18-gage terne plate. A discussion of the causes which produced these cracks is presented under "Weld Defects."

Figures 7 and 8 show the effect of a variation in electrode force on nugget penetration when the welding current is held constant. They pertain to 22-gage terne plate at 60 and 100 ipm, respectively. The decrease in penetration obtained with higher electrode force is due to decreased interface-contact resistance causing less heat generation. The macrographs in Fig. 9 illustrate the decrease in penetration obtained with increased electrode force in 22-gage material at a constant current of 17,000 amp.

As shown in Figs. 7 and 8, the curvature of the penetration lines changed from convex to concave when the welding speed was changed from 60 to 100 ipm. It is believed that this occurrence is due to the "tear-drop" nugget shape which reduces the average nugget penetration for high welding speeds. With an electrode force of 900 lb and a welding current of 17,000 amp, 60% penetration was obtained at 60 ipm as compared to 48% at 100 ipm. It appears that intermediate welding speeds would

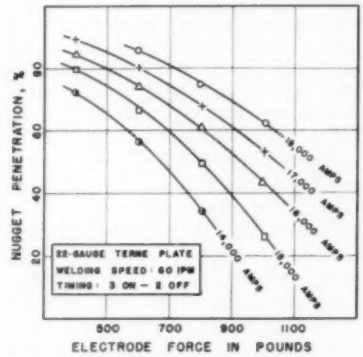

Fig. 7—Effect of electrode force on nugget penetration with welding current held constant. 22-gage terne plate; welding speed 60 ipm

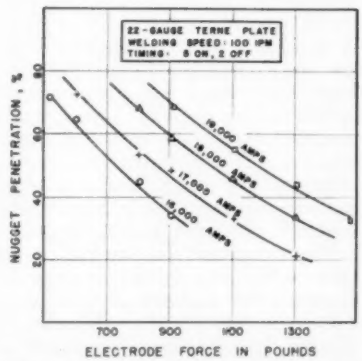

Fig. 8—Effect of electrode force on nugget penetration with welding current held constant. 22-gage terne plate; welding speed 100 ipm

produce transition configurations from convex to concave, and that a particular welding speed would produce a linear relationship between nugget penetration and electrode force.

Effect of Current-timing Variation. Briefly stated, the biggest problem associated with seam welding is control of the "heat input" at the weld area. Selection of an electrode force and a welding current provides a certain amount of heating control, but fine adjustment can best be accomplished by current timing. The effect of current timing is to distribute the current impulses along the weld. Current timing is referred to as "heat" time and "cool" time or as "on" time and "off" time. The heat time governs the amount of heat available to produce the weld nugget; while the cool time determines the nugget-to-nugget spacing and allows time for heat dissipation, which is necessary to prevent overheating in the weld areas.

Heat-time Variation. Change in heat time (while holding the cool time constant) was found to have little effect on the penetration ob tained in any of the three materials. Figures 10 and 11 show this result for 22-gage terne plate at speeds of 60 and 100 ipm, respectively. This finding indicates that, for a given gage of terne plate, the amount of penetration obtained depends primarily upon the welding current used to make the weld. The welding current, however, is determined by the current timing and the percent heat setting. Percent heat is the ratio of the heat produced with an altered sine wave to the heat produced by an unaltered, full-sine wave. Increased heating time was found to produce a slight

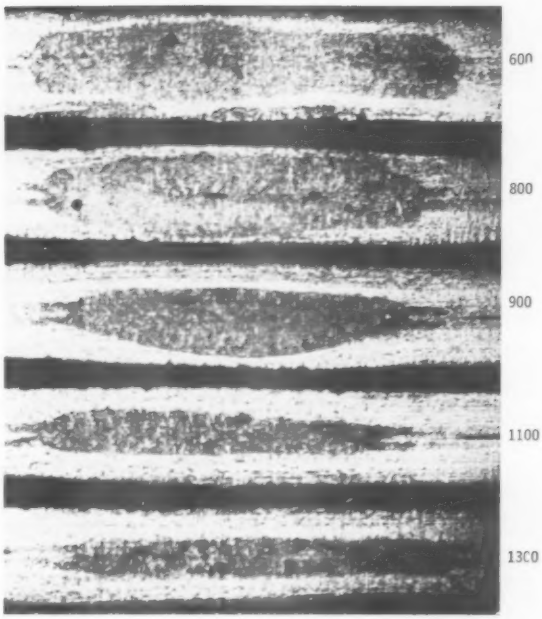

Fig. 9—Macrograph showing the decrease in nugget size produced by increased electrode force in 22-gage terne plate welded at 60 ipm with a welding current of 17,000 amp. × 12. (Reduced by 20% upon reproduction)

increase in nugget size which was helpful in improving nugget overlap, but tended to cause large voids in the nugget interior.

Cool-time Variation. For 22- and 20-gage terne plates the effect of increasing the cool time, while holding the heat time constant, was to sharply reduce the amount of current required to produce a given nugget penetration. Figures 12 and 13 illustrate this result for 22-gage terne plate at speeds of 60 and 100 ipm, respectively. This was the result expected because the increased cool time increased nugget spacing thereby reducing shunting effects and allowing more time for heat dissipation between current impulses. The time available for heat dissipation is important for it lowers the temperature and

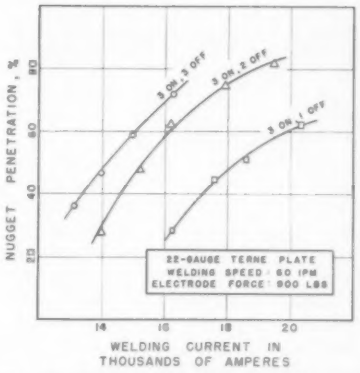
NUGGET PENETRATION, %
WELDING CURRENT IN THOUSANDS OF AMPERES
3 ON, 3 OFF
3 ON, 2 OFF
3 ON, 1 OFF
22-GAUGE TERNE PLATE
WELDING SPEED · 60 IPM
ELECTRODE FORCE · 900 LBS

Fig. 12—Effect of cool-time variation on nugget penetration and welding current. 22-gage terne plate; 900-lb electrode force; welding speed, 60 ipm

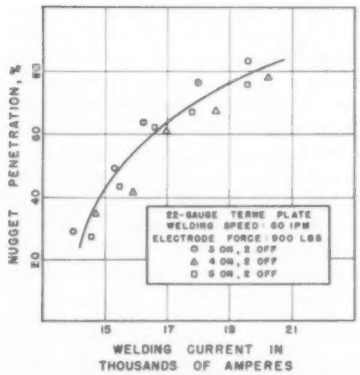
NUGGET PENETRATION, %
WELDING CURRENT IN THOUSANDS OF AMPERES
22-GAUGE TERNE PLATE
WELDING SPEED · 60 IPM
ELECTRODE FORCE · 900 LBS
3 ON, 2 OFF
4 ON, 2 OFF
5 ON, 2 OFF

Fig. 10—Effect of heat-time variation on nugget penetration and welding current. 22-gage terne plate; 900-lb. electrode force; welding speed, 60 ipm

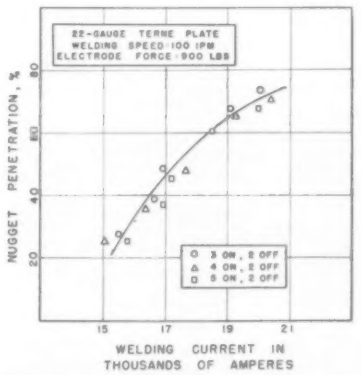
NUGGET PENETRATION, %
WELDING CURRENT IN THOUSANDS OF AMPERES
22-GAUGE TERNE PLATE
WELDING SPEED · 100 IPM
ELECTRODE FORCE · 900 LBS
3 ON, 2 OFF
4 ON, 2 OFF
5 ON, 2 OFF

Fig. 11—Effect of heat-time variation on nugget penetration and welding current. 22-gage terne plate; 900-lb electrode force; welding speed, 100 ipm

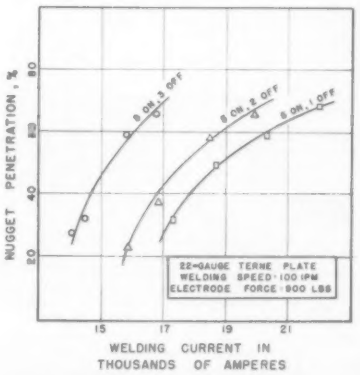
NUGGET PENETRATION, %
WELDING CURRENT IN THOUSANDS OF AMPERES
3 ON, 3 OFF
3 ON, 2 OFF
3 ON, 1 OFF
22-GAUGE TERNE PLATE
WELDING SPEED · 100 IPM
ELECTRODE FORCE · 900 LBS

Fig. 13—Effect of cool-time variation on nugget penetration and welding current. 22-gage terne plate, 900-lb electrode force; welding speed, 100 ipm

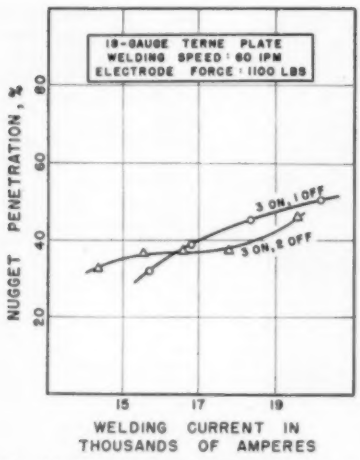

Fig. 14—Effect of cool-time variation on nugget penetration and welding current. 18-gage terne plate; 1100-lb electrode force; welding speed, 60 ipm

the electrical resistance of the weldment at the point of the next current impulse. The slight reduction in resistance tends to cause less total heat to be generated between the electrodes; however, this loss is more than offset by the heating effect produced by the proportional increase in the current which flows through the weld area, since heat is proportional to RI^2.

The findings in the 18-gage material were not at all similar to the results obtained in the 22- and 20-gage terne plate as may be seen in Fig. 14. This is because increased cool time increased the current required to achieve a given pene tration. Apparently, the heavier gage material introduces some new consideration to the welding operation; possibly an increase in electrical resistance or an increase in heat dissipation due to larger amounts of surrounding metal. Either one of these possibilities or a combination of two of them might account for the increase in current required to obtain a given penetration, but they provide no ready explanation for the transition range in which penetration remained unchanged by substantial increases in current.

Continuous Current. Continuous current was investigated because it offered a means of achieving nugget overlap at high welding speeds. It was found that nugget overlap was consistent, but that close control of the welding current was mandatory to minimize weld defects. Slight overheating of the weld produced large voids and longitudinal cracks as shown in Fig. 15. The defects pictured in Fig. 15 occurred in a weld possessing only 35% penetration made with 900-lb electrode force, at a welding speed of 150 ipm, and with welding current of 22,000 amp. Welds with higher penetrations contained larger voids.

Welds made with currents insufficient to produce weld nuggets were sporadic combinations of soldering and solid phase bonding. The solid-phase bonding appeared very much as that pictured in Fig. 17. It appears that, if sound welds are to be produced by continuous current, the nugget formation should be avoided, especially for high welding speeds where the release of the electrode force is premature; also, emphasis should be placed on the pressure welding obtained with low welding current.

The sporadic solid-phase bonding obtained might be improved by reducing the width of the electrode face or by increasing electrode force. If dependable pressure welding were achieved, then it might also be possible to increase welding speed.

Weld Defects. Weld quality in each of the three gages of terne plate was found to be most affected by electrode force and cool time. Generally, welds made with less than optimum electrode force were degraded by the presence of inclusions and widely distributed porosity. Welds made with electrode force above the optimum suffered from surface indentation and severe squeezing of the weld nugget.

The cool time employed to produce a weld was also a factor in determining weld quality. Generally, reducing the cool time to one cycle tended to overheat the weld area and cause porosity and shrinkage cracks in the nugget. A cool time of two cycles normally produced welds with less porosity and shrinkage defects. Welds made with three cooling cycles were about equal in quality to the two-cooling-cycle welds except that nugget overlap was lacking.

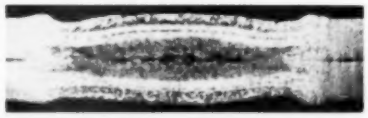

Fig. 16—Shrinkage defect caused by excessive heat time. Surface indentation and bulging at center of weld due to defective electrode face. × 12. (Reduced by 1/2 upon reproduction)

The over-all effect of cool time, however, must be judged with consideration given to heat time, material thickness and current magnitude. Excessive current produces welds having porosity and shrinkage defects. Figure 16 shows a weld made with an excessive heat time of 6 cycles which was partially remedied by 2-cycles cool time; but even so, the nugget in the 18-gage specimen was overheated and displayed a large shrinkage defect.

Lack of nugget overlap was a problem associated with the 22- and 20-gage terne plate at the higher welding speed of 100 ipm. Nugget overlap was found to be improved with an increase in material thickness, due to the increased heating associated with the increase in resistance. For this reason, nugget overlap improved from marginal in the 22-gage terne plate to moderate in the 20-gage terne plate, and to more than adequate in the 18-gage material.

Figure 17 is a micrograph of the region between two of the layers or bands of martensite, and reveals that solid-phase bonding has been accomplished. In pillow tests, welds of this nature displayed no pin-hole leaks up to 100 psi and

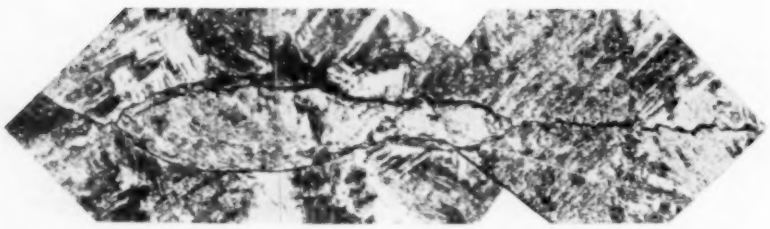

Fig. 15—Composite micrograph of weld defect found in a weld produced in 22-gage terne plate with 900-lb electrode force, welding speed of 150 ipm, and 22,000 amp of continuous current. Nugget penetration was 35%. Micrograph shows less than half of the actual defect. × 156. (Reduced by 1/2 upon reproduction)

withstood pressure of over 200 psi before failure occurred outside the seam weld.

Transverse cracking was a weld defect that was found rather frequently in 22-gage terne plate, occasionally in 20-gage terne plate and not at all in the 18-gage material. These cracks were detected largely in welds of higher penetration, and occurred invariably in the depressions which were formed in the weld surface by the knurled electrode faces. Figure 18 is a macrograph of a longitudinal section of two welds showing unusually large cracks which pass completely through the weld. It was found that the cracks ranged in size from the microscopically small to the visibly large. The consistent location of the transverse cracks in the impressed furrows suggests that these cracks are caused by thermal and vibrational stresses. Depressions would serve to concentrate the stresses and trigger the crack propagation. This view is somewhat supported by the routine observation that the 22-gage weldments were subjected to severe vibration due to the fluctuating magnetic field surrounding the welding operation.

To test this idea, a simple fixture was added to the backup plate used to guide the strips between the electrodes. A small shelf was placed about four inches to the side and a quarter inch above the point of contact with the electrodes. The purpose of the shelf was to lift the weldments and maintain a slight spring tension in them as they emerged between the electrodes. With this device, welds were made in the 22-gage material at the same conditions which produced cracking in the first welds. There was a definite reduction in the vibration observed during the welding operation, and no large cracks were found in the metallurgical specimens. Some small transverse cracking occurred, but magnification was required to detect the small and infrequently spaced cracks.

Nugget Hardness. A survey of the hardness across a weld area was made using a Knoop hardness tester. It was found that the dark etched layers at the upper and lower surfaces of the weld were harder than any other structure in the weld area, possessing a Rockwell "B" hardness of 108. This exceeded the Rockwell "B" hardness of 95, which is the maximum hardness obtainable in steel with the carbon content involved in this investigation. A similar structure and hardness had been encountered by Volek[1] in his investigation of galvanized steel, and an investigation into the source of the unexpected hardness found that carbon concentration occurred in some areas and produced the high hardness.

That a similar structure and events occur in terne plate should be expected, since the chemical analyses for the terne-coated and galvanized steels were very similar. The fact that the structures and hardness were similar, also detracts from the idea that the "extra" hardness was due to alloying of the coating with the steel. If this were the case, then it would be expected that the hardness of the "galvanized" dark areas would differ from the "terne plate" dark areas.

For the welds made in this investigation there was a heat-affected zone (HAZ) composed of large grains in the region between the dark etched layers and the nugget. The hardness of the heat-affected zone was about 72 on the Rockwell "B" scale. Across the nugget the hardness was near the maximum attainable with 0.06%-carbon steel. The nugget hardness was 93 on the Rockwell "B" scale. Figure 19 presents the findings of the hardness survey. A hard material possesses high strength, but it is also brittle; therefore, the presence of the dark etched layers near the surface was conducive to cracking and contributed to the production of transverse cracks.

Corrosion Resistance. For comparison, a few galvanized-steel specimens were included with the terne-plate specimens in the corrosion test. The welds in the galvanized material quickly developed a white "frosting" over their entire surface; while the terne-plate specimens in the same interval developed rust areas on and near the seam weld.

The corrosion specimens were 1-x 2-in. sections cut from the test weld strips. In the 100% humidity room, the specimens were inclined at an angle from the vertical. Since a fine spray was ejected into the test chamber near the ceiling, the inclination of the specimens tended to produce a wet upper and a dry lower surface on each specimen. The abundance of water on the upper surface caused extensive rusting, and the surface was heavily coated with a layer of red and orange oxide. The lower surface, however, was only locally attacked, with the rust areas developing where there were irregularities in the weld surface. Corrosion on the dry side of the specimen was limited, and in the four-month test period appeared to do no great harm to the weld. However, the aqueous attack on the upper side of the specimen was severe and concentrated along the edge of the weld. The welding operation did not remove all of the terne from the path of the weld,

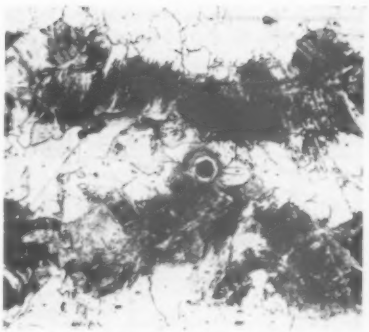

Fig. 17—Micrograph of solid-phase bonding achieved between the bands of hard constituent which connect the nugget. × 156. (Reduced by 1/2 upon reproduction)

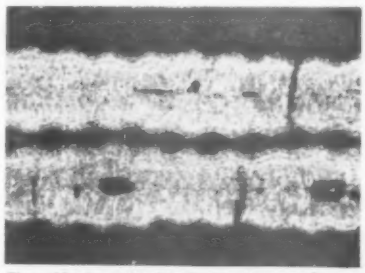

Fig. 18—Longitudinal sections of two welds possessing unusually large transverse cracks completely through the weld. × 10. (Reduced by 1/3 upon reproduction)

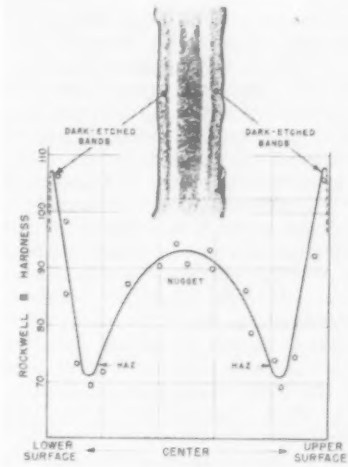

Fig. 19—Survey of the hardness across a weld nugget

Table 2—Recommended Schedule for Seam Welding 22-, 20- and 18-Gage Terne Plate

THICKNESS		ELECTRODE FACE WIDTH,	ELECTRODE FORCE		WELDING SPEED,	CURRENT TIMING, cycles		WELDING CURRENT,	PERCENT HEAT
inches	gauge	inches	MIN. lbs.	MAX. lbs.	ipm	ON	OFF	amperes	
.031	22	9/32	800	1000	50	3	2	17,000	78
					100	5	2	18,000	74
.036	20	9/32	900	1100	60	2	1	17,500	74
					100	5	1	18,500	70
.049	18	9/32	1000	1200	60	2	1	18,000	70
					100	4	1	19,000	70

but enough was removed to expose the steel to corrosion attack. The corrosion resistance of welded terne plate was only moderate and was much less than that of welded galvanized steel.

Electrode Life. Alloying of terne metal with the electrodes occurred in the seam-welding operation and produced a marked change in weld-surface appearance and electrode contour. The first welds were made with new and freshly machined electrodes and were accompanied by flashing and a tendency for electrode sticking. As welding continued, the alloy coating on the electrodes increased and the weld surfaces lost their sticky, melted appearance and began to show distinct ridge impressions from the knurled electrode face. Flashing and electrode sticking were reduced even for high welding currents. After 600 ft of welding, the alloying on the electrodes had produced a line depression in the middle of the electrode face which encircled the electrode wheel. Also, the contour of the electrode face had been changed from flat to concave. Other effects were increased electrode indentation at the edge of the weld and bulging at the center of the weld. Reference is made to Fig. 16 to illustrate the indentation and bulging produced in the weld.

For the concave shape to have developed, more alloying must have occurred at the center of the electrode face than at its edges. The conditions surrounding the welding event were such as to produce increased wear at the center of the electrode face. The heat generated at the weld surfaces was dissipated by conduction and water cooling. The center of the electrode face was less affected by these cooling processes than were the edges; therefore, its higher temperature was conducive to more alloying and wear.

Electrode life was not much greater than 500 ft due to the bulge in weld thickness. This compares to an estimated electrode life of over a thousand feet for galvanized steel. The vaporization of zinc removed it from the weld area so that little remained to alloy with the electrodes; whereas, with the melting of terne alloy, the coating remained in close contact with the electrodes and was readily available for electrode pickup. It is expected that electrode life could be greatly improved if additional cooling were available.

Conclusions

Based upon an evaluation of the results obtained in this investigation, the seam-welding schedule in Table 2 is given as a guide for welding 22-, 20- and 18-gage terne plate, and the following conclusions are presented:

1. The optimum electrode force for a given gage of terne plate is independent of the welding speed.

2. For a given gage of material, the optimum electrode force is the same for terne plate and galvanized steel.

3. The welding current recommended for welding terne plate is in line with that recommended for galvanized steel.

4. The optimum current timing is the most difficult evaluation to make and the timings presented in Table 2 should be interpreted as being approximate rather than final determinations.

5. A fitted knurled driving roller is necessary to remove pickup from the electrodes and to prevent mushrooming.

6. The most common weld defect was porosity, which was present, more or less, in all welds.

7. Transverse cracking can be eliminated or greatly reduced by restricting the vibration of the weldments after passing between the electrodes.

8. The corrosion resistance of welded terne plate is much less than that of welded galvanized steel, and judgment should be exercised in using such welds where they would be exposed to water for long periods.

9. Electrode life is limited in seam welding terne plate, but this difficulty might be removed if a means were provided for increased cooling.

10. Lack of nugget overlap does not necessarily imply a "leaky" seam weld, since "martensitic" pressure welds occur between the nuggets.

11. By employing continuous current and higher interface pressures to produce solid-phase bonding, it seems likely that welding speed could be increased.

Acknowledgment

The copper-base RWMA Class II alloy electrodes were donated by P. R. Mallory and Company; the hot-dip coated 22-, 20- and 18-gage commercial-quality steel sheets were contributed by Republic Steel Corp.

References

1. Volek, C. W. and Begeman, M. L., "Effect of Zinc Coatings on Resistance Seam Welding of Sheet Steel," THE WELDING JOURNAL, **38** (3) Research Suppl., 113-s to 121-s (1959).

2. Allen, W. J. and Begeman, M. L., "Seam Welding Galvanized Steel," *Ibid.*, **37** (4) Research Suppl., 138-s to 143-s (1958).

3. Resistance Welder Manufacturers' Association, *Resistance Welding Manual*, Revised Edition, Philadelphia, Pa (1948).

Arc Welding of 5% Cr–0.5% Mo Alloy-Steel Pipe

Wide use of low-chromium-molybdenum steels in petroleum industry prompts study on properties of weldments of these steels, particularly with reference to extent to which thermal treatments are required to obtain satisfactory properties

BY J. BLAND AND G. F. TISINAI

ABSTRACT. Unrestrained weldments were made using 5% Cr – ½% Mo alloy-steel pipe and 5% Cr – ½% Mo, 1¼% Cr – ½% Mo, 25% Cr – 12% Ni or 25% Cr – 20% Ni electrodes. The hardness and tensile properties were correlated for both 5% Cr – ½% Mo alloy-steel pipe material and 5% Cr – ½% Mo alloy weld deposits. The heat-affected zones of the 5% Cr – ½% Mo alloy-steel pipe had adequate ductility even in the absence of preheat or postheat treatments. Postheat temperatures of 1250° F and above imparted appreciable ductility to 5% Cr – ½% Mo weld metal; however, a temperature of 1400° F gave markedly more ductility and is preferred. If 1¼% Cr – ½% Mo, 25% Cr – 12% Ni or 25% Cr – 20% Ni electrodes were used for unrestrained weldments of 5% Cr – ½% Mo alloy-steel pipe, no preheat or postheat treatments were needed to obtain adequate weld ductility. However, refinery experience has indicated that austenitic stainless-steel welds on ferritic base metals may crack eventually when subjected to thermal cycling.

Introduction

The wide use of low-chromium-molybdenum steels in the petroleum industry has prompted a series of studies on the properties of weldments of these steels, particularly in reference to the extent to which thermal treatments are required to obtain satisfactory properties. Three previous papers[1–3] have described the results of welding 0.5% Cr – 0.5% Mo, 1.25% Cr – 0.5% Mo and 2.25% Cr – 1.0% Mo steels. This paper will describe the results of a similar study made on 5.0% Cr – 0.5% Mo steel. In the earlier papers, particular reference was made to the resistance of the Cr – Mo steels both to graphitization and to high-temperature hydrogen attack.

The American Standard Code for Pressure Piping[4] recommended a minimum preheat temperature of 450° F and a minimum stress-relieving temperature of 1200° F. This treatment is accepted also by the AMERICAN WELDING SOCIETY.[5] The Pipe Fabrication Institute[6] recommends a 250° F minimum preheat temperature before tack welding, and a 400 to 700° F preheat and interpass temperature or a partial stress relief between 1200 and 1400° F for 30 min or more if welding is interrupted. Postheat treatment of 1325 to 1400° F for 1 hr per in. of thickness, but not less than 1 hr, also is recommended by the Institute. The AWS Standard for Interruption of Heat Treatment[7] states that the heating cycle may be safely interrupted for the 5.0% Cr – 0.5% Mo steel in wall thicknesses 1 in. and below, provided it is welded under controlled procedures using low-hydrogen electrodes. However, the weld deposit should never be less than one-third the wall thickness or two layers, whichever is greater. Holmberg[8] reported on the weldability of the ferritic 5 to 9% Cr – 0.5 to 1% Mo steels and the use of austenitic electrodes when postheating could not be done readily.

As in the past studies of this series, particular emphasis was placed on a correlation of the hardness measurements of the weld metal and heat-affected zones with the ductility values exhibited in both tensile and bend specimens. The need of such a correlation is emphasized in particular when electrodes depositing high-strength weld metal are used, since deformation in these specimens under load occurs preferentially in the lower strength base metal.

The mechanical property most difficult to evaluate from the tests of weldments is ductility. A butt-weld tensile-test specimen, for example, involves a composite volume of metal including unaffected base metal, deposited weld metal and heat-affected base and weld metals. Each portion contributes to the over-all deformation to varying degrees. The extent of such variation can be determined most readily by a hardness survey across the weld section, providing the ductility of the particular zone can be correlated with the particular hardness level. If this correlation is unknown, there can be no sound basis in using the hardness measurements for the evaluation of the weld.

In the text of this paper, the following designations will be used: 1¼ Cr Mo for 1.25% Cr – 0.5% Mo steel, 5 Cr Mo for 5.0% Cr – 0.5% Mo steel, 25–12 Cr Ni for the 25% Cr – 12% Ni austenitic stainless steel and 25–20 Cr Ni for the 25% Cr – 20% Ni austenitic stainless steel.

Experimental Procedures

Portions of 5 in.-schedule 160, 5 Cr Mo steel pipe were heat treated to the 1700° F normalized, 1700° F water quenched, 1700° F water quenched and tempered, 1900° F normalized, 1900° F water quenched and 1900° F water quenched and tempered states. The analysis of the pipe is given in Table 1. Button-head, 0.505-in. diam tensile bars were made from such heat-treated materials, as well as from as-received stock, and tested to failure in a hydraulic testing

J. BLAND, formerly with Standard Oil Company (Indiana), is Consulting Engineer, Welding Metallurgy and Development, Knolls Atomic Power Laboratory, General Electric Co., Schenectady, N. Y., and G. F. TISINAI is a Project Supervisor, Engineering Research Department, Standard Oil Co. (Indiana), Whiting, Ind.

Alternate paper for AWS 41st Annual Meeting held in Los Angeles, Calif., April 25–29, 1960.

Table 1—Chemical Composition of Deposited Weld Metal and Alloy Pipe Material

Brand code	AWS class	Covering type	Chemical composition, % C	Mn	P	S	Si	Cr	Mo
Electrode No. 1	E502-15	Low hydrogen	0.04	0.43	0.011	0.013	0.87	4.50	0.64
Electrode No. 2	E502-15	Low hydrogen	0.10	0.47	0.011	0.015	0.82	4.33	0.71
Electrode No. 3	E502-15	Low hydrogen	0.06	0.55	0.014	0.012	0.24	5.19	0.59
Electrode No. 4	E502-18	Iron powder-low hydrogen	0.06	0.64	0.022	0.014	0.45	4.18	0.64
Pipe material	...	...	0.13	0.42	0.014	0.014	0.39	4.85	0.57

machine. The button heads of all tensile specimens were cut off and their hardnesses determined by Rockwell B and C tests. These hardness values then were converted to Brinell hardness values. Equations correlating the hardness and tensile data were obtained by analyzing the data on an IBM 705 digital computer. Particular emphasis will be placed on the equation correlating hardness with percent elongation in 2 in. (hereafter referred to as "ductility").

Test plates for all-weld-metal specimens of four different brands of 5 Cr Mo electrodes were made in accordance with AWS specifications. Analyses of the as-deposited metals are given in Table 1. The test plates were made with combinations of 300, 500° F and no preheats with both 1350° F and no postheats. Duplicate all-weld-metal, button-head, 0.505-in. diam tensile bars were made from each weld deposit and tested to failure in a hydraulic testing machine. The button heads of all tensile specimens were cut off and their hardnesses determined by Rockwell B and C tests. These hardness values then were converted to Brinell hardness values. Equations correlating the hardness and tensile data were obtained by analyzing the data on the digital computer.

Full-thickness, multipass butt welds were made between $2^1/_2$-in. long sections of the 5-in., schedule 160, 5 Cr Mo steel pipe with electrode brand No. 1. All weld joints were 60-deg included-angle single vees with a $^1/_{32}$ to $^1/_{16}$-in. root face and a $^3/_{32}$ to $^1/_8$-in. root opening. Backing straps were not used. One weldment was made with each of 300° F, 500° F and no preheats. All welds were made in the flat position (pipe horizontally rolled) with welding current in the range recommended by the manufacturer of the electrode. Each welded ring was cut longitudinally into 16 pieces, and the individual pieces were postheated for $^1/_2$, 1, 2 and 4 hr at each of the temperatures 1250, 1300, 1350 and 1400° F. Hardness measurements were made of the welds, heat-affected zones and base metals on each of the 48 pieces after they had been polished suitably.

Full-thickness multipass butt welds were made between 6-in. long sections of the 5-in., schedule 160, 5 Cr Mo steel pipe with each of the electrodes listed in Table 1. All weld joints were 60 deg included-angle single vees with a $^1/_{32}$ to $^1/_{16}$-in. root face and a $^3/_{32}$ to $^1/_8$-in. root opening. Backing straps were not used. The welds were made with four preheat-postheat combinations, viz., 300–1250° F, 500–1250° F, 300–1350° F and 500–1350° F. All postheat times were 1 hr. All welds were made in the flat position (pipe horizontally rolled) with welding currents in the range recommended by the manufacturers of the particular electrodes. Side-bend, notch-bend, hardness-measurement and Charpy V-notch impact specimens were prepared from the weldments. Longitudinal bend specimens were prepared from full-thickness longitudinal butt welds made between 6-in. long quarter sections of the pipe under similar welding conditions described above.

Full-thickness multipass butt welds were made between 6-in. long sections of the 5-in., schedule 160, 5 Cr Mo pipe with austenitic stainless-steel electrodes of the 25–12 Cr Ni and 25–20 Cr Ni compositions and the low-alloy ferritic electrode of the $1^1/_4$ Cr Mo composition. Conditions of welding were similar to those described previously for 5 Cr Mo electrodes except for preheat-postheat conditions. The welds made with the austenitic stainless-steel electrodes were made both with no preheat and with a 500° F preheat. No postheats were made. The welds made with the $1^1/_4$ Cr Mo electrode were made with a 300° F preheat followed by both no postheat and a 1250° F-1 hr postheat. Side-bend, notch-bend and hardness-measurement specimens were prepared from the weldments.

Results

Hardness–Tensile Properties of 5 Cr Mo Pipe Metal. The tensile properties of heat-affected zones of pipe welds are virtually impossible to obtain directly because of their small volume. However, the microstructures of such zones usually are intermediate between the microstructures of the base metal in the normalized and in the water-quenched (from austenitizing temperatures) conditions. Through the heat treatments given this pipe metal, a variety of microstructures was obtained which had various hardness values. The data obtained in these experiments showed that the hardness and tensile properties produced by any given tempering treatment were very similar whether the temperature from which the sample was water quenched was either 1700 or 1900° F (see Table 2 and Fig. 1). The correlation between the hardness and tensile data obtained by the digital computer analysis are given below. The precision limits for the quadratic equations were much better than those for the linear equations:

	Precision limits for corresponding linear equations
Yield strength, psi $= 1331.1\ \text{Bhn} - 1.73\ (\text{Bhn})^2 - 122{,}230$ ($\pm 11{,}160$ psi)	±18,090 psi
Tensile strength, psi $= 246.52\ \text{Bhn} + 0.503\ (\text{Bhn})^2 + 26{,}480$ (± 7120 psi)	±9,170 psi
% Elongation in 2 in. $= 69.92 - 0.314\ \text{Bhn} + 0.00044\ (\text{Bhn})^2$ (i.e., ductility) (±2.42%)	±4.34%
% Reduction of area $= 56.98 + 0.211\ \text{Bhn} - 0.00056\ (\text{Bhn})^2$ (±4.74%)	±6.60%

The curves for the above equations were drawn by the 705 computer and the one correlating ductility and hardness is shown in Fig. 2. By applying the equations to hardness data obtained in heat-affected zones of pipe welds, the tensile properties of the heat-affected zones can be approximated.

Table 2—Mechanical Properties of Heat-treated 5 Cr Mo Steel Pipe

Specimen no.	Thermal treatment	Hardness, Bhn[a]	Yield strength, psi[b]	Ultimate strength, psi	Elongation, % in 2 in.	Reduction of area, %
1	As received	151	44,100	76,000	33.5	75.5
2	1700 F—1 hr—air cool	362	121,000	190,000	14.0	55.0
3	1700 F—1 hr—H_2O	372	140,000	190,000	12.0	62.0
4	1700 F, H_2O, 1100 F—$^1/_2$ hr	322	135,000	153,000	15.5	72.0
5	1700 F, H_2O, 1100 F—1 hr	283	122,000	138,000	16.0	74.0
6	1700 F, H_2O, 1100 F—2 hr	270	117,000	134,500	17.5	73.5
7	1700 F, H_2O, 1100 F—4 hr	260	109,000	126,000	18.5	73.5
8	1700 F, H_2O, 1200 F—$^1/_2$ hr	250	102,800	121,000	18.5	74.5
9	1700 F, H_2O, 1200 F—1 hr	240	95,000	112,700	19.0	76.0
10	1700 F, H_2O, 1200 F—2 hr	222	89,000	108,000	21.0	75.0
11	1700 F, H_2O, 1200 F—4 hr	222	84,500	104,000	21.5	74.5
12	1700 F, H_2O, 1300 F—$^1/_2$ hr	216	81,000	101,000	23.0	76.0
13	1700 F, H_2O, 1300 F—1 hr	210	77,000	99,000	24.0	77.0
14	1700 F, H_2O, 1300 F—2 hr	195	71,000	94,600	25.0	77.0
15	1700 F, H_2O, 1300 F—4 hr	190	66,000	91,000	25.5	76.0
16	1700 F, H_2O, 1400 F—$^1/_2$ hr	200	69,500	93,700	26.0	77.0
17	1700 F, H_2O, 1400 F—1 hr	190	64,500	89,000	28.0	78.0
18	1700 F, H_2O, 1400 F—2 hr	176	60,000	86,000	30.0	76.0
19	1700 F, H_2O, 1400 F—4 hr	169	55,400	83,600	30.0	78.0
20	1900 F—1 hr—air cool	362	119,000	184,000	14.5	51.0
21	1900 F—1 hr—H_2O	382	139,000	187,000	13.0	59.0
22	1900 F, H_2O, 1100 F—$^1/_2$ hr	322	133,000	150,000	14.0	70.0
23	1900 F, H_2O, 1100 F—1 hr	276	124,000	140,000	16.5	72.0
24	1900 F, H_2O, 1100 F—2 hr	270	115,000	133,000	18.0	73.0
25	1900 F, H_2O, 1100 F—4 hr	265	110,000	127,000	18.5	72.0
26	1900 F, H_2O, 1200 F—$^1/_2$ hr	250	103,000	120,000	19.0	73.0
27	1900 F, H_2O, 1200 F—1 hr	240	95,500	113,500	19.0	74.5
28	1900 F, H_2O, 1200 F—2 hr	228	89,000	107,000	20.0	74.5
29	1900 F, H_2O, 1200 F—4 hr	216	85,000	104,000	19.5	76.0
30	1900 F, H_2O, 1300 F—$^1/_2$ hr	216	81,000	101,000	22.5	78.0
31	1900 F, H_2O, 1300 F—1 hr	216	79,000	101,000	23.5	76.0
32	1900 F, H_2O, 1300 F—2 hr	210	74,500	96,000	24.0	77.0
33	1900 F, H_2O, 1300 F—4 hr	185	70,300	93,000	24.0	77.0
34	1900 F, H_2O, 1400 F—$^1/_2$ hr	185	71,800	95,500	25.0	78.0
35	1900 F, H_2O, 1400 F—1 hr	190	67,000	91,700	25.0	77.0
36	1900 F, H_2O, 1400 F—2 hr	185	61,700	87,000	27.5	77.0
37	1900 F, H_2O, 1400 F—4 hr	172	56,400	83,000	27.5	77.0

[a] Converted from Rockwell hardness measurements.
[b] 0.2% permanent set.

Table 3—Mechanical Properties of Deposited Weld Metal

Electrode no.	Preheat, °F	Postheat, °F	Hardness, Bhn[a]	Yield strength, psi[b]	Ultimate strength, psi	Elongation, % in 2 in.	Reduction of area, %
1	None	None	290	91,500	118,000	8.0	15.0
1	None	None	245	97,500	119,000	17.5	53.5
1	300	1350	240	91,500	104,000	21.0	67.0
1	300	1350	228	89,600	102,000	21.0	67.0
2	None	None	240	87,000	113,000	15.0	50.5
2	None	None	240	89,600	115,000	8.0	28.0
2	None	1350	185	71,000	88,700	23.0	64.0
2	None	1350	195	71,500	89,000	22.5	67.0
2	300	None	223	89,600	114,500	16.0	49.0
2	300	None	240	91,500	114,500	7.5	31.0
2	300	1350	195	70,700	88,700	25.0	63.0
2	300	1350	195	72,500	89,500	22.5	65.5
2	500	None	220	83,500	114,000	16.5	49.5
2	500	None	240	87,500	118,000	12.5	42.5
3	None	None	332	121,000	145,000	2.0	6.5
3	None	None	322	116,000	148,000	12.0	42.0
3	300	1350	190	74,700	90,000	22.0	70.0
3	300	1350	190	77,500	92,100	22.0	68.5
4	300	1350	216	84,000	98,500	19.0	56.0
4	300	1350	210	83,700	98,500	21.5	68.0

[a] Converted from Rockwell hardness measurements.
[b] 0.2% permanent set.

Hardness–Tensile Properties of 5 Cr Mo Weld Metal. The tensile properties of weld metal in pipe welds cannot be obtained readily by direct tests because tensile bars made from weldments usually fail in the base metal rather than in the weld metal. The hardness and tensile data obtained from the samples made from the all-weld-metal specimens are listed in Table 3. The correlation between the hardness and tensile data obtained by the digital computer analysis is given in adjacent column. The equations are given in linear form since the precision limits for the corresponding quadratic equations are not much different.

	Precision limits for corresponding quadratic equations
Yield strength, psi = 300.14 Bhn + 17,400 (±9360 psi)	±9,590 psi
Tensile strength, psi = 376.17 Bhn + 20,485 (±12,190 psi)	±11,865 psi
% Elongation in 2 in. = 51.88 − 0.154 Bhn (i.e., ductility) (±6.82%)	±6.94%
% Reduction of area = 154.15 − 0.451 Bhn (±19.52%)	±20.08%

The curves for the above equations were drawn by the 705 computer and the one correlating ductility and hardness also is shown in Fig. 2. By applying the equations to hardness data obtained from weld metal in pipe welds, the tensile properties of the weld metal can be approximated.

These data indicate that the pipe metal has a greater ductility at a given hardness value than the weld metal. This difference is very pronounced at hardnesses above 225 Brinell. In comparing all of the tensile properties at various hardness levels, those of the pipe metal generally show much less deviation from the curves than do those of the weld metal.

Table 4—Effect of Preheat and Postheat (Time and Temperature) on Hardness–Ductility of Welds Made on 5% Cr – ½% Mo Steel Pipe Using Brand No. 1 (5% Cr – ½% Mo) Electrode

Preheat, °F	Postheat, F and Hr	Brinell hardness[a] Weld	Brinell hardness[a] Heat-affected zone	Brinell hardness[a] Pipe	Calculated ductility[b] Weld	Calculated ductility[b] Heat-affected zone
0	1250—½	250	233	141	13.1	20.4
300	1250—½	257	237	142	12.1	20.2
500	1250—½	249	240	144	13.3	19.8
0	1250—1	242	235	139	14.2	20.1
300	1250—1	240	233	140	14.7	20.3
500	1250—1	249	229	144	13.2	21.2
0	1250—2	240	235	141	14.7	20.1
300	1250—2	250	237	144	13.1	20.2
500	1250—2	247	226	139	13.6	21.5
0	1250—4	240	233	139	14.7	20.4
300	1250—4	248	213	137	13.4	22.8
500	1250—4	247	224	139	13.6	21.6
0	1300—½	231	215	147	16.1	22.4
300	1300—½	231	199	140	16.1	24.8
500	1300—½	231	209	140	16.1	23.5
0	1300—1	228	209	139	16.6	23.5
300	1300—1	229	210	141	16.5	23.6
500	1300—1	231	200	141	16.1	24.8
0	1300—2	233	212	140	15.8	23.0
300	1300—2	229	210	140	16.5	23.6
500	1300—2	228	213	142	16.6	22.8
0	1300—4	226	210	144	16.7	23.6
300	1300—4	224	213	144	16.9	22.8
500	1300—4	233	205	142	15.8	23.8
0	1350—½	240	228	144	14.7	21.2
300	1350—½	235	231	137	15.5	20.9
500	1350—½	240	220	140	14.7	22.0
0	1350—1	238	218	142	14.9	22.3
300	1350—1	231	226	145	16.1	21.5
500	1350—1	240	210	145	14.7	23.6
0	1350—2	237	224	144	15.0	21.6
300	1350—2	233	210	144	15.8	23.6
500	1350—2	231	215	144	16.1	22.4
0	1350—4	234	195	142	15.7	25.4
300	1350—4	240	215	140	14.7	22.4
500	1350—4	233	220	143	15.8	22.0
0	1400—½	215	202	145	18.7	24.4
300	1400—½	215	209	143	18.7	23.5
500	1400—½	213	199	142	18.9	24.8
0	1400—1	235	216	145	15.5	22.4
300	1400—1	235	215	143	15.5	22.4
500	1400—1	231	211	148	16.1	23.3
0	1400—2	207	187	151	19.7	26.7
300	1400—2	209	185	142	19.4	27.0
500	1400—2	204	182	143	20.1	27.3
0	1400—4	187	182	145	23.0	27.3
300	1400—4	191	177	140	22.5	28.1
500	1400—4	190	170	142	22.6	29.2

[a] Converted from Rockwell C hardness.
[b] As calculated from the appropriate equations.

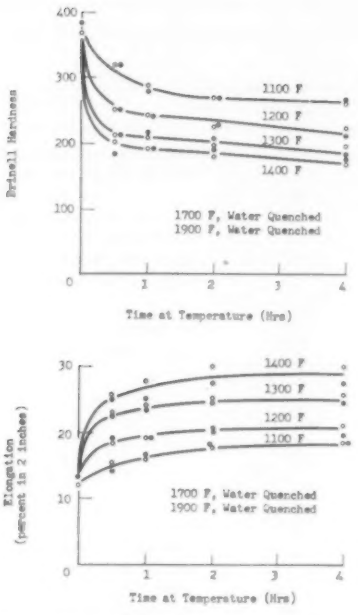

Fig. 1—Effect of temperature and time of tempering on hardness and ductility of 5 Cr Mo steel, water quenched from 1700° F and from 1900° F

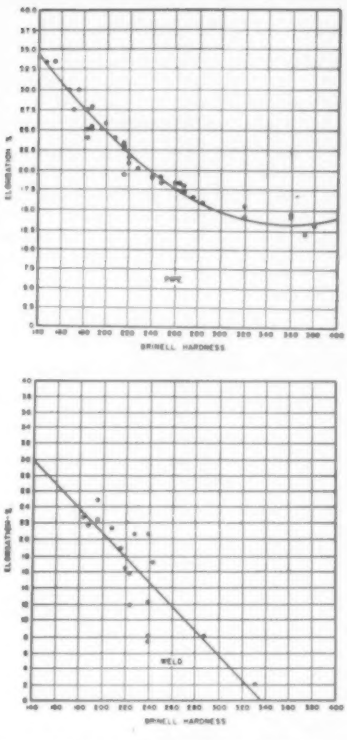

Fig. 2—The curves drawn by the 705 computer for the equations relating the hardness and ductility for the pipe and the weld metals

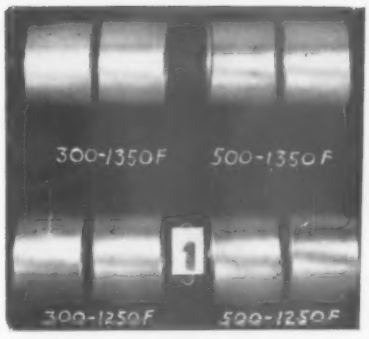

Fig. 3—Longitudinal bend specimens of weldments made on 5 Cr Mo pipe with the 5 Cr Mo electrode No. 1. Approximately × 1/4

Effect of Various Preheats and Postheats on the Hardness of 5 Cr Mo Weldments. The hardness measurements and the calculated ductility values of the welds and heat-affected zones on each of the 48 pieces of pipe weld made with electrode brand No. 1 with the variety of preheats and postheats are given in Table 4.

The ductility of weld metal using normal welding practice is less for any given preheat-postheat treatment than the ductility of weld metal made according to AWS specifications for producing all weld-test samples. This discrepancy is due to the differences in techniques in making the welds and does not indicate that the pipe welds are unacceptable. The data show that preheats up to 500° F do not affect the final hardnesses of welds and heat-affected zones whereas postheats do. The calculated ductilities of welds is between 12.1 and 14.7% for a 1250° F postheat, 15.8 and 16.9% for a 1300° F postheat, 14.7 and 16.1% for a 1350° F postheat and 15.5 and 23.0 % for a 1400° F postheat. It must be remembered that in the all-weld-metal samples, the measured ductilities of samples given a 1350° F postheat were between 19.0 and 25.0%. In comparing the data for the 1400° F postheat, an anomaly appears. The 1/2-hr treated samples show ductilities of 18.7 to 18.9% whereas the 1-hr treated samples show ductilities of 15.5 to 16.1%. However, the ductilities of the 2- and 4-hr treated samples are all above 19.4%. The calculated ductilities of the heat-affected zones for all postheats ranged between 19.8 and 29.2%.

Weldments on 5 Cr Mo Pipe Made

Table 5—Effect of Preheat and Postheat on Hardness–Ductility of 5 Cr Mo Steel Pipe Welds Using 5 Cr Mo Electrodes

Electrode no.	Preheat, ° F	Postheat, ° F[a]	Brinell hardness[b] Weld	Brinell hardness[b] Heat-affected zone	Brinell hardness[b] Pipe	Calculated ductility[c] Weld	Calculated ductility[c] Heat-affected zone
1	300	1250	250	210	132	13.5	23.6
	500	1250	240	228	137	14.5	21.2
	300	1350	234	210	132	15.9	23.2
	500	1350	240	222	135	14.5	21.8
2	300	1250	228	210	132	16.6	23.6
	500	1250	228	210	135	16.6	23.6
	300	1350	265	260	141	10.9	17.7
	500	1350	210	205	130	19.5	23.8
3	300	1250	216	210	135	16.6	23.6
	500	1250	240	216	135	14.5	22.4
	300	1350	240	216	132	14.5	22.4
	500	1350	210	210	130	19.5	23.6
4	300	1250	235	222	127	15.1	21.8
	500	1250	234	216	135	15.9	22.4
	300	1350	313	276	139	3.5	16.6
	500	1350	222	222	135	17.3	21.8

[a] Postheat treatment for 1 hr at temperature.
[b] Converted from Rockwell B and C hardness values.
[c] As calculated from the appropriate equation.

Table 6—Bend Tests of Welds in 5 Cr Mo Steel Pipe Using 5 Cr Mo Electrodes

			Longitudinal bend[a]			Side bend[d]		
Electrode, no.	Preheat, °F	Postheat[b] °F	Bend angle, deg	Elongation, %[c]	Remarks	Bend angle, deg	Pass[e] or fail	Remarks
1	300	1250	180	22	.....	180	4P	One sample had a 1/16-in. tear at edge
1	500	1250	180	22	.....	180	4P	.....
1	300	1350	180	22	.....	180	4P	1/8-in. tear in center of finish pass on surface
1	500	1350	180	22	.....	180	4P	One sample had a 1/16-in. tear in final pass
2	300	1250	180	22	.....	180	4P	.....
2	500	1250	180	22	One very small pinhole opened up	180	4P	One sample had a small tear in finish pass
2	300	1350	180	22	One very small pinhole opened up	180	4P	.....
2	500	1350	180	22	.....	180	4P	.....
3	300	1250	180	22	Two-minute surface defects 1/32 to 1/16-in. long opened up	180	4P	.....
3	500	1250	180	22	.....	180	4P	.....
3	300	1350	180	22	.....	180	4P	Two samples show minor lack of penetration at root but did not open up
3	500	1350	180	22	.....	180	4P	One sample had a 1/16-in. opening in root caused by lack of penetration
4	300	1250	180	22	.....	180	4P	
4	500	1250	180	22	.....	180	4P	
4	300	1350	180	22	.....	180	4P	
4	500	1350	180	22	.....	180	4P	

[a] Averages of two specimens.
[b] Postheat treatment for 1 hr at temperature.
[c] Elongation in outer fiber—percent in 2 in.
[d] Averages of four specimens.
[e] Cracks or tears longer than 1/8 in. constitute failure.

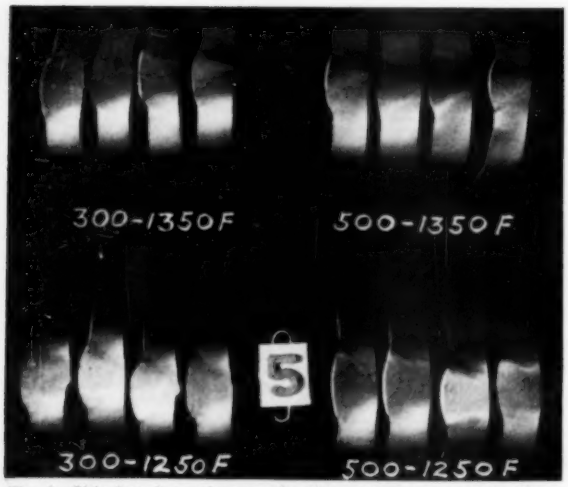

Fig. 4—Side-bend specimens of weldments made on 5 Cr Mo pipe with the 5 Cr Mo electrode No. 1. Approximately × 2/5

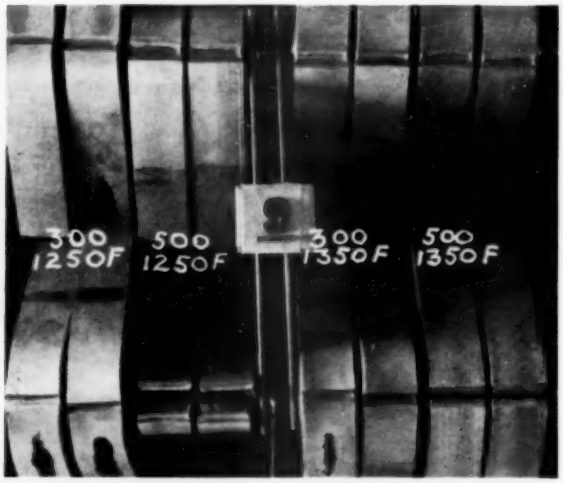

Fig. 5—Notch-bend specimens of weldments made on 5 Cr Mo pipe with the 5 Cr Mo electrode No. 1. The top specimens contained the notch in the heat-affected zone and the bottom specimens contained the notch in the weld metal. Approximately × 2/5

Table 7—Notch-bend Tests of Welds in 5 Cr Mo Steel Pipe

Specimen	Thermal treatment Preheat, °F	Thermal treatment Postheat, °F[a]	Notch location	Max load, lb	Deflection At max load, in.	Deflection After max load, in.	Energy To max load, ft-lb	Energy After max load, ft-lb	Extent of cracking at notch root
Base metal	...	1250	Base metal	1880	1.10	1.10	143.2	150.6	Slight
Base metal	...	1350	Base metal	1880	1.10	1.10	143.2	150.6	Slight
Electrode no. 1	300	1250	Weld	2600	0.95	1.25	170.3	234.0	Slight
	300	1250	Weld	2600	0.95	1.25	170.3	234.0	Slight
	300	1250	Heat-affected zone	2520	1.12	[b]	200.1	[b]	Slight
	300	1250	Heat-affected zone	2400	1.12	[b]	190.7	[b]	Moderate
	500	1250	Weld	2780	0.96	1.21	184.1	237.7	Severe
	500	1250	Weld	2760	0.96	1.08	184.1	211.5	Severe
	500	1250	Heat-affected zone	2620	0.94	1.26	173.7	230.0	Severe
	500	1250	Heat-affected zone	2440	1.04	1.16	184.9	196.9	Severe
	300	1350	Weld	2550	0.96	1.24	166.9	431.0	Slight
	300	1350	Weld	2550	0.96	1.24	166.9	431.0	Slight
	300	1350	Heat-affected zone	2280	0.97	1.23	131.3	205.5	Moderate
	300	1350	Heat-affected zone	2420	0.97	1.23	164.9	217.0	Severe
	500	1350	Weld	2700	0.94	0.62	180.3	102.5	Severe
	500	1350	Weld	2600	0.94	0.52	173.5	92.3	Severe
	500	1350	Heat-affected zone	2420	0.98	1.20	166.5	210.6	Severe
	500	1350	Heat-affected zone	2420	0.98	1.20	166.5	205.8	Severe
Electrode no. 2	300	1250	Weld	2600	0.92	1.26	166.9	171.5	Severe
	300	1250	Weld	2540	0.98	1.20	177.0	152.6	Severe
	300	1250	Heat-affected zone	2500	1.08	[b]	196.0	[b]	Slight
	300	1250	Heat-affected zone	2500	1.08	[b]	196.0	[b]	Moderate
	500	1250	Weld	2600	0.94	0.86	168.4	105.5	Severe
	500	1250	Weld	2600	0.94	0.86	168.4	81.7	Severe
	500	1250	Heat-affected zone	2400	1.0	0.90	168.2	196.4	Severe
	500	1250	Heat-affected zone	2340	1.05	1.15	176.8	180.8	Moderate
	300	1350	Weld	2500	[c]	[c]	[c]	[c]	Severe
	300	1350	Weld	2500	0.96	1.24	169.8	128.6	Severe
	300	1350	Heat-affected zone	2400	0.98	1.22	166.3	212.1	Moderate
	300	1350	Heat-affected zone	2400	0.98	1.22	166.3	212.1	Moderate
	500	1350	Weld	2460	0.94	1.24	168.0	196.4	Severe
	500	1350	Weld	2440	0.94	1.28	168.0	145.5	Severe
	500	1350	Heat-affected zone	2200	1.0	1.2	154.8	188.8	Moderate
	500	1350	Heat-affected zone	2200	1.0	1.2	154.8	188.8	Moderate
Electrode no. 3	300	1250	Weld	2680	0.94	1.26	175.8	230.4	Severe
	300	1250	Weld	2680	0.94	1.26	175.8	189.0	Severe
	300	1250	Heat-affected zone	2470	1.08	[b]	192.5	[b]	Slight
	300	1250	Heat-affected zone	2470	1.08	[b]	192.5	[b]	Moderate
	500	1250	Weld	2750	0.92	1.28	173.5	194.7	Severe
	500	1250	Weld	2750	0.92	1.28	171.4	163.4	Severe
	500	1250	Heat-affected zone	2460	0.95	1.35	166.8	198.8	Severe
	500	1250	Heat-affected zone	2400	0.95	0.95	166.5	166.8	Severe
	300	1350	Weld	2500	0.92	0.80	163.8	133.3	Severe
	300	1350	Weld	2460	0.92	1.16	159.7	130.7	Severe
	300	1350	Heat-affected zone	2320	0.96	1.24	158.0	208.5	Slight
	300	1350	Heat-affected zone	2360	0.96	1.24	158.0	208.5	Moderate
	500	1350	Weld	2450	0.94	1.24	164.4	219.5	Slight
	500	1350	Weld	2400	0.94	1.24	159.5	217.5	Slight
	500	1350	Heat-affected zone	2320	1.02	1.14	165.8	197.3	Slight
	500	1350	Heat-affected zone	2300	1.02	1.14	165.8	197.3	Slight
Electrode no. 4	300	1250	Weld	2700	0.92	1.20	169.5	72.7	Severe
	300	1250	Weld	2680	0.92	1.20	169.5	241.0	Moderate
	300	1250	Heat-affected zone	2360	0.93	0.68	154.8	122.5	Severe
	300	1250	Heat-affected zone	2360	0.93	1.27	154.8	181.4	Severe
	500	1250	Weld	2760	0.92	0.85	176.0	171.7	Severe
	500	1250	Weld	2760	0.92	0.85	176.0	171.7	Severe
	500	1250	Heat-affected zone	2500	1.06	1.14	191.8	201.9	Moderate
	500	1250	Heat-affected zone	2500	1.06	1.14	191.8	201.9	Moderate
	300	1350	Weld	2580	0.94	0.77	169.6	145.4	Severe
	300	1350	Weld	2500	0.78	0.11	133.7	22.1	Severe
	300	1350	Heat-affected zone	2420	0.96	0.78	163.5	147.4	Severe
	300	1350	Heat-affected zone	2380	1.0	1.2	169.6	199.5	Moderate
	500	1350	Weld	2500	1.04	0.27	184.6	55.0	Severe
	500	1350	Weld	2420	1.01	1.19	176.3	209.0	Slight
	500	1350	Heat-affected zone	2250	1.0	1.16	158.7	192.8	Moderate
	500	1350	Heat-affected zone	2200	1.0	1.16	158.8	188.7	Moderate

[a] Postheat treatment for 1 hr.
[b] Recording instrument was improperly set to obtain the full deflection after maximum loading for these specimens.
[c] Improper loading prevented the obtaining of these data.

with Various 5 Cr Mo Electrodes. The hardness measurements and the calculated ductility values of the welds and heat-affected zones of the 16 weldments of 5 Cr Mo pipe made with the four 5 Cr Mo electrodes are given in Table 5.

The calculated ductilities for all 16 weldments are on the order of 15% for the weld metal and 20% for the heat-affected zones. These results, therefore, correspond closely to those described in Table 4 for the previous study on weldments made only with the No. 1 electrode. Three discrepancies were noted, however. In two instances (Nos. 2 and 4 electrodes with the 300–1350° F treatments), decided reductions in ductility occurred and in one instance (No. 2 electrode with the 500–1350° F treatment), a decided increase in ductility occurred. The reasons for the anomalies are not evident readily.

The longitudinal bend-test results (duplicates) for each weldment are given in Table 6 and illustrated for those made with electrode No. 1 in Fig. 3. All samples responded excellently to this test. The elongation in the outer fibers of this particular size sample was 22% at the zone of maximum straining.

Table 8—Impact Properties of Weld Metal in 5 Cr Mo Steel Pipe Weldments[a]

Electrode no.	Thermal treatment Preheat, °F	Thermal treatment Postheat, °F[b]	Transition temperature and energy ranges: ½ energy level energy, ft-lb	½ energy level Temperature, °F	15 ft-lb level, temperature, °F	Room temperature energy, ft-lb
1	300	1250	45	+90 ± 20	+50 ± 20	30 ± 10
2	300	1250	45	+10 ± 15	−35 ± 20	75 ± 5
3	300	1250	55	+45 ± 15	0 ± 50	85 ± 5
4	300	1250	45	+100 ± 15	+20 ± 40	30 ± 5
1	500	1250	45	+25 ± 25	− 5 ± 35	70 ± 5
2	500	1250	45	−10 ± 20	−65 ± 25	70 ± 10
3	500	1250	50	+10 ± 20	−35 ± 30	80 ± 10
4	500	1250	50	+100 ± 40	+20 ± 45	35 ± 15
1	300	1350	45	+60 ± 25	−30 ± 20	50 ± 5
2	300	1350	20	+15 ± 60	−40 ± 30	30 ± 10
3	300	1350	50	−15 ± 10	−50 ± 10	90 ± 1
4	300	1350	35	+135 ± 35	+70 ± 50	10 ± 2
1	500	1350	50	+60 ± 30	−20 ± 30	55 ± 11
2	500	1350	35	−20 ± 25	−70 ± 15	65 ± 2
3	500	1350	55	−15 ± 15	−70 ± 10	95 ± 2
4	500	1350	55	+50 ± 55	−40 ± 35	65 ± 10

[a] Averages of duplicate or triplicate specimens.
[b] Postheat treatment for 1 hr at temperature.

The side-bend test results (quadruplicates) for each weldment are given in Table 6 and illustrated for those made with electrode No. 1 in Fig. 4. All weldments responded excellently to this test.

The notch-bend test results (duplicates) for each weldment are given in Table 7 and illustrated for those made with electrode No. 1 in Fig. 5. The results indicate that all of the weld metals and base-metal heat-affected zones could sustain maximum loads greater than those for the base metal. In all instances, there was a definite measurable

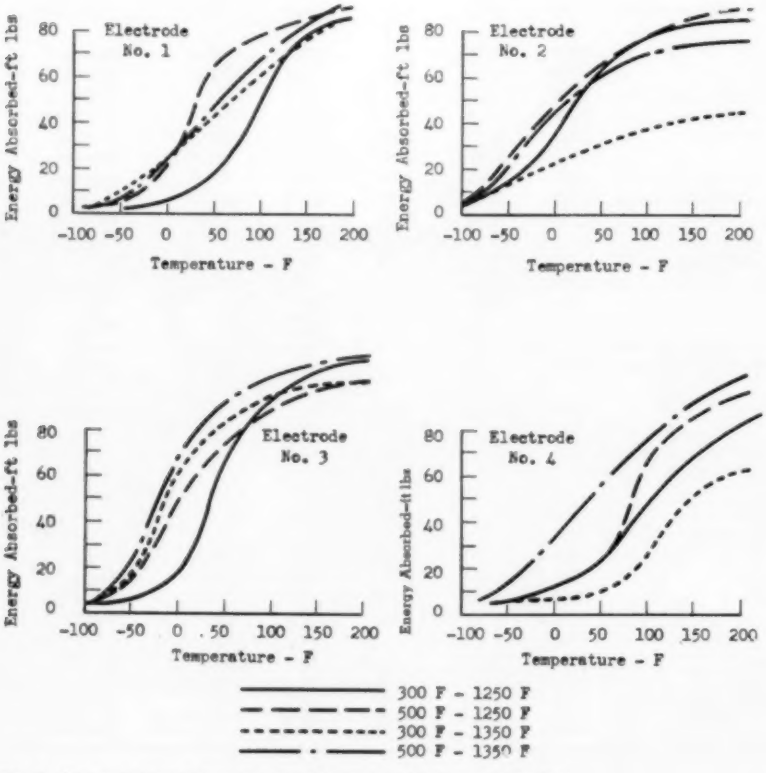

Fig. 6—Charpy V-notch impact transition-temperature curves for 5 Cr Mo weld metals deposited in weldments on 5 Cr Mo steel pipe

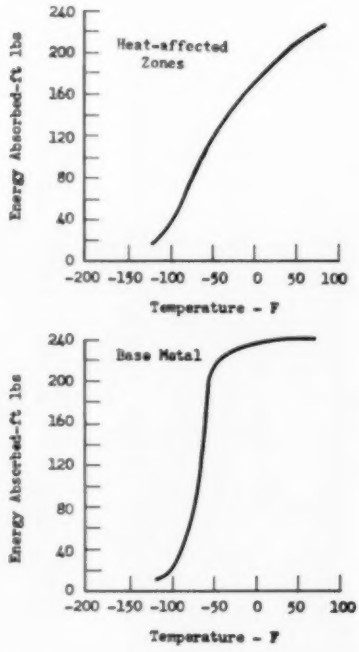

Fig. 7—Charpy V-notch impact transition-temperature curves for both heat-affected zone and base metals of the 5 Cr Mo pipe welded under the various preheat-postheat conditions of 300–1250° F, 500–1250° F, 300–1350° F and 500–1350° F

deflection (or energy absorption) after maximum loading. As indicated in Table 7, many of these samples had severe cracks at the completion of the test. It is not known when these cracks were initiated during the bend test but, in no instance, did they prevent a definite deflection after maximum loading. This observation indicates that these welds would not be subject to a catastrophic failure because of a notch brittleness of the welds or heat-affected zones. On this basis, both the 1250 and 1350° F postheats were beneficial in preventing notch embrittlement.

The impact-test results are given in Table 8 and Fig. 6 for the weld metals and in Fig. 7 for the heat-affected zones and the base metal. The data obtained for the weld metals showed a considerable scatter so that individual tests often differed greatly from the average curves drawn in Fig. 7. There was some suggestion that the weld metal deposited by Electrode No. 4 had somewhat inferior impact-resistance properties. Also, the 500–1350° F preheat-postheat combination appeared to impart the most consistently satisfactory impact resistance to the weld metals.

The data obtained for heat-affected zones and the base metal showed that both zones have better impact resistance than that of the weld metal. Also, the various preheat treatments had virtually no effect in changing these impact properties.

Weldments on 5 Cr Mo Steel Pipe with 25–12 Cr Ni, 25–20 Cr Ni and 1¼ Cr Mo Electrodes. The hardness measurements and the calculated ductility values of the heat-affected zones (and weld metal of the 1¼ Cr Mo electrode using an equation developed in a previous study[2]) and side-bend-test results are given in Table 9 and Fig. 8. As expected, the austenitic welds are relatively soft and would be expected to have excellent ductility. The 1¼ Cr Mo weld metal also has an excellent (calculated) ductility even with no postheat treatment. The heat-affected zones of the 5 Cr Mo pipe have excellent (calculated) ductilities even in the absence of any preheat and postheat treatments. The side-bend-test results on all weldments showed excellent responses with the only failures being a lack of penetration in a few of the weld roots; an effect which preheat and postheat treatments would not have prevented. The notch-bend-test results are given in Table 10. The results show that all of the specimens absorbed appreciable energy after maximum loading. As indicated in Table 10, many of these samples had severe cracks at the completion of the test. It is not known when these cracks were initiated during the bend test but in no instance did they prevent a definite deflection after maximum loading. This observation indicates that these welds would not be subject to a catastrophic failure because of a notch brittleness of the welds or heat-affected zones.

Conclusions

1. The hardness and tensile properties can be correlated for both 5 Cr Mo alloy-steel pipe material and for 5 Cr Mo weld deposits. At high hardness values, the ductility of the pipe metal (including heat-affected zones) remains relatively high but the ductility of weld metal becomes rather low. This fact indicates that postheat treatments of such weldments are essential to impart ductility to the 5 Cr Mo weld metal but are not needed to impart ductility to the heat-affected zones of the 5 Cr Mo base metal. Even at a Brinell hardness of 380, the pipe metal has a ductility (as measured by elongation) of about 12.5%.

2. Ductilities of weld metal of pipe welds are less than those of all-weld-metal specimens made according to AWS specifications. This difference probably is due to the welding-technique differences followed in each instance.

3. Preheating up to 500° F has only a very slight effect in improving the ductility of weld metal and heat-affected zones in 5 Cr Mo alloy-steel pipe welded with 5 Cr Mo electrodes. Postheat treatments of 1250 and 1350° F are effective in imparting ductility to 5 Cr Mo weld metal but a 1400° F treatment increases the ductility markedly.

4. The ductility of all welds made on 5 Cr Mo alloy steel pipe with 5 Cr Mo electrodes using postheats of 1250 and 1350°F were entirely satisfactory as evidenced by the results of side-bend and longitudinal-bend tests.

5. Notch-bend-test results indicate that the 1250 and 1350° F postheat treated weldments of 5 Cr Mo electrodes on 5 Cr Mo alloy-steel pipes are not subject to notch embrittlement during slow bending.

6. The impact properties of heat-affected zones of 1250 and 1350° F postheat treated 5 Cr Mo alloy-steel pipe are as good as those of the base metal. However, the 5 Cr Mo weld metal has impact properties substantially lower than those of the heat-affected zones and base metal.

7. When unrestrained welds are made in 5 Cr Mo alloy steel with 25–12 Cr Ni, 25–20 Cr Ni and 1¼ Cr Mo electrodes, there appears to be no need for either preheat or postheat to obtain ductile weldments. Previous studies have shown that 1¼ Cr Mo weld metal does not need either preheat or

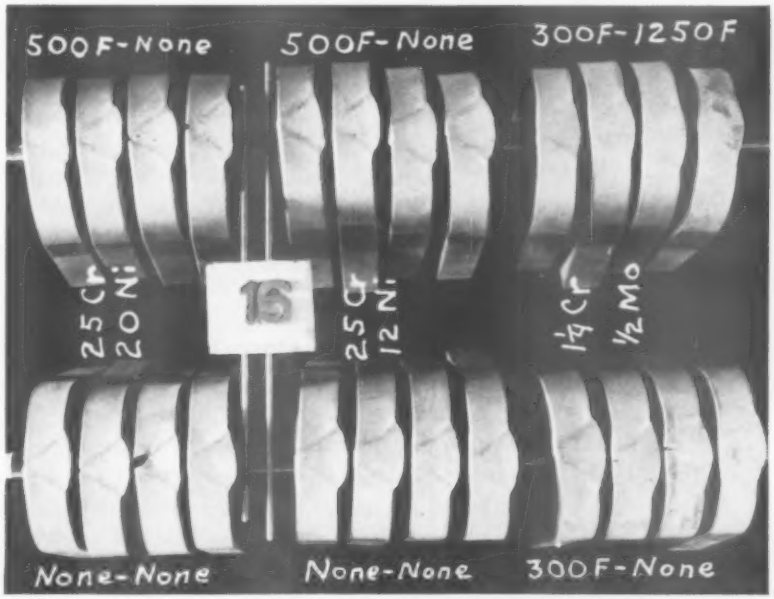

Fig. 8—Side-bend specimens after testing. The tests were made in quadruplicate and the identifications of welding-electrode composition, preheat and postheat are given in the photograph. Approximately × ½

Table 9—Effect of Preheat or Postheat on Hardness–Ductility and Side-bend Tests of Welds Made on 5 Cr Mo Pipe Using 25–12 Cr Ni, 25–20 Cr N and 1¼ Cr Mo Electrodes

Electrode	Preheat, °F	Postheat, °F	Brinell hardness[a] Weld	Brinell hardness[a] Heat-affected zone	Brinell hardness[a] Pipe	Calculated ductility, Heat-affected[b] zone	Side-bend-test results[c] Bend angle, deg	Side-bend-test results[c] Pass or fail[d]	Remarks
25–12 Cr Ni	None	None	169	210	132	23.6	180	All passed	No. 1—1/16-in. opening in root
	500	None	169	228	130	21.2	180	3 passed 1 failed	No. 4—1/8 crack in. root pass—not lack of fusion
25–20 Cr Ni	None	None	169	210	139	23.6	180	3 passed 1 failed	No. 3 lack of fusion in root prop. into weld 1/4-in.
	500	None	162	216	132	22.4	180	All passed	Lack of fusion in root stopped in weld
						Weld[e] / Heat-affected zone[e]			
1¼ Cr Mo	300	None	228	228	137	20.8 / 21.2	180	All passed	Nos. 2, 3—slight lack of fusion in root—did not propagate into weld
	300	1250—1 hr	205	210	127	23.8 / 23.6	180	All passed	

[a] Converted from Rockwell B hardness values.
[b] As calculated from the appropriate equation.
[c] Four side bends made for each condition.
[d] Cracks or tears longer than 1/8 in. constitute failure.
[e] This data obtained from equations developed in previous studies.

Table 10—Notch-bend Tests of Weldments of 5 Cr Mo Pipe with Various Electrodes

Specimen	Thermal treatment Preheat, °F	Thermal treatment Postheat, °F	Notch location	Max load, lb	Deflection At max load, in.	Deflection After max load, in.	Energy To max load, ft-lb	Energy After max load, ft-lb	Extent of cracking at notch root
5 Cr Mo pipe welded with 25–20 Cr Ni	None	None	Weld	2000	0.58	0.50	81.6	64.8	Severe
	None	None	Weld	1900	0.44	0.96	47.6	79.3	Severe
	None	None	Heat-affected zone	2200	0.94	0.96	144.0	138.7	Moderate
	None	None	Heat-affected zone	2180	0.96	1.24	149.6	160.8	Moderate
	500	None	Weld	2040	0.58	0.72	85.0	76.5	Severe
	500	None	Weld	2050	0.60	0.68	86.3	71.2	Severe
	500	None	Heat-affected zone	2250	1.0	1.2	162.3	197.0	Moderate
	500	None	Heat-affected zone	2170	0.76	1.44	113.5	113.5	Severe
5 Cr Mo pipe welded with 25–12 Cr Ni	None	None	Weld	2020	0.56	0.72	78.4	53.6	Severe
	None	None	Weld	1900	0.49	0.65	67.5	52.3	Severe
	None	None	Heat-affected zone	2200	1.02	1.18	160.8	184.6	Moderate
	None	None	Heat-affected zone	1940	0.56	0.77	78.9	47.2	Severe
	500	None	Weld	2070	0.61	0.56	86.4	52.3	Severe
	500	None	Weld	2000	0.60	0.56	84.0	54.2	Severe
	500	None	Heat-affected zone	2300	1.12	1.08	185.8	136.8	Severe
	500	None	Heat-affected zone	2250	1.02	1.18	166.7	177.0	Severe
5 Cr Mo pipe welded with 1¼ Cr Mo	300	None	Weld	2600	0.90	0.64	166.5	70.7	Severe
	300	None	Weld	2640	0.92	0.58	172.8	70.7	Severe
	300	None	Heat-affected zone	2260	0.82	0.25	132.5	45.0	Severe
	300	None	Heat-affected zone	2500	0.86	0.56	152.7	105.5	Severe
	300	1250° F	Weld	2270	0.92	1.28	148.5	131.5	Severe
	300	1250° F	Weld	2320	1.0	1.2	166.7	130.5	Severe
	300	1250° F	Heat-affected zone	2260	0.96	1.24	156.5	181.5	Moderate
	300	1250° F	Heat-affected zone	2200	1.0	1.2	156.5	193.5	Moderate

postheat for good ductility. It is well known that 25–12 Cr Ni and 25–20 Cr Ni weld metals are ductile. This study has shown that heat-affected zones of 5 Cr Mo pipe material are ductile even in the absence of preheat and postheat (although the 5 Cr Mo weld metal does need the postheat treatment). Therefore, it follows that when unrestrained welds are made on 5 Cr Mo alloy-steel pipe with an electrode which deposits ductile weld metal, the weldment should need no preheat or postheat treatments. However, refinery experience has shown that weldments of ferritic base metals with the austenitic 25–12 Cr Ni and 25–20 Cr Ni electrodes may crack eventually in or adjacent to the weld when subjected to thermal cycling. The stresses causing such cracks are developed because of the difference in the coefficients of thermal expansion of the austenitic weld metal and ferritic base metal. The $1^1/_4$ Cr Mo weld metal, being ferritic, will not cause this type of cracking in 5 Cr Mo weldments exposed to thermal cycling.

Acknowledgment

The authors wish to acknowledge the assistance of C. F. Braun, J. M. Backus and other personnel of the Engineering Research Department for the preparation of the welds and test specimens and in securing the data.

The permission of the Standard Oil Company (Indiana) to publish this paper is greatly appreciated, as are the advice and encouragement given by C. H. Samans, Associate Director, Materials Division, Engineering Research Department.

References

1. Bland, J., Privoznik L. F., and Windsor, F. J., "The Arc Welding of Low Chromium-Molybdenum Steel Pipe," THE WELDING JOURNAL, **31** (9), 783–791 (1952).

2. Bland, J., "Arc Welding of Low Chromium-Molybdenum Steel Pipe," *Ibid.*, **32** (9) 803–814 (1953).

3. Bland, J., "The Arc Welding of 2.25% Cr – 1.0% Mo Alloy Steel Pipe," *Ibid.*, **35** (4), Research Suppl., 181-s to 194-s (1956).

4. American Standard Code for Pressure Piping, ASME, ASA B31.1-1955.

5. "Rules for Welding Piping in Marine Construction—Ferritic Alloy Steels," AWS Std. D3.4-52 (tent.), p. 1.

6. "Recommended Preheat and Postheat Welding Practices for Low Chromium-Molybdenum Steel Pipe," Pipe Fabrication Institute Standard FS(M) 8-1955.

7. "Recommended Practices for Interruption of Heat Treatment Cycles for Low Chromium-Molybdenum Steel Pipe Materials," AWS Std. D-10.3-55 (tent.)

8. Holmberg, M. F., "Welding Alloy Steels for High-Temperature Service," THE WELDING JOURNAL, **28** (2), 141–148 (1949).

Selection of Projects

The **Welding Research Council** is receptive to new ideas for research projects from any source. Naturally before any project can be approved or undertaken, certain yardsticks have to be applied. For the most part there are rather obvious yardsticks developed over the years:

1. Is the **Welding Research Council** the best agency to undertake the work?
2. Is the problem a "doable" one?
3. Will it be possible to secure the necessary funds, talent and research facilities?
4. Is the problem of broad general interest?

The answer to question 1 is in most cases not too difficult as this question implies other questions:

(a) What other agencies are working in this general field?
(b) What work has already been done or is being done in the general field?
(c) Is there some other agency that could be considered a more logical agency?

Problem 2 is sometimes more difficult. The **Welding Research Council** believes, however, that before any experimental work is undertaken that a literature survey of existing information should be made by the investigator to learn what has been done before—the successes and failures. A breakdown of the problem into its fundamental elements should help provide this answer.

The answer to the third question, inasfar as funds are concerned, should be readily available. A project should not be undertaken unless the sponsors are willing to put up a third of the funds. In developing a program and budget one should have bids from at least two laboratories which in itself would provide part of the answer to this question. However the ideas of Committee members and the original sponsors should be secured.

The answer to the fourth question is generally available as the result of securing the answers to the first three questions.

Submerged-Arc Welding HY-80 Steel

Study is conducted to develop methods for making submerged-arc welds capable of withstanding severe impact loading at low temperatures

BY W. J. LEWIS, G. E. FAULKNER, D. C. MARTIN AND P. J. RIEPPEL

Introduction

One of the prime considerations in the construction of submarine hulls is the ability of the hull to withstand severe impact loading at temperatures of 30° F. Most of the submarine hulls being fabricated today are made from Grade HY-80 steel using standard low-hydrogen welding electrodes and preheating operations. The Grade HY-80 steel base plate and the welded joints meet the property requirements for submarine-hull construction. Although many of the joints in hull construction are suitable for automatic welding techniques such as the submerged-arc process, the properties of weldments deposited with the submerged-arc process with conventional techniques are not satisfactory for submarine applications.

This study was conducted to develop methods for making submerged-arc welds which will withstand severe impact loading at low temperatures. The specific objectives were to obtain submerged-arc weld metals with yield strengths of at least 80,000 psi and Charpy V-notch toughness of 20 ft-lb at −100° F or a nil-ductility temperature of −100° F[a] in both the as-welded and stress-relieved conditions. Submarine hulls with notch toughness and nil-ductility temperature values in this range will withstand severe impact loading at service temperatures.

This program was conducted in two phases. The first phase of the program consisted of preparing and evaluating several experimental filler wires. The compositions of the experimental wires were within the range of compositions of commercial covered electrodes and filler wires for the inert-gas-shielded metal-arc process which produce weld metals with good Charpy V-notch-toughness properties. It was found that submerged-arc welds made with similar filler-metal compositions had lower V-notch toughness than that reported for manual and inert-gas-shielded metal-arc welds.

In order to determine methods for improving the notch toughness of submerged-arc welds, studies were made to compare the mechanical properties, metallurgical characteristics and compositions of welds made by the submerged-arc process with those made by the inert-gas-shielded metal-arc process. The information obtained from these comparisons led to Phase II of this program in which the effects of flux composition on weld-metal properties were studied. For this phase of the program, experimental fluxes were prepared and evaluated. The information obtained in the flux studies will be presented in a subsequent paper.

This paper describes the results obtained in evaluating several experimental filler wires for use in submerged-arc welding HY-80 steel. The effects of nickel, manganese and molybdenum on weld-metal properties are discussed and the properties of submerged-arc welds and inert-gas-shielded metal-arc welds made with the same filler wire and conditions are compared.

W. J. LEWIS, G. E. FAULKNER, D. C. MARTIN and P. J. RIEPPEL are associated with Battelle Memorial Institute, Columbus, Ohio.

Paper presented at AWS 40th Annual Meeting held in Chicago, Ill., April 6-10, 1959.

Table 1—Composition of 1-in. Thick HY-80 Steel Plates

Heat designation	Chemical composition, % C	Mn	P	S	Si	Ni	Cr	Mo
Heat 20120-15	0.15	0.36	0.020	0.032	0.18	1.97	1.06	0.18
Heat 20739	0.16	0.23	0.011	0.028	0.19	2.33	0.89	0.25

HY-80 Steel Base Material

The base metal used in the welding studies was 1-in. thick HY-80 steel plate. Plates from two different heats were obtained for these studies. The compositions of these plates were as given in Table 1. Tension and impact tests were made on the base metals. The results of these tests are listed in Table 2. From the data obtained, both plates met the requirements of MIL-S-16216W (Navy). However, Heat 20739 had superior tensile and impact properties. Because tests were concerned primarily with weld-metal properties rather than base-metal properties, both of the heats were used during this program.

Experimental Procedures

Weld-metal studies were made on

Table 2—Tension and Impact Properties of 1-in.-thick HY-80 Steel Plates[a, b]

Heat designation	Yield strength, psi	Ultimate tensile strength, psi	Elongation in 2 in., %	Reduction in area, %	V-notched Charpy notch toughness, ft-lb 78° F	−40° F	−100° F
Heat 20120-15	82,000	98,000	23	63	84	80	57
Heat 20739	90,000	104,000	21	66	[c]	[c]	[c]

[a] Testing direction transverse to the direction of rolling.
[b] Average of two specimens.
[c] Did not break.

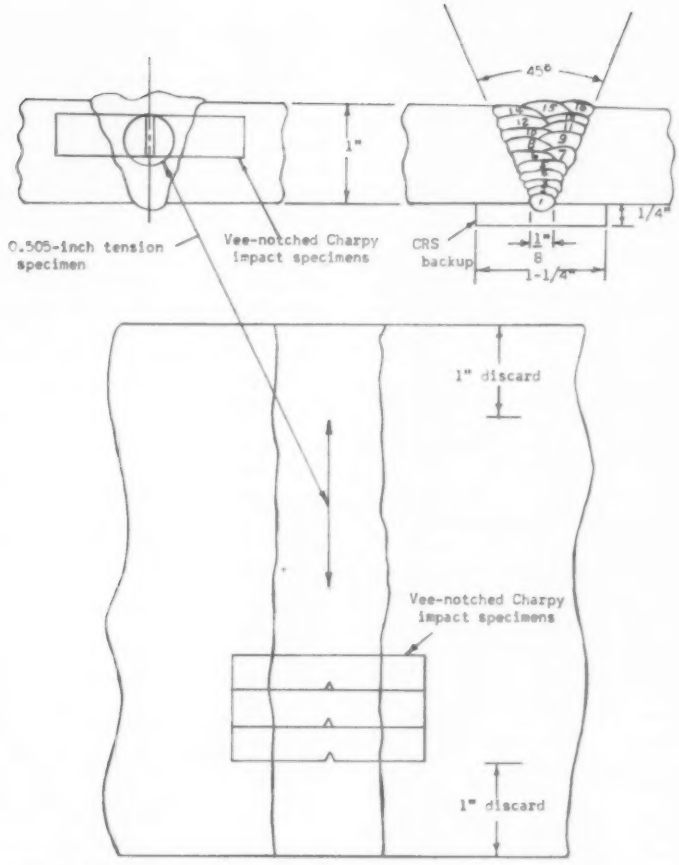

Fig. 1—Joint design, pass sequence and location of tension and impact specimens in a multipass weld

joints prepared with 9 experimental filler wires. The welds were made under closely controlled conditions and were evaluated on the basis of Charpy V-notch properties and tensile properties.

The heats of steel for the experimental filler wires were prepared in a MgO-lined electric-induction furnace under an argon atmosphere. The heats were prepared from high-grade melting stock, which included electrolytic iron as the base to keep sulfur and phosphorus contents at a minimum. The chemical composition of each of the additions was known prior to the preparation of the heats, and the amount of each element added to the heats of steel was carefully weighed in preparing these materials. Approximately 0.075% aluminum was added to each heat as a deoxidizer. All alloy and deoxidation additions were made in the furnace.

The normal pouring temperature for all experimental heats was 2980° F. Big-end-up ingot molds were used for all of the experimental heats. The size of the heats varied from 110 lb from which three 35-lb splits were made to 310-lb heats which were subsequently divided into three 100-lb splits.* The ingots were then forged, rolled and

* Two or more ingots cast from one heat. Except for variations in one alloying element, each split had the same composition.

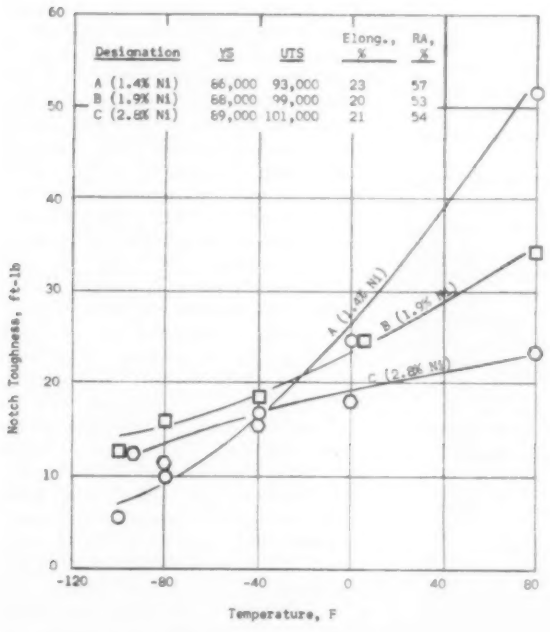

Fig. 2—Effect of nickel on weld-metal notch toughness (as-welded)

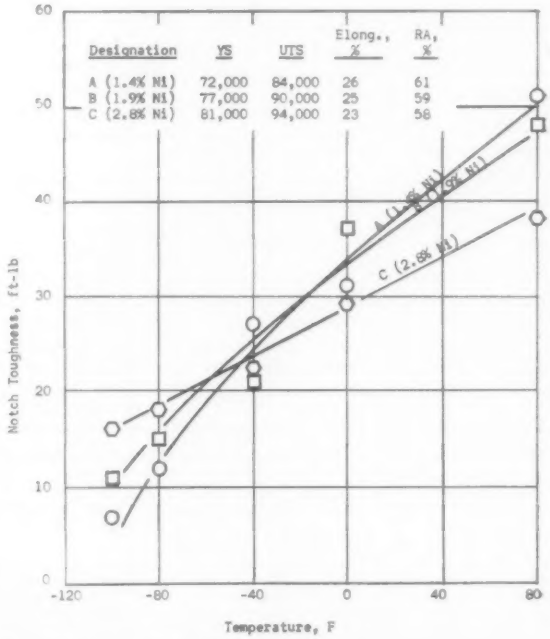

Fig. 3—Effect of nickel on weld-metal notch toughness (stress relieved)

Table 3—Chemical Composition of Experimental Wires

Wire designation[a]	Chemical composition, %				
	C	Mn	Si	Ni	Mo
A	0.09	1.27	0.13	1.40	0.56
B	0.08	1.18	0.26	1.91	0.57
C	0.08	1.14	0.24	2.88	0.53
D	0.09	1.94	0.12	2.15	Trace
E	0.08	2.84	0.04	2.14	Trace
F	0.11	1.26	0.01	3.44	Trace
G	0.08	1.34	0.10	3.16	0.52
H	0.10	1.27	0.05	3.40	0.62
I	0.11	1.20	0.02	3.36	1.07

[a] The wires were taken from split heats: heat No. 1—A and G; heat No. 2—B and C; heat No. 3—D and E; heat No. 4—F, H and I.

drawn to $^{5}/_{32}$-in. diam wire for welding.

All of the wires were used to make submerged-arc welds in 1-in. thick HY-80 steel plate. The joint geometry was a single-vee 45-deg butt joint with a $^{1}/_{8}$-in. root opening (Fig. 1). Welding conditions which gave a 45,000 joules/in. heat input were used. This heat input was selected on the basis of studies made on weld metals and heat-affected zones of submerged-arc welds made with various amounts of heat per inch of weld. The aim was to use the highest heat input per inch of weld possible and still maintain good heat-affected-zone properties. In using 45,000 joules/in., a relatively narrow and high-hardness heat-affected zone was obtained. It appeared that weld metals with better properties might be obtained if lower heat inputs were used than those made with 45,000 joules/in., but the difference at low testing temperatures did not appear significant. The welding conditions used to make submerged-arc welds with experimental wires were:

Arc voltage, v	30
Amperage, amp	550
Travel speed, ipm	22
Preheat and interpass temperature, ° F	250
Flux	Neutral

Weld-metal notch toughness and tensile properties were determined in both the as-welded and stress-relieved conditions using standard V-notch Charpy specimens and standard 0.505-in. tensile specimens (Fig. 1). The stress-relieving treatment consisted of heating the welded joints for 1 hr at 1200° F.

Experimental Results and Discussion

The compositions of the experimental wires were selected on the basis of available information[4] on welds made with manual electrodes. This information showed that good Charpy V-notch-toughness properties were obtained in weld deposits containing approximately 3% nickel, 1% manganese and 0.6% molybdenum. However, it was found in this program that submerged-arc welds made with similar compositions had lower notch toughness than that reported for manual welds. Attempts were made to obtain satisfactory weld properties by modifying the nickel, manganese and molybdenum contents of the wires. None of the modified wires produced satisfactory weld properties. However, the selection of compositions allowed a study of the effect of nickel, manganese and molybdenum on weld-metal properties.

The chemical compositions of the experimental filler wires studied are listed in Table 3. Of the first two heats studied, one wire contained 2% nickel and the other contained 3% nickel. Both wires had manganese contents of 1% and molybdenum contents of 0.50%. These wires did not produce weld metals which met the target requirements. However, the results showed that increased nickel lowered notch toughness and also increased yield strength. The 2 and 3% nickel wires were then modified for further studies. First, the manganese content of the 2% nickel wire was increased with and without molybdenum additions and, second, molybdenum content of the 3% nickel wire was varied in an effort to increase notch toughness without lowering the yield strength too much. In addition, a $1^{1}/_{2}$% nickel wire was used to further study the effects of nickel on weld properties.

The results presented in succeeding sections are from single and duplicate tests. In most cases, tensile data are obtained from single specimens and Charpy V-notch-toughness data are obtained from duplicate specimens.

Effect of Nickel on Weld-metal Properties

The effect of nickel on weld-metal properties was studied over the range of 1.4 to 2.8% nickel. This study involved three different welding wires designated A, B and C. Chemical compositions of submerged-arc welds made with these wires are given in Table 4. It can be seen that the weld-metal compositions were similar except for the nickel content.

The effects of nickel on weld-metal notch toughness and tensile properties are shown in Fig. 2. The notch toughness of the weld metals decreased with increasing nickel contents, especially at temperatures above −40° F. For example, at room temperature, the notch toughness of A weld metal (1.4% nickel) was 52 ft-lb; whereas the notch toughness of C weld metal (2.8% nickel) was 22 ft-lb. However, at subzero temperatures, the increased nickel did not appear to be harmful. At −80° F, the notch toughness of A and C weld metals was similar and at −100° F the notch toughness of A weld metal (1.4% nickel) was 7 ft-lb and that of C weld metal (2.8% nickel) was 12 ft-lb.

The tensile properties of the welds were obtained from single tests. Although the differences in properties are small, there is a trend that tensile and yield strengths increased slightly with increased nickel contents, and the ductility was slightly decreased. All of the welds had yield strengths above the minimum required 80,000 psi.

The effect of nickel on weld-metal notch toughness and tensile proper-

Table 4—Composition of Experimental Filler Wires and Weld Metals with Three Levels of Nickel

Filler-wire designation	Chemical composition, %						
	C	Mn	Si	Ni	P	S	Mo
A wire	0.09	1.27	0.13	1.40	...	...	0.56
A weld metal	0.07	0.86	0.42	1.35	...	...	0.50
B wire	0.08	1.18	0.26	1.91	0.012	0.002	0.57
B weld metal	0.05	1.08	0.52	1.92	0.012	0.005	0.59
C wire	0.08	1.14	0.24	2.88	0.012	0.002	0.53
C weld metal	0.06	0.94	0.49	2.76	0.011	0.005	0.56

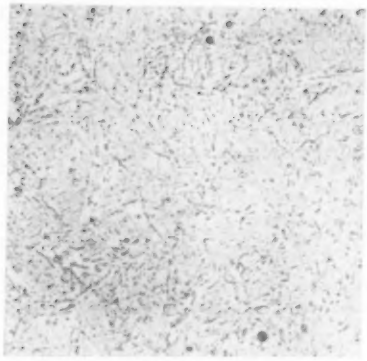

Fig. 4—Typical acicular as-welded microstructure within the weld pass. X 500. (Reduced by 1/2 upon reproduction)

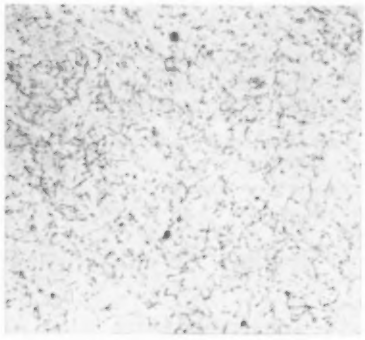

Fig. 5—Typical stress-relieved microstructure within the weld pass. X 500. (Reduced by 1/2 upon reproduction)

Table 5—Composition of Experimental Filler Wire and Metals with Two Levels of Manganese

Filler-wire designation	Chemical composition, %				
	C	Mn	Si	Ni	Mo
D wire	0.09	1.94	0.12	2.15	Trace
D weld metal	0.07	1.26	0.41	2.12	0.08
E wire	0.06	2.84	0.04	2.14	Trace
E weld metal	0.08	1.81	0.42	2.14	0.05

ties in the stress-relieved condition is shown in Fig. 3. The notch toughness of the stress-relieved weld metals were not affected appreciably by nickel content. In comparing Figs. 2 and 3, it can be seen that weld-metal notch toughness was higher and the tensile strength was lower in the stress-relieved condition than in the as-welded condition. The change in properties was attributed to the change in microstructure observed in the joints. In the as-welded condition, carbide occurred predominantly at the edge of acicular ferrite plates, resulting in an acicular pattern (Fig. 4). During stress-relieving operations (Fig. 5), the carbide was spheroidized and this apparently improved notch properties.

Effect of Manganese on Weld-metal Properties

Two filler wires were fabricated which allowed a study on the effects of manganese on weld-metal properties. The compositions of the wire and weld metals are listed in Table 5. The nickel and molybdenum contents of the wires were about 2 and 0%, respectively. The manganese content ranged from 2 to 3% in the wire and 1.26 to 1.81% in the deposited weld metals.

The notch toughness and tensile properties of weld metals made with wires D and E are shown in Fig. 6. At temperatures above −40° F, the notch toughness of weld metals with high manganese (1.8%) was 10 to 20 ft-lb lower than the welds containing low manganese (1.26%). However, at temperatures below −40° F, the notch toughness of the welds was essentially the same.

With increasing manganese content, the yield and tensile strengths were increased, and the ductility was decreased. The yield strength of both weld metals was above the 80,000-psi minimum yield requirements.

The effects of manganese on the notch toughness and tensile properties of weld metals in the stress-

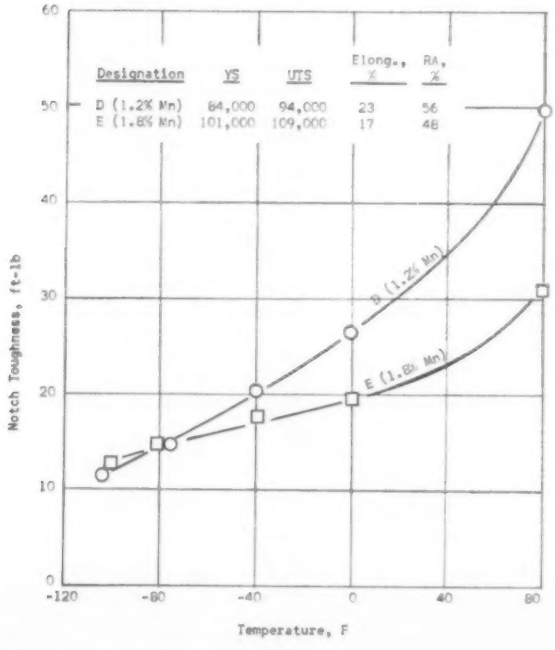
Designation YS UTS Elong., % RA, %
D (1.2% Mn) 84,000 94,000 23 56
E (1.8% Mn) 101,000 109,000 17 48
D (1.2% Mn)
E (1.8% Mn)
Notch Toughness, ft-lb
Temperature, F

Fig. 6—Effect of manganese on weld-metal notch toughness (as welded)

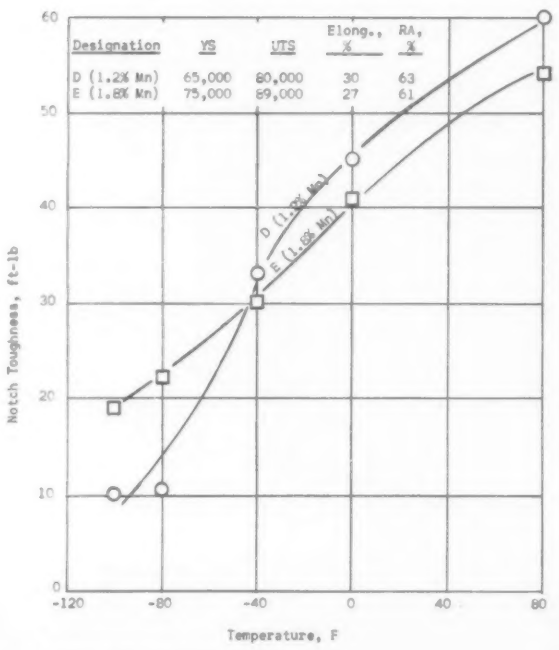
Designation YS UTS Elong., % RA, %
D (1.2% Mn) 65,000 80,000 30 63
E (1.8% Mn) 75,000 89,000 27 61
D (1.2% Mn)
E (1.8% Mn)
Notch Toughness, ft-lb
Temperature, F

Fig. 7—Effect of manganese on weld-metal notch toughness (stress relieved)

relieved condition are shown in Fig. 7. At temperatures above −40° F, the notch toughness of the weld metals was similar. However, at low-testing temperatures the high-manganese content appears beneficial. At −100° F, E weld metal (1.81% manganese) was 10 ft-lb higher than D weld metal (1.26% manganese). In comparing Figs. 6 and 7, it can be seen that weld-metal notch toughness was improved and the yield strength was lowered by stress relieving.

Table 6—Composition of Experimental Filler Wires and Weld Metals with Four Levels of Molybdenum

Filler-wire designation	Chemical composition, %				
	C	Mn	Si	Ni	Mo
F wire	0.11	1.26	0.01	3.44	Trace
F weld metal	0.08	0.93	0.34	3.08	0.05
G wire	0.08	1.34	0.10	3.16	0.52
G weld metal	0.07	0.92	0.39	2.94	0.43
H wire	0.10	1.27	0.05	3.40	0.62
H weld metal	0.09	0.97	0.32	3.00	0.50
I wire	0.11	1.20	0.02	3.36	1.07
I weld metal	0.07	0.86	0.28	2.97	0.76

Effect of Molybdenum on Weld-metal Properties

The effects of molybdenum were studied in weld metal containing about 3% nickel – 1% manganese. The chemical analysis of the wires and weld metals are given in Table 6. The molybdenum content of the weld metals ranged from 0.05 to 0.76%.

The effects of molybdenum on the weld-metal notch toughness and tensile properties of the 3% nickel wires are shown in Fig. 8. It can be seen that, with increased molybdenum contents, impact properties were generally lowered and the tensile and yield strengths were increased. The notch toughness, however, of (G) 0.43% molybdenum and (H) 0.50% molybdenum weld metal were not comparable. The reason for this is not known. Both weld metals were made with the same welding conditions and the microstructures and compositions were similar. The tensile and yield strengths of weld metal (G) were high, but the weld from which these data were obtained was made with an 80° F interpass temperature instead of the 250° F interpass temperature used for the other welds.

The effect of molybdenum on weld-metal notch toughness and tensile properties in the stress-relieved condition is shown in Fig. 9. The same trend that was observed on the welds in the as-welded condition prevailed in the stress-relieved welds; that is, with increased molybdenum contents, weld-metal notch toughness decreased and tensile and yield strengths increased. In comparing Figs. 8 and 9, it can be seen again that weld-metal notch toughness was improved and tensile strength was lowered by stress relieving.

The tensile properties of welds deposited from experimental wires F, G, H and I showed that increased molybdenum content generally improves yield and tensile properties in both the as-welded and stress-relieved conditions.

Comparison of Submerged-arc and Inert-gas-shielded Metal-arc Weld Metal

In the filler-wire study, it was expected that better notch toughness results than were observed would be obtained since the notch toughness of weld metals made with other processes with similar compositions were good. Therefore, further studies were made to determine if the experimental filler wires inherently produced low notch toughness or whether the low notch toughness was due to some metallurgical or chemical change that normally

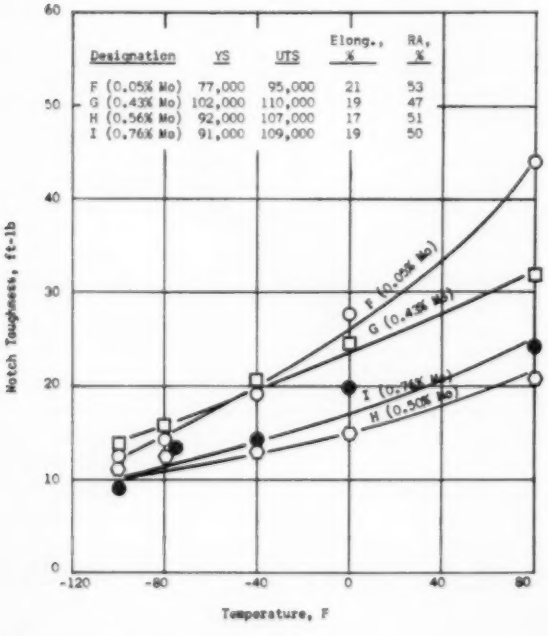

Fig. 8—Effect of molybdenum on weld-metal notch toughness (as welded)

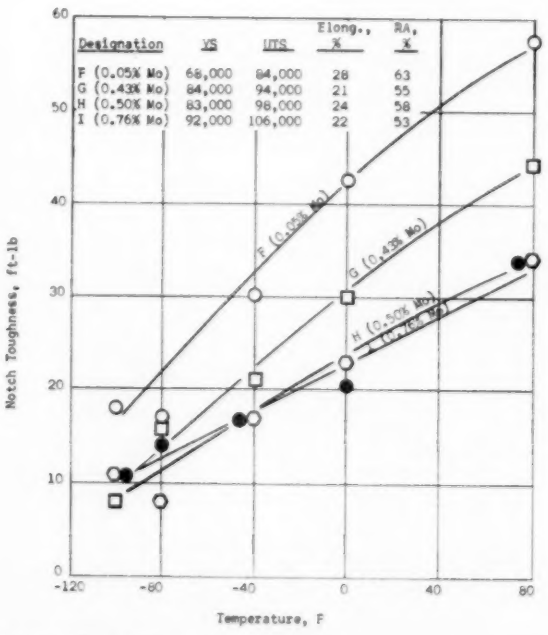

Fig. 9—Effect of molybdenum on weld-metal notch toughness (stress relieved)

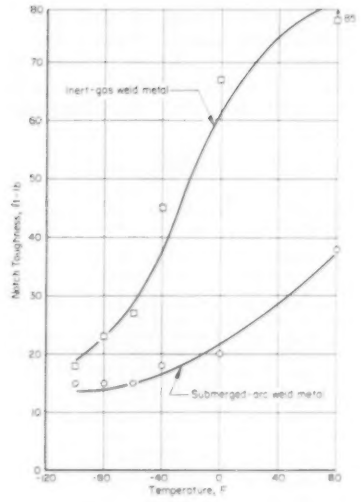

Fig. 10—Comparison of notch toughness of weld metals made with the submerged-arc welding process and the inert-gas-shielded metal-arc process

occurs in using the submerged-arc welding process.

Studies were made to compare the mechanical properties, metallurgical characteristics and composition of weld metals deposited with the submerged-arc and inert-gas-shielded metal-arc processes. These studies were made to determine if differences in weld-joint properties could be associated with microstructure or composition of the welds.

Submerged-arc and inert-gas-shielded metal-arc welds were made using the same base plate, joint design, filler wire (B) and welding conditions. The welding conditions were: 450 amp, 26 arc v, 15.6-ipm welding speed, and a 250° F interpass temperature. The submerged-arc welds were made with a neutral flux. The inert-gas-shielded metal-arc welds were made with argon shielding.

Weld-metal notch toughness and tensile properties were determined for both types of welds using standard V-notch Charpy specimens and standard 0.505-in. tensile specimens. The welds were tested in the as-welded condition. The results of the notch-toughness tests are shown in Fig. 10. As this figure shows, the notch toughness of the welds made by the inert-gas-shielded process was considerably higher than that of the welds made by the submerged-arc process. The tensile properties of the welds are shown in Table 7. The tensile properties of both welds were practically the same.

Metallographic examinations and chemical and vacuum-fusion analyses were made on both weld metals to try to determine the causes of the difference in notch-toughness properties. Metallographic examinations showed that the microstructure of the welds made with both processes was essentially the same. However, the submerged-arc welds contained a considerable number of silicate inclusions and the inert-gas welds were relatively clean (Fig. 11).

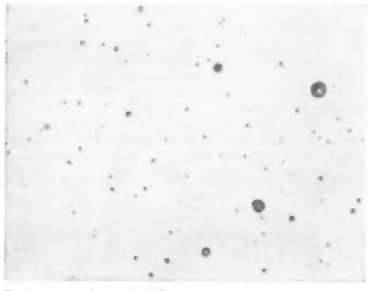

Submerged-arc weld

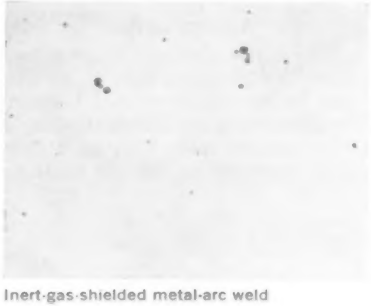

Inert-gas-shielded metal-arc weld

Fig. 11—Comparison of cleanliness of submerged-arc and inert-gas-shielded metal-arc weld metals. X 1500. (Reduced by 1/2 upon reproduction)

The results of chemical and vacuum-fusion analyses are shown in Table 8. The wire composition is included for comparison. As this table shows, the major differences in the compositions of the weld metal are in silicon and oxygen contents. The silicon content of the submerged-arc welds was about twice that of the inert-gas welds. The oxygen content of the submerged-arc welds was about 6 times that of the argon-shielded welds.

This study showed that the major differences between the submerged-arc welds and the inert-gas-shielded metal-arc welds were:

1. Number of inclusions.
2. Oxygen content.
3. Silicon content.

On the basis of this information, studies were made to improve weld-metal notch toughness by modifying the neutral flux or developing a new flux. The modifications were aimed at altering the fluidity of the flux or changing arc characteristics so as to obtain less trapped silicates than were observed in weld metals made with the neutral flux. The information obtained from the flux studies

Table 7—Tensile Properties of Submerged-arc and Inert-gas Welds Made with the Same Filler Wire and Welding Conditions

Welding process	Yield strength (0.2% offset), psi	Ultimate tensile strength, psi	Elongation in 2 in., %	Reduction in area, %
Submerged arc	100,000	114,250	17.1	52.6
	100,000	114,250	19.8	52.3
Inert gas	98,000	107,750	18.2	51.0
	102,500	111,750	21.4	68.3

Table 8—Composition of Experimental Filler Wire and Weld Metals

	Chemical composition, %											
	C	Mn	P	S	Si	Cr	Ni	Mo	Al[a]	N_2	H_2	O_2
Filler wire	0.08	1.18	0.012	0.002	0.26	...	1.91	0.57	...	...	...	...
Submerged-arc weld metal	0.07	0.81	0.014	0.016	0.44	0.43	2.15	0.32	0.03	0.007	0.00007	0.096
Inert-gas weld metal	0.10	0.74	0.013	0.021	0.22	0.42	2.13	0.36	0.02	0.006	0.00005	0.016

[a] Total aluminum—Al_2O_3 and residual Al.

will be presented in a subsequent paper.

Conclusions

Nine experimental filler wires were prepared for submerged-arc welding studies. The compositions of these wires were such that a study of the effects of nickel, manganese and molybdenum could be made. The ranges of alloy content studied were: nickel, 1.4 to 3.0%; manganese, 1.2 to 1.8%; molybdenum, 0.05 to 0.80%. The weld metals were evaluated on the basis of notch toughness and tension tests. In analyzing the data, the following important observations were made:

1. Increasing nickel content lowered weld-metal notch toughness, especially at testing temperatures above −40° F. However, at testing temperatures below −40° F, increased nickel appeared to be beneficial.

2. Increasing manganese content also lowered weld-metal notch toughness at testing temperatures above −40° F, but at testing temperatures below −40° F, the notch toughness of the welds was about the same.

3. Increasing molybdenum content generally lowered weld-metal notch toughness.

4. The tensile and yield strengths of the weld metals were improved by increasing the nickel, manganese or molybdenum contents. However, the improvement in strength obtained by increasing the manganese or molybdenum contents was greater than that obtained by increasing the nickel content.

5. The notch toughness of the weld metals was improved and the tensile and yield strengths were lowered by stress-relieving operations.

Studies to find the differences between submerged-arc and inert-gas-shielded metal-arc weld metals showed the following:

1. The notch toughness of weld metals made by the inert-gas-shielded metal-arc process was higher than the notch toughness of weld metals made by the submerged-arc process.

2. The difference found in the notch toughness of weld metals made by the two processes was attributed to the number of inclusions, oxygen content and silicon content.

3. The tensile properties of weld metals made by the two processes were practically the same.

Acknowledgment

The authors wish to express their appreciation to the Bureau of Ships and to Battelle Memorial Institute for permission to publish this paper. The authors also wish to express their appreciation for the technical counsel offered by C. E. Sims, of the Battelle staff.

Acknowledgment is also due to J. A. Hincks and R. Pollock for the preparation and testing of the weld-joint specimens and to R. D. Buchheit for the metallographic work.

References

1. Rienbolt, J. A., and Harris, W. J., Jr., "Effect of Alloy Elements on Notch Toughness of Pearlitic Steels," *Am. Soc. Metals, Trans.*, **43** 1175–1201 (1951).

2. Boulger, F. W., Frazier, R. H., and Lorig, C. H., *Investigation of the Influence of Deoxidation and Chemical Composition on Notched-Bar Properties of Ship Plate Steel*, Welding Research Council, Bull. No. 26, April 1956.

3. Puzak, P. P., and Pellini, W. S., "Effect of Temperature on the Ductility of High-Strength Structural Steels Loaded in the Presence of Sharp Crack," Naval Research Laboratory, Report 4545.

4. Wepfer, G. S., "The Development and Investigation of High-Tensile High-Impact Electrode," THE WELDING JOURNAL, **35** (3), 229–235 (1956).

5. Hatch, W. P., Jr., and Hartbower, C. E., "Vee-Notch Charpy Impact Testing of Weld Metal and Heat-Affected Zone Simultaneously," *Ibid.*, **35** (3), Research Suppl., 120-s to 126-s (1956).

6. Simon, W., "Effect of Silicon in Submerged-Arc Welds," *Materials and Methods* (July 1955).

7. Stern, I. L., Kohn, N. A., and Nagler, H., "Notch-Toughness Characteristics of Submerged-Arc Weld Deposits," WELDING JOURNAL, **36** (5), Research Suppl., 226-s to 234-s (1957).

8. Battelle Memorial Institute, "Development of Filler Wire for Welding Army Ordnance Armor by the Inert-Gas-Shielded Consumable-Electrode Process," Summary Report WAL 641/17, dated March 31, 1956, to Watertown Arsenal Laboratory (Contract DAI-33-019-505-ORD-(P)-2, Subcontract TB4-31).

9. Air Reduction Co., "The Welding of HY-80 Steel by Inert-Gas-Shielded Metal-Arc Welding," Final Report dated Feb. 28, 1957, to Department of the Navy (Contract NObs 72087).

To Prospective Authors for 42nd Annual Meeting!

All authors interested in presenting papers at the AWS 42nd Annual Meeting to be held in New York City on April 17–21, 1961 are advised of a change in preliminary arrangements.

The usual forms, "An Invitation to Authors" and "Authors Application Form", have been printed as a detachable insert on pages 509–510 of the May issue of the Welding Journal instead of being sent through the mails.

Anaconda Memo to Management

This is a penny's worth of bronze

It's a piece of Anaconda welding rod that could be worth its weight in gold to you. It might save you a big capital investment or important production time by salvaging equipment that seems beyond repair. Take the experience of Jessup Steel Co., for example. A while back their production stopped dead in its tracks when the 60-ton semisteel base of a big forging hammer fractured. A replacement base? Of course—in nine months. Jessup called specialists in repairing heavy machinery. The base was repaired by braze welding in a week —at 20% of replacement cost. About a ton of Tobin Bronze®-481 rod was used. But sometimes a few ounces can make equally significant savings in building up worn surfaces or repairing a broken part that has immobilized a big machine. *And don't overlook braze welding in production.* It's a practical way to get flexible, low-cost production assembly of tubular and sheet steel products —like furniture and appliances. American Motors uses it to add strength, prevent squeaks, leaks, and rattles in unit construction of the Rambler's body, supplementing electric welding in some 30 areas. Anaconda-997 (Low Fuming) Bronze Rod has proved to be the best welding rod for these production uses.

6080

We'd be glad to send you (or anyone else in your company) a copy of Publication B-13 which gives detailed and practical information on Anaconda Welding Rods in repair and production jobs. If you have a special problem, the services of an Anaconda specialist are at your disposal. Write: The American Brass Company, Waterbury 20, Conn. In Canada: Anaconda American Brass Ltd., New Toronto, Ont.

ANACONDA®

WELDING RODS

products of The American Brass Company

For details, circle No. 46 on Reader Information Card

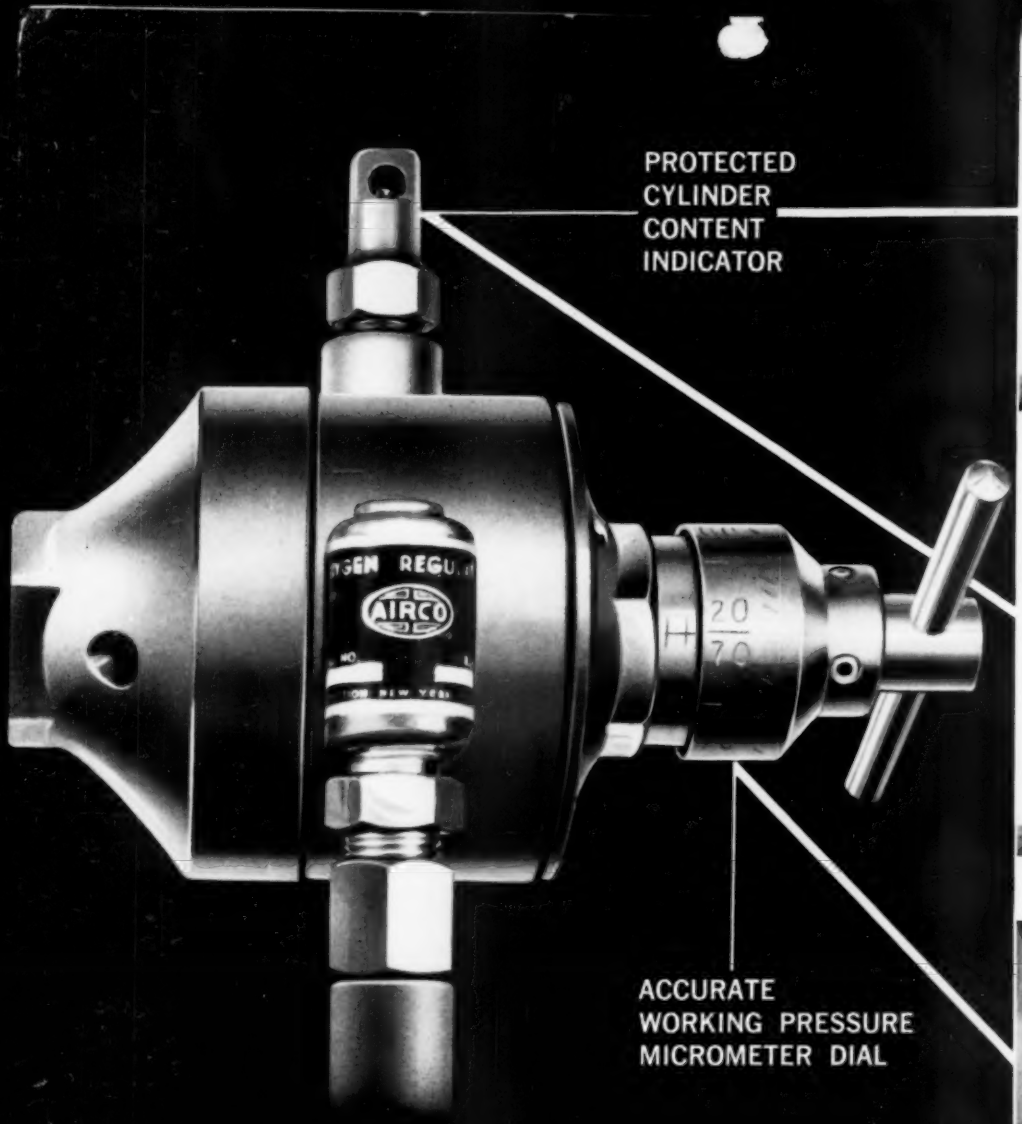

Indicator at top of protective housing indicates a full cylinder.

Cylinder content indicator at half-full position.

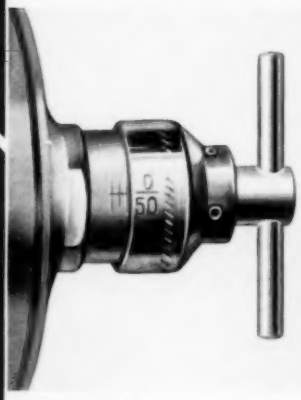

Read working pressure directly from micrometer markings engraved on dial. Regulators for oxygen and acetylene service are available.

All new...accurate...and toughest yet! Airco Gaugeless Regulators ...backed by the *most experience*

The new Airco Gaugeless Regulators for oxygen and acetylene give you the *pressure accuracy* you need, plus the *ruggedness* that regulators should have for construction and maintenance work, where rough handling is constant fare. That's because of the regulator's protected cylinder content indicator, and adjustable micrometer working pressure dial.

These rugged regulators are the newest in Airco's extensive quality line . . . two more examples of how *Airco experience* brings you better welding equipment. Whether you need regulators, gas welding and cutting equipment, tips, supplies or industrial gases – your nearby Authorized Airco Distributor has them in stock. Look in your Classified Telephone Directory, under "Welding Equipment and Supplies," for your nearest Authorized Airco Distributor.

AIRCO®

AIR REDUCTION SALES COMPANY

A division of Air Reduction Company, Incorporated

150 East 42nd Street, New York 17, N. Y.

More than 700 Authorized Airco Distributors Coast to Coast

On the west coast–
Air Reduction Pacific Company

Internationally–
Airco Company International

In Cuba–
Cuban Air Products Corporation

In Canada–
Air Reduction Canada Limited

All divisions or subsidiaries of Air Reduction Company, Inc.

For details, circle No. 47 on Reader Information Card